**Two Subunits Contribute to the Integrity of the TRAPP II**

**Complex Through Intra-Molecular Interactions**

BY

DAVID TAUSSIG

B.S. Wheaton College, 2006

THESIS

Submitted as partial fulfillment of the requirements
for the degree of Doctor of Philosophy in Biological Sciences
in the Graduate College of the
University of Illinois at Chicago, 2013

Chicago, Illinois

Defense Committee:

Nava Segev, Advisor, Biochemistry and Molecular Genetics
Donald Morrison, Chair, Biological Sciences
Brian Kay, Biological Sciences
David Stone, Biological Sciences
Sojin Shikano, Biochemistry and Molecular Genetics

## ACKNOWLEDGMENTS

I would like to thank my advisor, Nava Segev, for her expansive technical advice, scientific analysis, and patience, all of which were greatly needed and deeply appreciated. Furthermore, her extensive contributions toward the writing of my publications, as well as this dissertation, are highly valued. In addition, I am sincerely grateful for the contributions of my current and former committee members: Dr. Kay, Dr. Stone, Dr. Shikano, Dr. Morrison, and Dr. Liebman. Their out-of-the-box scientific ideas, constructive criticism, and professional support was greatly treasured and sought-after. Also, I wish to acknowledge the current and former lab members who collaborated with me on research projects, providing experimental advice and, in many cases, experimental results which I include in this dissertation. These include Andrei Tokarev, Geetanjali Sundaram, Zhanna Lipatova, XiuQi Zhang, and Jane Kim.

Lastly, a big thank you to my parents Paul and Martha Taussig, as well as remaining family and very good friend Vidhu Mathur, for their unwavering emotional (and sometimes technical) support—they celebrated with me during the good times, and kept me going when times were tough.

## TABLE OF CONTENTS

TABLE OF CONTENTS (CONTINUED)

## LIST OF TABLES

## LIST OF FIGURES

**LIST OF FIGURES** (CONTINUED)

FIGURE PAGE

## LIST OF ABBREVIATIONS

| | |
|---|---|
| ER | endoplasmic reticulum |
| GDP | guanine diphosphate |
| GTP | guanine triphosphate |
| GEF | guanine nucleotide exchange factor |
| GAP | GTPase activating protein |
| GDI | Rab GDP dissociation inhibitor |
| GDF | GDI displacement factor |
| REP | Rab escort protein |
| SEDT | spondyloepiphyseal dysplasia tarda |
| GST | glutathione s-transferase |
| MBP | maltose binding protein |
| GFP | green fluorescent protein |
| YFP | yellow fluorescent protein |
| CFP | cyan fluorescent protein |
| PCR | polymerase chain reaction |
| TRAPP | transport protein particle |
| BiFC | bi-molecular fluorescence complementation |

## SUMMARY

Intracellular protein transport in yeast is a highly regulated process controlled by several layers of regulatory elements, most of which are conserved in higher eukaryotes. The master regulators of transport are Rab GTPases, which are in turn regulated by other factors known as GEFs and GAPs. In this dissertation, I report the findings of research pertaining to a large protein complex acting as a GEF on multiple Rab GTPases in yeast.

This complex, known as TRAPP, is found in three alternative arrangements, each governing a different transport step. One such arrangement, TRAPP II, contains 11 conserved subunits, 8 of which are essential for viability. However, the precise architecture of this complex remains poorly understood, as do the specific roles of two subunits, Trs20 and Trs33, in the context of the TRAPP complex.

Here I provide and discuss evidence clarifying the functions of Trs33 and Trs20. Using approaches involving yeast genetics, protein biochemistry, and fluorescence microscopy, I demonstrate that each subunit contributes to the structure and function of TRAPP II through novel interactions with a third subunit, Trs120. Moreover, a mutation in *TRS20*, analogous to one which causes a disease in humans, disrupts the interaction of Trs20 with Trs120.

Together, these results shed light on the structural interdependencies of the TRAPP II complex, and elucidate the roles of two subunits in the structure and function of this complex. In addition, the finding of defective interaction between Trs20 and Trs120 caused by a disease-associated mutation has implications for further research into the molecular basis of the disease, as well as possible therapeutic targets.

# CHAPTER I: INTRODUCTION

## A. Overview of vesicular transport

One of the hallmarks of eukaryotic cells is compartmentalization. Membrane-bound compartments, or organelles, vary in size, content, and most importantly, function. Each compartment has a unique repertoire of proteins and lipids which define its role within the cell. For example, the endoplasmic reticulum (ER) is an organelle rich in chaperone proteins and post-translational modifiers (Araki and Nagata 2011), whereas the lysosome contains many proteases to support its role as the recycling organelle of the cell (Ciechanover 2012). The budding yeast *Saccharomyces cerevisiae*, a unicellular organism, contains more than six different organelles during actively-growing conditions, each with a distinct set of resident proteins. Furthermore, like most eukaryotic cells, yeast actively secrete many proteins, in a process known as exocytosis, as well as import proteins from the plasma membrane to intra-cellular organelles, which is called endocytosis.

Given this complexity, one can appreciate the need for a controlled set of transport pathways, through which proteins can be shuttled to various destinations. The first to report evidence of directed protein transport were Lucien Caro and George Palade, who report the results of a study in which they visualized radio-labeled proteins progressing from the ER to the Golgi apparatus in mammalian pancreatic cells (Caro and Palade 1964). Palade later established that transport of secretory proteins occurs within membrane-bound structures we now refer to as vesicles (Palade 1975).

Since then, a vast amount of research has helped to elucidate the various transport pathways which exist in eukaryotic cells. A picture has emerged of an extensive network of transport pathways, including secretion, endocytosis, and transfer of proteins from one organelle to another. Figure 1 illustrates a few examples of transport steps found in yeast. In addition to identifying the various pathways, decades of research have illuminated, for many pathways, distinct steps in the transport process, and the identity of specific regulators involved in each.

A typical transport pathway involves four steps, diagrammed in Figure 2 (Bonifacino and Glick 2004). First, proteins destined for transport are recruited near a region of the membrane of a donor compartment, which then undergoes membrane curvature and budding, forming a vesicle. Second, vesicles are transported by motor proteins along actin cables or microtubules toward the acceptor compartment. Third, long range factors known as tethers physically connect the vesicle with the acceptor compartment. Finally, long coiled-coiled proteins termed SNAREs orchestrate fusion of the vesicular and organelle membranes, effectively adding the contents of the vesicle to the destination compartment.

A great deal has been discovered regarding the mechanisms of each of these four steps, as well as proteins required for each. Surprisingly, most factors involved in the transport steps are specific to a particular pathway, rather than being generic elements. For example, the tethering factors connecting vesicles moving from the ER toward the cis-Golgi are different from those connecting vesicles headed from the trans-Golgi to the plasma membrane. Similarly, the coat protein orchestrating membrane budding from the plasma membrane during endocytosis, clathrin, is different from COP I, a complex responsible for budding of vesicles from the Golgi directed to the ER (Bonifacino and Lippincott-Schwartz 2003). While exceptions exist, most transport steps have their own set of regulatory elements.

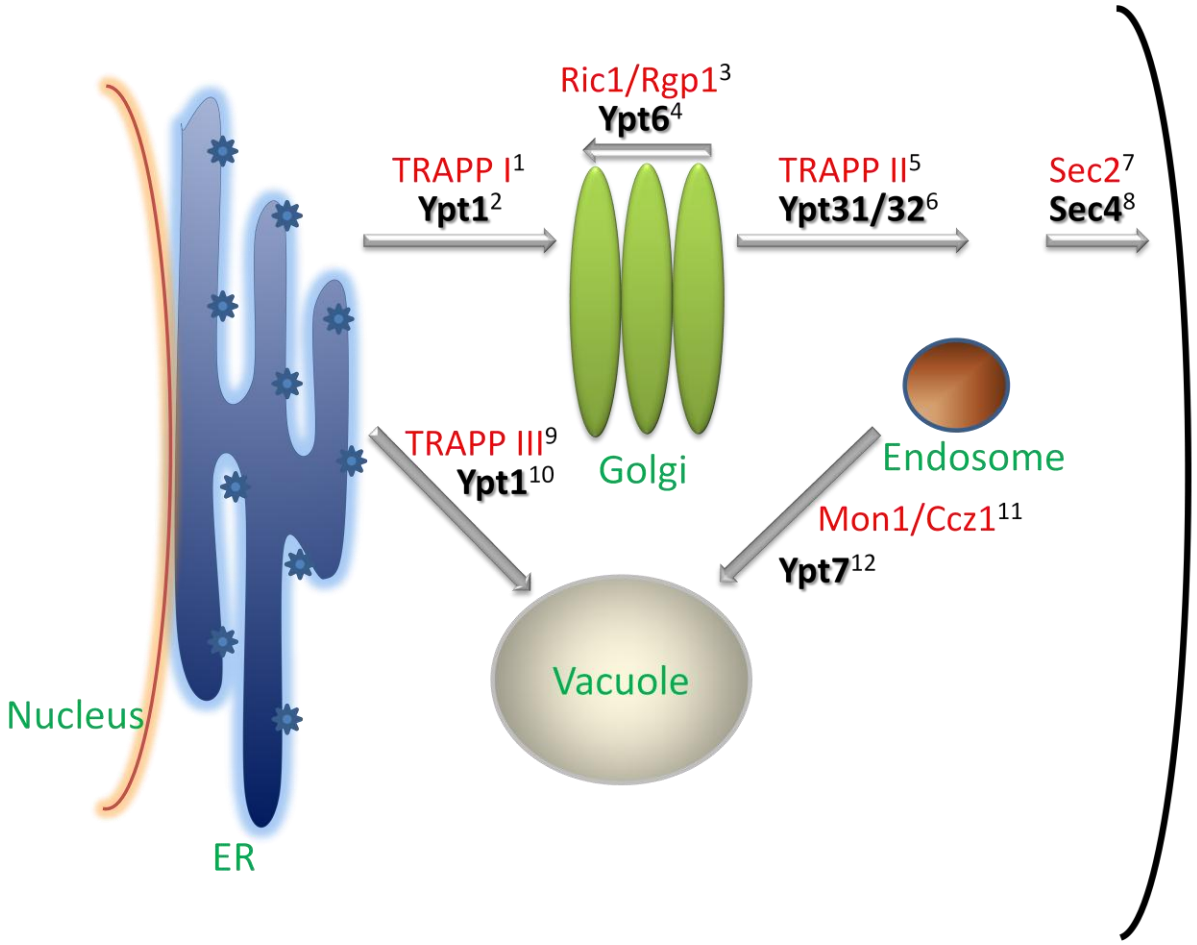


**Figure 1: Examples of protein trafficking steps in yeast, and their regulatory elements.** Cellular landmarks are labeled in green. The Rab-GTPase regulating each step is written in black, and the GEF activating each Rab in red. References: [1](Sacher et al. 1998; Kim et al. 2006) [2](Segev et al. 1988) [3](Siniossoglou et al. 2000) [4](Jones et al. 2000) [5](Jedd et al. 1997) [6](Walch-Solimena et al. 1997) [7](Salminen and Novick 1987) [8](Lynch-Day et al. 2010) [9](Nordmann et al. 2010) [10](Schimmoller and Riezman 1993)

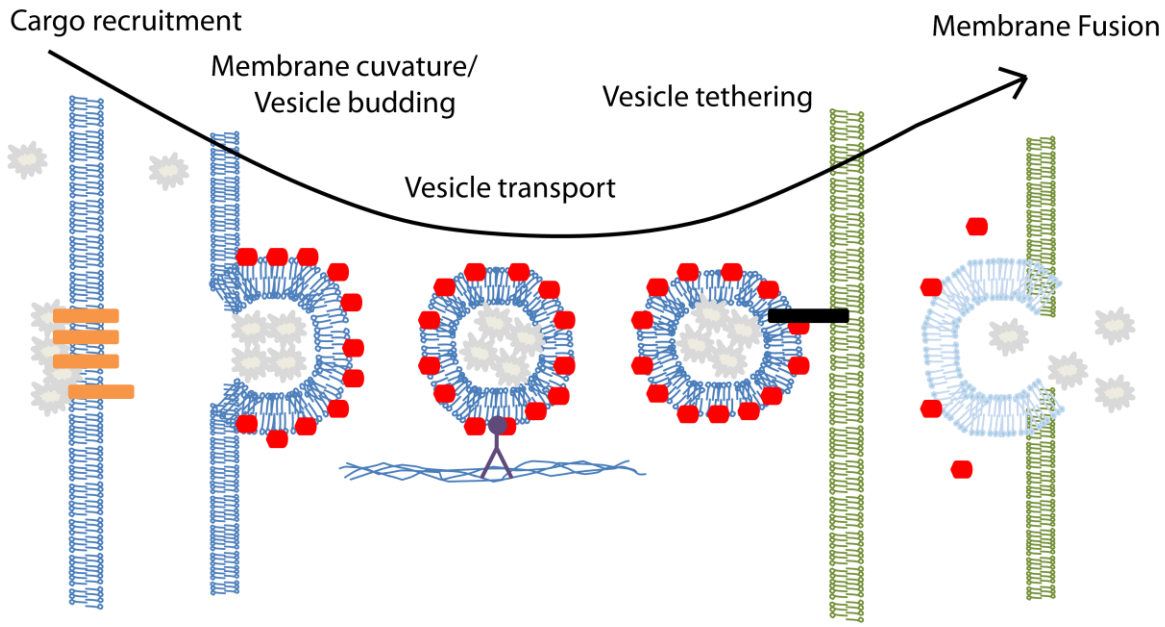


**Figure 2: Schematic of a typical protein transport reaction.** Cargo (gray structures) is recruited to a particular domain of the donor membrane (blue) by receptor trans-membrane proteins (yellow). Budding is initiated by membrane curvature caused by the binding of coat proteins (red) to the donor membrane. After budding, the vesicle is transported along the cytoskeleton by motor proteins. Upon arrival at the target membrane (green), the vesicle docks at the membrane by binding to long-range tethering factors residing on the destination membrane. Finally, the membranes undergo SNARE-mediated fusion, thereby emptying the vesicle cargo into the lumen of the destination compartment.

Most proteins involved in these transport in steps are constitutively functional, meaning that they have no intrinsic method of shutting themselves off, thereby halting transport. These include coat proteins, tethering factors, and SNAREs. However, such rigidity limits the ability of the cell to adapt to changing conditions, such as environmental variables or growth cycle progression. To address this issue, each transport step is under the control of a specific Rab GTPase. These proteins are often referred to as "molecular switches," due to their nature of cycling between active and inactive forms. Rab GTPases are considered the master regulators of intracellular protein transport.

**B. Rab GTPases**

The first Rab GTPase discovered, called Ypt1 for its role in yeast protein transport, was identified in yeast in 1983. It was recognized as a homolog of the Ras GTPase, the latter studied extensively due to its oncogenic properties (Gallwitz et al. 1983). A few years later Ypt1 was shown to play a role in autophagy and secretion, as well as other cellular processes (Segev and Botstein 1987; Segev et al. 1988). Many similar proteins have been subsequently found in both yeast and higher eukaryotes, often through sequence similarity to Ras or each other, forming what is now known as a family of GTPases known as Rabs (Salminen and Novick 1987; Touchot et al. 1987). Currently there are 11 Rabs known in yeast, and ≈70 in mammals (Mizuno-Yamasaki et al. 2012). According to the current dogma, each Rab governs a specific transport step. In higher eukaryotes, the expression of some Rab proteins is cell-type specific. Figure 1 illustrates some examples of pathways controlled by Rabs in yeast.

Rabs exert their function by binding to transport components, termed effectors. A large number of effectors have been identified, and cover a great diversity of different roles. Just a few

examples include tethering factors such as the exocyst, an effector of Sec4 (Guo et al. 1999), motor proteins such as the Ypt31/32 effector Myo2 (Lipatova et al. 2008), or adaptor proteins such as the Rab9 effector TIP47 (Carroll et al. 2001).

Importantly, Rabs can exist in one of two conformations. When bound to the nucleotide GTP, the protein folds in such a way that it can bind to its effectors. This is referred to as the 'on' state, in which case the transport step regulated by the Rab progresses. GTP hydrolysis by the Rab, after which the Rab is bound to GDP, results in a change in protein shape to a form which cannot binds its effectors, therefore no longer facilitating transport. The nucleotide binding, GTP or GDP, defines the Rab's state as a molecular switch, and controls transport progression.

Unsurprisingly, the nucleotide bound state of a Rab is tightly controlled by other regulatory factors (Segev 2001): GTPase activating proteins (GAPs) catalyze the GTPase activity of the Rab, causing a GTP-bound Rab to become GDP-bound. On the other side, guanine nucleotide exchange factors (GEFs), dissociate the GDP from the Rab, allowing the Rab to bind GTP, which is roughly ten times more concentrated in the cell than GDP. Thus, GAPs are the factors which turn 'off' a Rab GTPase, and GEFs are the factors which turn them 'on.'

. Many GEFs and GAPs have been identified. The GEFs for 7 of the Rabs in yeast are indicated in Figure 1. While GEFs are generally regarded as specific, activating only one Rab, GAPs demonstrate promiscuity among different Rabs *in vitro*. For example, one of the GAPs found in yeast, Gyp3, can catalyze GTPase activity on 6 different Rabs *in vitro*. (Albert and Gallwitz 1999). However, there is still debate concerning whether GAPs are specific *in vivo*.

Another critical element of Rab function is membrane attachment. Rabs do not have a transmembrane domain, but are prenylated with a duel geranylgeranyl lipid moiety shortly after synthesis, which is required for correct localization and, therefore, function of the Rab GTPase

(Seabra 1998). The enzyme which carries this out, Rab geranylgeranyl transferase, forms a ternary complex with the Rab and another protein, called Rab escort protein, or REP, which is required for the prenylation (Anant et al. 1998).

After initial prenylation, the Rab's membrane attachment is closely linked to its guanine nucleotide-bound state. According to the currently accepted model, and illustrated in Figure 3, Rabs are recruited to membranes in their GDP-bound state, where they encounter their GEF. Upon interaction with the GEF, the Rab dissociates from GDP and binds GTP, at which point it attaches to the membrane through its geranylgeranyl moiety. In this state it binds to effectors, driving forward the specific transport step under the Rab's control. After the transport cycle is complete, the Rab encounters and binds to its GAP, which catalyzes hydrolysis of GTP to GDP. At this point the Rab interacts with a new partner, which acts promiscuously on multiple Rabs, called guanine dissociation inhibitor, or GDI. GDI extracts the Rab from the membrane, and holds it in the cytosol until another round of transport begins (Garrett et al. 1994). Thus the Rab cycles between a GTP-bound state at the membrane, and a GDP-bound state in the cytoplasm (Hutagalung and Novick 2011).

The crystal structures of many Rab GTPases, from yeast and mammals, have been solved, both in GTP-bound and GDP-bound states. Examples include the mammalian Rab3A bound to a GTP analog (Dumas et al. 1999), the GTP and GDP-bound forms of Sec4, from yeast (Stroupe and Brunger 2000), and Ypt1, from yeast, in complex with its GEF (Cai et al. 2008). These structures, and many others, have revealed several structural features found in Rabs. One such feature is a GTPase region, composed of a β-sheet bordered by α-helixes, common to all Rabs as well as Ras. Another important feature is the hypervariable domain, which is different for each Rab, and shown to be important for Rab localization (Chavrier et al. 1991). At or very

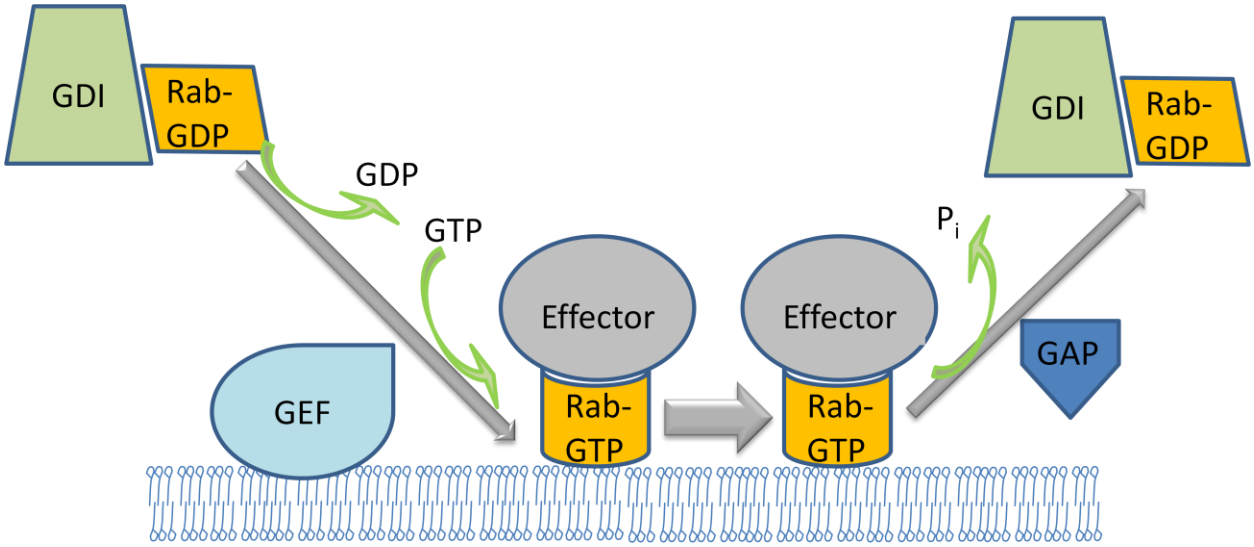


**Figure 3: The steps of the Rab cycle.** Cytosolic Rab is bound to GDP, and in complex with Rab-GDI. To facilitate transport, the Rab is recruited to a membrane and activated by its specific GEF, which removes GDP from the Rab. Subsequent binding by GTP results in a conformational shift, allowing the Rab to interact with its effectors. After the transport step is complete (broad arrow), the Rab GTPase activity is catalyzed by its GAP, changing it back to the inactive form. The GDP-bound Rab is extracted from the membrane by Rab-GDI, and is held in the cytosol until another round of transport begins.

near the carboxy terminus are two conserved cysteine residues to which are attached the geranylgeranyl lipid groups, critical for the Rab's membrane attachment (Calero et al. 2003). And finally, all Rabs contain two regions termed switch 1 and switch 2, which dramatically change conformation depending on the guanine nucleotide bound. It is the switch 1 and switch 2 regions which bind effectors in the GTP-bound state (Lee et al. 2009).

The Rab GTPases most relevant to this dissertation are the yeast proteins Ypt1, Ypt31, and Ypt32. Ypt1 has been shown to act in at least three distinct pathways: ER-Golgi, intra-Golgi, and autophagy transport. The only Ypt1 effector for ER-Golgi and intra-Golgi transport reported to date is the Sec34/Sec35 complex, which plays a role in intra-Golgi transport (Suvorova et al. 2002). However, several effectors of its mammalian ortholog, Rab1, have been identified. These include the tethering factor p115 (Allan et al. 2000), and Golgi matrix protein GM130 (Moyer et al. 2001; Weide et al. 2001). Atg11, a scaffold protein which organizes the pre-autophagosomal structure (PAS), has been reported as an effector for Ypt1 in the autophagy pathway (Lipatova et al. 2012).

Ypt31 and Ypt32 are a pair of highly similar (90%) Rab GTPases which act at the trans-Golgi. Deletion of either causes no apparent growth defect, but deletion of both is lethal (Benli et al. 1996). No evidence has been reported of any functional differences; hereafter they will be referred to as Ypt31/32, and considered functionally redundant. They have been shown to be required for exit from the Golgi (Jedd et al. 1997), as well as endosome to Golgi transport (Chen et al. 2005). Several effectors have been identified, including motor protein Myo2 (Lipatova et al. 2008), F-box protein Rcy1, required for endosome-Golgi transport (Chen et al. 2005), and Sec2, the GEF for Sec4 (Ortiz et al. 2002).

Coordination among Rabs acting sequentially in transport pathways is currently a hot topic in Rab research. This concept demonstrates the cross-talk between steps within a transport pathway, and legitimizes the nature of Rabs as molecular switches, which are ‘on’ or ‘off’ depending on their nucleotide-bound state. In other words, if each step in a pathway were an isolated event, with no coordination between the transport processes, there would be no advantage to having an ‘off’ state for the master regulator.

Evidence of several examples of coordination has been found. Most often, coordination occurs through Rab-GEF cascades, where one Rab recruits the GEF for the next Rab in the pathway. A good example of this is the Ypt31/32-Sec2-Sec4 cascade, in which Ypt31/32 recruit Sec2, the GEF for Sec4, which acts immediately downstream of Ypt31/32 (Ortiz et al. 2002). Another, found in mammalian cells, is the Rab22-Rabex-5-Rab5, where Rab22 recruits the GEF for Rab5, which acts later in the endocytic pathway (Zhu et al. 2009), Another type of cascade involves GAPs, where the downstream Rab recruits the GAP for its predecessor, effectively turning it ‘off.’ An example of this is the Ypt31/32-Gyp1-Ypt1 cascade, where Ypt31/32 recruit Gyp1, the GAP for Ypt1, which acts prior to Ypt31/32 (Rivera-Molina and Novick 2009).

While many examples of coordination have been elucidated, there is little doubt there are more as yet undiscovered. A good candidate for coordinating transport steps in yeast is the TRAPP (for Transport Protein Particle) complex. Alternative arrangements of this complex act as GEFs for Ypt1 and Ypt31/32, which together regulate at least three different transport steps (illustrated in Figure 1). While no confirmation of crosstalk through TRAPP complexes has been reported, a better understanding of the relationship between the complexes may yield evidence that these complexes coordinate the functions of Ypt1 and Ypt31/32.

**C. TRAPP structure and function**

The first TRAPP subunit discovered was Bet3, found during a genetic interaction screen to detect proteins involved in secretion (Rossi et al. 1995). Bet5, another TRAPP subunit, was identified as a high-copy suppressor of *bet3-1*, a temperature sensitive strain (Jiang et al. 1998). Three other members were identified by mass spectrometry following immuno-precipitation of Bet3 from a yeast lysate. This study further showed that Bet3 exists as part of a large complex localizing to the Golgi apparatus, and required for docking vesicles to the Golgi in ER-Golgi transport (Sacher et al. 1998). Another five TRAPP subunits were discovered by the same group shortly after, who also reported evidence that the complex exhibits properties of a peripheral membrane protein (Sacher et al. 2000). The last remaining protein currently considered a subunit of TRAPP, Tca17, was discovered much later, identified through a screen for proteins defective in recycling the SNARE Snc1, and shown to bind to TRAPP subunits (Montpetit and Conibear 2009).

TRAPP is now known to exist as at least 3 alternative complexes, each with different but overlapping sets of subunits (Yu and Liang 2012). The first TRAPP variants to be distinguished were TRAPP I and TRAPP II (Sacher et al. 2001). A third complex, TRAPP III, was shown to exist more recently, and implicated in autophagy (Lynch-Day et al. 2010). Each TRAPP subunit is listed in Table I, along with its complex assignments and mammalian ortholog.

Of the TRAPP complexes, the role of TRAPP I is most well understood. As illustrated in Figure 4, TRAPP I contains 6 unique subunits: Bet3, Bet5, Trs23, Trs20, Trs31, and Trs33. Each is present as a single copy except Bet3, which is present in two copies. TRAPP I is known to localize to the cis-Golgi, and act in ER-Golgi transport (Sacher et al. 2001). Two roles of this

**Table I: List of TRAPP subunits found in yeast, complex association(s), closest mammalian homolog, and putative function**. References: [1](Turnbull et al. 2005), [2](Kim et al. 2006), [3](Venditti et al. 2012), [4](Montpetit and Conibear 2009), [5](Lynch-Day et al. 2010), [6](Liang et al. 2007), (Yip et al. 2010), [8](Morozova et al. 2006)

| Subunit | Complex | Mammalian Ortholog | Function |
|---|---|---|---|
| Bet3 | I, II, III | TRAPPC3 | Required for membrane attachment[1], Ypt1 GEF activity[2] |
| Bet5 | I, II, III | TRAPPC1 | Required for Ypt1 GEF activity[2] |
| Trs23 | I, II, III | TRAPPC4 | Required for Ypt1 GEF activity[2] |
| Trs31 | I, II, III | TRAPPC5 | Required for Ypt1 GEF activity[2] |
| Trs20 | I, II, III | TRAPPC2/Sedlin | Involved in ER exit in mammals[3] |
| Trs33 | I, II, III | TRAPPC6 | Required for attachment of Tca17[4] |
| Trs85 | III | TRAPPC8/GSG1 | Autophagy specific[5] |
| Trs65 | II | C5orf44 | Contributes to attachment of Trs130/Trs120[6]; required for dimerization[7] |
| Trs120 | II | TRAPPC9/NIBP | Required for attachment of Trs130[8] |
| Trs130 | II | TRAPPC10/EHOC-1 | Required for Ypt31/32 GEF activity[8] |
| Tca17 | II | TRAPPC2L | Contributes to attachment of Trs65[4] |

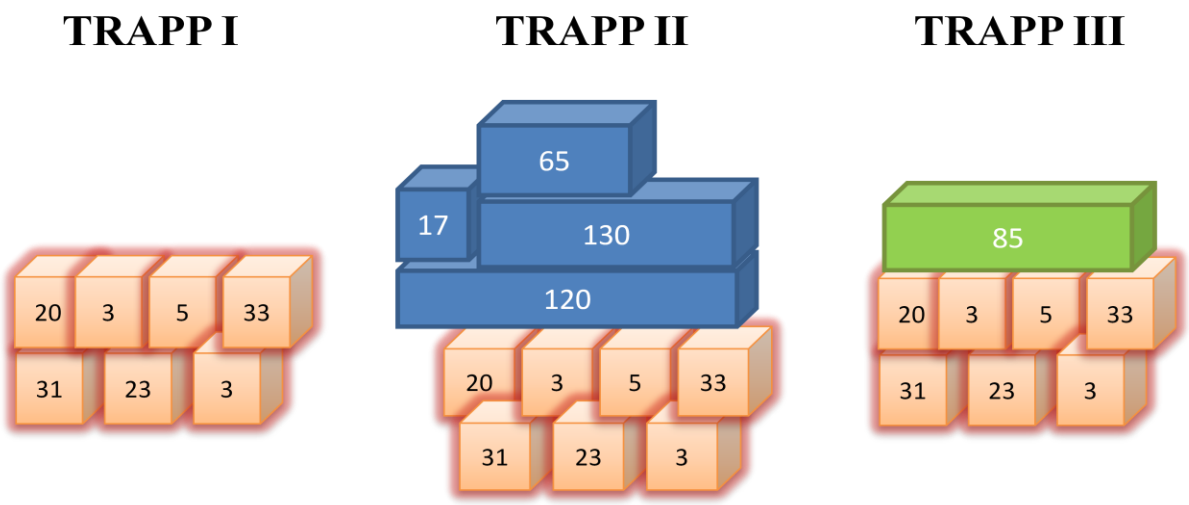


**Figure 4: Arrangement of subunits in three alternative TRAPP complexes.** TRAPP I contains 6 unique subunits: Trs20, Trs31, Bet3, Trs23, Bet5, and Trs33 (two copies of Bet3). TRAPP II contains all of those plus 4 additional subunits: Tca17, Trs65, Trs120, and Trs130. TRAPP III contains all 6 TRAPP I subunits, plus Trs85. While the arrangement of all other subunits is based on interaction data, the position of Trs85 with respect to other TRAPP III subunits was chosen arbitrarily, as no direct interactions of Trs85 with other TRAPP subunits have been reported.

complex in contributing to this transport step have been reported: as a GEF for the Rab GTPase Ypt1, and as a tethering factor docking ER-derived COPII vesicles at the cis-Golgi.

The GEF activity on Ypt1 is universally accepted (Jones et al. 2000; Wang et al. 2000). It has been conclusively shown that the central 4 subunits, Bet3, Bet5, Trs23, and Trs31 (hereafter referred to as core TRAPP I), are necessary and sufficient to exchange nucleotide on Ypt1 *in vitro* (Kim et al. 2006). The latter role, of tethering COPII vesicles to the cis-Golgi, is less well established. Several other large protein complexes acting in membrane transport in yeast have known tethering functions, including the exocyst (Wiederkehr et al. 2004), GARP (Conibear and Stevens 2000), and C-VPS (Sato et al. 2000), among others. The fact that TRAPP is reminiscent of these complexes suggests a likely tethering function for TRAPP. However, the only direct evidence for such a role reported to date is genetic and physical interaction demonstrated between the TRAPP subunit Bet3 and COPII subunit Sec23, a coat protein present on the surface of vesicles transported from the ER to the Golgi (Cai et al. 2007).

The structure of each TRAPP I subunit has been solved, either individually or in complex with other proteins. These include, in part, complexes composed of Bet3-Trs33 (Kim et al. 2005), Bet3-Trs31-Trs20, Bet3-Trs33-Bet5-Trs23 (Kim et al. 2006) and even Bet3-Bet5-Trs23-Trs31-Ypt1 (Cai et al. 2008). These structures and others have provided strong evidence that TRAPP I exists as a relatively long and flat molecule, with the arrangement of subunits depicted in Figure 4. This structure was shown to be dependent on a specific domain of Trs23, one of the middle subunits of TRAPP I (Brunet et al. 2012).

Another TRAPP complex, known as TRAPP III, has been shown to act in autophagy. This complex is thought to contain all of the TRAPP I subunits plus another subunit, Trs85, based on co-precipitation analysis (Choi et al. 2011). A role for Trs85 in autophagy was

originally reported based on the mis-localization of autophagy-specific protein Atg8 in a strain with *TRS85* deleted (*trs85Δ*) (Meiling-Wesse et al. 2005), and the inability of this strain to process preApeI to its mature form, an established assay for selective autophagy (Nazarko et al. 2005). Later, Trs85 was localized to the pre-autophagosomal structure, or PAS, which is the focal point from which the autophagosome is thought to originate (Lynch-Day et al. 2010).

Based on this evidence, as well as the known requirement of Ypt1 for autophagy, the current understanding is that Trs85 is part of a complex with other subunits, forming TRAPP III, which activates Ypt1 for its regulation of the autophagy pathway. While there have been data reported regarding the subunit composition of TRAPP III, the arrangement of Trs85 with respect to the other subunits remains completely unknown. Further work is needed, specifically determining direct interaction between Trs85 and other TRAPP subunits, to elucidate the structure of TRAPP III.

The largest TRAPP complex shown to exist in yeast is called TRAPP II. This complex contains all the TRAPP I subunits as well as 4 additional proteins specific to TRAPP II: Trs65, Tca17, Trs120, and Trs130. Moreover, the complex was recently shown to be present as a dimer in yeast lysates (Yip et al. 2010; Choi et al. 2011), bringing the complex to a combined size of over one megadalton.

While the subunit composition of TRAPP II is broadly accepted in the field, as is its localization predominantly to the trans-Golgi (Cai et al. 2005; Liang et al. 2007), there is much uncertainty regarding its structure and function. The TRAPP II complex has been shown to act as a GEF for the Rab GTPases Ypt31/32 *in vitro* (Jones et al. 2000; Morozova et al. 2006) Moreover, genetic evidence has suggested that TRAPP II functions upstream of Ypt31/32, based on the suppression of growth defects in TRAPP II-mutant strains by the over-expression of

Ypt31 (Yamamoto and Jigami 2002; Sciorra et al. 2005). However, other reports have contradicted the claim that TRAPP II acts as a GEF on Ypt31/32 (Wang and Ferro-Novick 2002; Cai et al. 2008), and it is still considered by some to be an open question in the field. Roles for TRAPP II subunits have been suggested in trans-Golgi-associated transport (Cai et al. 2005), Golgi-ER retrograde transport (Chen et al. 2011), and even autophagy (Zou et al. 2013). With such varied roles proposed for TRAPP II, there remains much to be learned regarding the function of the complex in regulating protein transport.

Given here (and summarized in Table I) is a brief description of the role of each TRAPP II subunit, as currently understood. Bet3, a core TRAPP I subunit, and therefore also present in TRAPP II and III, is present in a 2:1 ratio relative to all of the other TRAPP subunits (Sacher et al. 2000). Furthermore, Bet3 is the only TRAPP subunit with the capability to directly bind membranes. When the crystal structure of mammalian Bet3 was solved, it was found to possess a hydrophobic pocket conjugating a palmitoyl group (Turnbull et al. 2005), which presumably allows membrane binding of Bet3, and thus the TRAPP complexes.

The other core TRAPP I subunits: Bet5, Trs23, and Trs31, are also part of TRAPP II, but have no clear role in its enzymatic function. However, they are required to connect the membrane-binding Bet3 subunit with Trs20 and Trs33. Likely, the TRAPP I subunits together form a scaffold for the attachment of TRAPP II-specific subunits. Trs33 and Trs20 connect to each end of core TRAPP I, and along with them are present in all three TRAPP complexes. They are the primary subjects of this dissertation, and their roles will be discussed in detail in Chapters 2 and 3, respectively.

The subunits specific to TRAPP II include Trs120, Trs130, Trs65, and Tca17. Of these, Trs65 and Tca17 are non-essential to growth in yeast. Yeast 2-hybrid assays have revealed

interaction of Trs120 with Trs130, Trs65, and TRAPP I subunits (unpublished data). Furthermore, deletion of *TRS120* in yeast prevents the co-precipitation of Trs130 with a Bet5-containing complex from yeast; the resulting complex does not have GEF activity on Ypt31. Mutation of *TRS130* prevents its co-precipitation with Bet5, and inhibits the GEF activity of the latter on Ypt31. However, mutation of *TRS130* does not affect the attachment of Trs120 to the complex (Morozova et al. 2006). Taken together, this suggests that Trs130 is required for enzymatic activation of Ypt31/32, and its attachment to the TRAPP complex relies on Trs120. Whether Trs120 or other TRAPP subunits contribute directly to the GEF activity of TRAPP II on Ypt31/32, or merely for the stability and localization of Trs130, is so far unknown.

Trs65, a non-essential TRAPP II-specific subunit, was originally shown to be important for cell wall biogenesis (Brown and Bussey 1993). Currently that phenotype is attributed to the role of TRAPP II in anterograde post-Golgi transport. More recently, an interaction was identified between Trs65 and Gea2, an Arf1 GEF involved in Golgi and post-Golgi transport, based on a yeast 2-hybrid screen (Chen et al. 2011). However, the function of this interaction remains unclear. Within the context of TRAPP II, Trs65 was shown to play a role in the attachment of essential subunits Trs130 and Trs120 to the complex, based on co-precipitation experiments and genetic interactions (Liang et al. 2007). Moreover, the dimerization of TRAPP II is completely dependent upon Trs65 (Yip et al. 2010; Choi et al. 2011).

Tca17, the other non-essential TRAPP II-specific subunit, has also been suggested to affect TRAPP II stability. Analysis of a *tca17Δ* strain revealed a minor defect in localization of TRAPP subunits as well as Ypt31. Furthermore, the association of Tca17 with TRAPP II is abolished in *trs33Δ* and *trs65Δ* strains, while Trs65 association with TRAPP is diminished in *tca17Δ* (Montpetit and Conibear 2009). These observations suggest that a network of interactions

works synergistically to stabilize the complex. While the physical interactions between Tca17 and other TRAPP subunits have not been extensively mapped, interaction has been reported for Tca17 with Trs130 by yeast 2-hybrid (Choi et al. 2011), and with a Bet3-Trs31 sub-complex by co-precipitation of recombinant proteins (Scrivens et al. 2009). Interestingly, Tca17 is considered to be a homolog of Trs20, and shares significant structural similarity, but the relevance of this has yet to be determined. Trs20 and Tca17 co-precipitate from yeast lysates (Montpetit and Conibear 2009), indicating they are both present on the same TRAPP II complex.

Each of the TRAPP subunits has an identifiable mammalian ortholog (shown in Table 1). Moreover, two additional proteins, TRAPPC11 and TRAPPC12, have been reported as stable components of the mammalian complex (mTRAPP), but have no yeast counterpart (Scrivens et al. 2011). Importantly, components of mTRAPP have been localized to the ERGIC, a compartment between the ER and Golgi apparatus, and have been implicated in ER-Golgi transport (Yu et al. 2006; Zong et al. 2012). Furthermore, mTRAPP precipitated from mammalian lysates was shown to act as a GEF on Rab1, the mammalian ortholog of Ypt1 (Yamasaki et al. 2009).

However, to date there is little evidence for alternate TRAPP complexes in mammals, such as there are in yeast. And while trans-Golgi-associated transport has been connected with TRAPP in plant cells (Qi et al. 2011), there is yet to be found any connection between post-Golgi trafficking and mTRAPP in mammals. The nature of yeast TRAPP, acting in three distinct pathways through different complexes, makes it likely that there are undiscovered roles of mTRAPP. If coordination between transport steps in yeast is found to occur through TRAPP complexes, the relevance of this to humans would be minimal if mTRAPP indeed functions in only one pathway. Additional research is warranted on this topic.

**D. Protein transport and human disease**

Many human diseases are associated with altered protein transport pathways. In some cases this involves defective transport, and in others hyper-active or uncontrolled transport. In addition, drugs targeting transport regulators have been considered as therapeutic options, even when the disease itself does not directly affect transport.

Most of the research on transport related to disease has focused on Rab GTPases, the master regulators of protein transport. Rab1, the human ortholog of Ypt1, has been found to be over-expressed in several types of cancer, including tongue cancer (Shimada et al. 2005) and liver cancer (He et al. 2002). Rab1 has also been studied in association with Parkinson's disease. One popular hypothesis regarding the molecular basis for this disease is that misfolded α-synuclein aggregates in the ER, causing ER stress. Studies using a yeast model of the disease showed that the lethality caused by over-expression of α-synuclein can be rescued by the over-expression of Ypt1. In addition, Rab1 over-expression was shown to rescue neuron loss in *C. elegans* and rat models of the disease (Cooper et al. 2006).

Rab11 and Rab25, the closest human orthologs of Ypt31/32, have also been implicated in many human diseases. Like Rab1, Rab25 is also over-expressed in liver cancer (He et al. 2002). EVI5, a putative Rab11 GAP, has been identified as an oncogene (Westlake et al. 2007). Rab11 in particular has been studied as a possible drug target to affect post-Golgi transport, an important consideration in several diseases. One such example is diabetes, caused by improper function of the glucose transporter GLUT4. Rab11 has been shown to be responsible for the localization of GLUT4 (Zeigerer et al. 2002), and knock-down of Rab11 or one of its effectors has been shown to increase the proportion of GLUT4 localizing to the plasma membrane

(Schwenk et al. 2007). Another disease connected with Rab11 is cystic fibrosis. This disease is caused by mutation of the CFTR gene, which encodes an anion channel functioning at the plasma membrane. The mutations destabilize the encoded protein, and therefore impair anion and water transport through the plasma membrane. One study showed that over-expression of Rab11 increased the amount of wild-type or mutant CFTR protein localizing to the plasma membrane (Gentzsch et al. 2004), making it a potential therapeutic agent.

In addition to the Rabs GTPases whose mammalian orthologs are activated by TRAPP, two subunits of TRAPP have themselves been implicated in human disease. These include Sedlin, the ortholog of yeast Trs20, and TRAPPC9/NIBP, the ortholog of Trs120. Mutations in Sedlin cause an X-linked cartilage-specific disorder known as spondyloepiphyseal dysplasia tarda (SEDT). This disease affects roughly 1 in 150,000 people, and is characterized by short stature and severe skeletal abnormalities (Tiller et al. 2001). The molecular basis for SEDT remains unclear, and will be discussed in more detail in Chapter 3 and 4.

Mutations in TRAPPC9/NIBP have been linked to several neurological disorders, including mental retardation (Mir et al. 2009), intellectual disability (Marangi et al. 2013), and multiple sclerosis (Gourraud et al. 2013). While the precise mechanism through which the Trs120 ortholog affects these diseases is still unknown, one clue may be its interaction with NIK and IKKβ, two factors involved in a transcription activation pathway integral to the central nervous system (Hu et al. 2005). A more complete grasp of the functions of Trs20 and Trs120 in yeast may deepen our understanding of the molecular basis behind the diseases caused by mutations in their human counterparts.

**E. Open questions concerning TRAPP research**

Much is known about the various functions of TRAPP, the organization of its components, and the contributions of some individual subunits toward the functions of TRAPP. However, there remain some very important questions unanswered. One of these is the function of mTRAPP in mammalian cells, discussed above. Regarding the yeast complexes, I will discuss three issues I consider most worthy of additional research.

One of these questions concerns possible coordination of transport steps through the different TRAPP complexes. As stated above, other examples of traffic coordination have been found in yeast and mammals. The involvement of TRAPP in multiple transport events makes a role for TRAPP in coordinating those events an intriguing possibility. One way this might be done is though the assembly of TRAPP II. Hypothetically, TRAPP I, which functions at the cis-Golgi, could subsequently move through the Golgi and provides a scaffold for the assembly of TRAPP II. Since TRAPP II functions immediately after TRAPP I in the secretory pathway, this would ensure that post-Golgi transport is dependent upon pre-Golgi transport, a logical hypothesis. However, to date there is no direct evidence, beyond the circumstantial evidence of shared subunits, that TRAPP II is formed from pre-functional TRAPP I. Testing this possibility, or other possible examples of coordination through TRAPP, would greatly increase our appreciation for the role of the complexes in regulating transport.

A second question regarding TRAPP is the GEF activity of TRAPP II on Ypt31/32. Currently the field is split on this issue. While yeast-purified TRAPP complexes have been shown to dissociate nucleotide from Ypt31/32 *in vitro*, others have been unable to reproduce this result and dispute the claim that TRAPP II functions as a GEF on Ypt31/32. Furthermore, while there is evidence that the TRAPP II-specific subunit Trs130 is required for the GEF function of

TRAPP II, it is unknown whether other subunits directly contribute to this catalytic activity. In other words, which subunits are necessary and sufficient to activate Ypt31/32 *in vitro*? Attempts to address this using TRAPP precipitated from yeast lysates have so far proved inconclusive, as many proteins co-purify with any TRAPP subunit. To answer this question, it is essential to reconstitute Trs130-containing complexes using recombinant proteins. So far the size and instability of Trs130 have hindered such efforts. Through improvements in protein expression technology, or use of a more stable Trs130 ortholog, it may become possible to reconstitute TRAPP II *in vitro* and put to rest the debate concerning its GEF activity on Ypt31/32.

A third important question concerns the structure of TRAPP II. While many inter-dependencies among the TRAPP subunits have been found, the precise arrangement of the subunits remains unknown. Dramatic progress was made in our understanding of TRAPP II structure through visualizing TRAPP II complexes by electron microscopy (Yip et al. 2010), but the images could not clearly demonstrate the precise positions of each subunit. The core TRAPP I subunits: Bet3, Bet5, Trs23, and Trs31, are required for membrane attachment and GEF activity on Ypt1. Trs65, Tca17, and Trs120 have all been shown to play a role in the attachment of Trs130, required for GEF activity on Ypt31/32, to the complex. Trs85, the only subunit not in TRAPP II, has been implicated in autophagy. How do the two remaining subunits, Trs33 and Trs20, contribute to TRAPP II structure and function? A better understanding of TRAPP II structure, and the contributions toward that made by individual subunits, will also aid researchers in approaching the questions previously mentioned concerning TRAPP.

## CHAPTER II: TRS33

Most of the data presented in this chapter were published in (Tokarev et al. 2009). I am one of three "co-first authors" of this manuscript. The results were obtained in collaboration with several other researchers. The following list reports each individual's contributions to the results shown in this chapter:

Figure 5:

A: n/a

B: Geetanjali Sundaram

Figure 6 (A-B): Andrei Tokarev

Figure 7 (A-B): David Taussig

Figure 8:

A: Geetanjali Sundaram

B: Jonathan Mulholland

Figure 9: David Taussig

Figure 10: David Taussig

Figure 11:

A: David Taussig

B: Zhanna Lipatova

Figure 12: David Taussig

Figure 13:

A: Andrei Tokarev

B: David Taussig

## A. Introduction

Trs33 was originally identified through mass spectrometry of proteins co-precipitating with Bet3 from yeast lysates (Sacher et al. 1998). As the TRAPP complex became more fully characterized, Trs33 has been reported to be present in all three alternative TRAPP complexes. Its presence in TRAPP I and II was determined by applying a yeast lysate to a gel filtration column, fractionating according to size, and precipitating Bet3 from each fraction to identify other proteins in complex with Bet3. Two distinct peaks of Trs33 were observed, corresponding to sizes of roughly 250 and >750 kDa, which we now consider TRAPP I and II, respectively (Sacher et al. 2001). When TRAPP III was later identified, the presence of Trs33 in this complex was confirmed through co-precipitation of Trs33 with Trs85, the only TRAPP III-specific subunit (Choi et al. 2011).

Crystal structures of the mammalian ortholog of Trs33, which is conserved from yeast to man, in complex with other TRAPP subunits have revealed close structural similarity between Bet3 and Trs33, despite relatively little sequence similarity. Both subunits form globular structures composed of four α-helices and an antiparallel β-sheet. One marked difference, however, is the absence of a hydrophobic channel in Trs33 such as is found in Bet3 (Kim et al. 2005; Kim et al. 2006). This channel is thought to contain a palmitoyl group, thus allowing for the membrane attachment of the TRAPP complex.

The structure and TRAPP complex assignments of Trs33 are known, but its contribution to any TRAPP function has remained unclear. Trs33 is known to interact directly only with its nearest neighbor in TRAPP I, Bet3, based on co-precipitation of recombinant proteins (Kim et al. 2005). Its position in TRAPP I is at the end of the molecule opposite Trs20, which is present at the other end (Kim et al. 2006) (illustrated in Figure 4). Trs33 co-precipitates efficiently with

recombinant core TRAPP I (Bet5, Trs23, Trs31, and Bet3), but has no effect on the latter's GEF activity on Ypt1, suggesting that it plays no role in this function (Kim et al. 2006). Furthermore, it has not been reported to contribute to any tethering function of TRAPP I.

While the physical direct-interacting partners of Trs33 have given no clue regarding its function, it has been found to interact genetically with many other genes. *TRS33* is non-essential in yeast, and its deletion reveals no apparent growth defect. However, as illustrated in Figure 5A, *TRS33* exhibits synthetic lethality with other genes, including: *PIK1*, *SEC14*, *DRS2*, and *TRS65*. All four of these genes are related to secretory traffic at the trans-Golgi, suggesting that Trs33 may have a function in that process. Furthermore, over-expression of a constitutively active form of Ypt31, Ypt31Q72L, suppresses the lethality of a *trs33Δ/trs65Δ* strain (Sciorra et al. 2005), implicating both Trs33 and Trs65 in a pathway under the control of Ypt31/32—namely, post-Golgi protein transport.

As mentioned in Chapter 1, *TRS65* was shown to interact genetically with the other TRAPP II-specific subunits, *TRS120* and *TRS130*. Furthermore, it was shown to play a role in TRAPP II stability, as the attachment of the essential subunits Trs120 and Trs130 to a Bet5-containing complex was diminished in a *trs65Δ* strain (Liang et al. 2007). In this chapter I present evidence that Trs33 functions in a manner similar to Trs65, and as such plays an important role in stabilizing the TRAPP II complex.

## B. Results

### 1. Trs33 is similar to Trs65N

*TRS33* and *TRS65*, both non-essential genes in yeast, exhibit synthetic lethality when both genes are deleted (Figure 5A). Based on this observation, we investigated both TRAPP

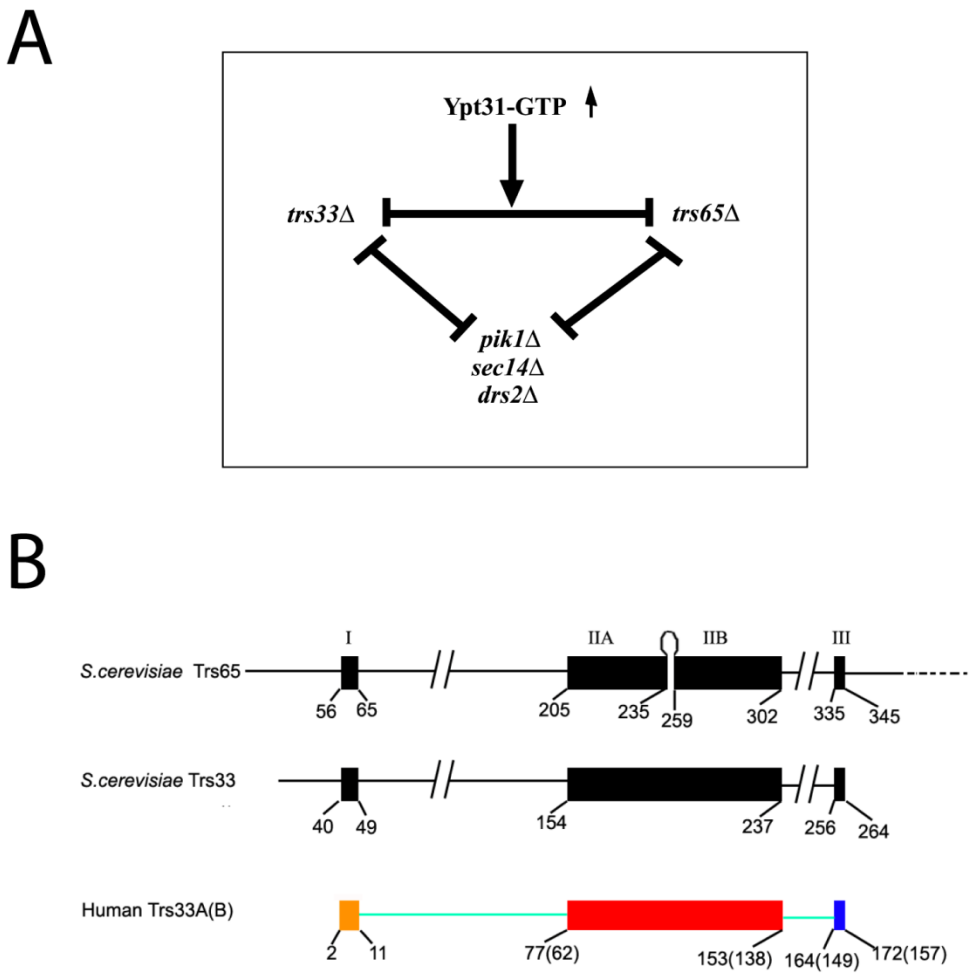


**Figure 5: Trs33 is structurally similar to Trs65N. A)** Summary of genetic interactions. *TRS65* exhibits synthetic lethality (illustrated with flat-head lines) with *TRS33*, and each of these with the trans-Golgi associated proteins *PIK1*, *SEC14*, and *DRS2*. The Ypt31-GTP arrows denote that *trs33Δ/trs65Δ* lethality can be rescued through over-expression of a GTP-locked form of Ypt31 (Sciorra et al. 2005).
**B)** Amino acid alignment of the amino-terminus of Trs65 with the yeast and human versions of Trs33, using $CLUSTALW_{2,}$ reveal highly conserved regions, implying a functional similarity between Trs65 and Trs33. Regions which are highly conserved in amino acid sequence are depicted as broad lines, and labeled with a domain assignment of I, IIA, IIB, or III. The numbers below each line represent amino acid number for each protein.

subunits in more detail, to see if any structural or functional similarities could be found. Indeed, an amino acid sequence alignment of Trs33 and Trs65 revealed that portions of Trs33 aligned closely with the N-terminal half of Trs65. Furthermore, these homologous regions were also conserved with *TRAPPC6*, the human ortholog of Trs33 (Figure 5B). This suggests a functional similarity between Trs65 and Trs33, since highly conserved regions generally indicate functional importance.

Previously it had been shown that Trs65 was important for the stability of TRAPP II—specifically, the attachment of Trs120 and Trs130 to the complex (Liang et al. 2007). In that study it was reported that Trs65 interacts directly with Trs120 and Trs130, and deletion of *TRS65*, coupled with manipulation of *TRS130* and *TRS120* on the chromosome, resulted in a temperature sensitive strain, hereafter referred to as *trs65ts*.

Since the portions of Trs65 which aligned with Trs33 were in the N-terminal half of Trs65 (Trs65N), we tested to see whether this half alone accounted for the defects observed in *trs65ts*. Full-length Trs65 and Trs65N, but not the C-terminal half (Trs65C), were found to interact with both Trs120 and Trs130 in a yeast 2-hybrid assay (Figure 6A). Furthermore, over-expression of Trs65N, but not Trs65C, from a 2 μ plasmid suppressed the temperature sensitive growth defect observed in *trs65ts* (Figure 6B). Together, these findings strongly suggest that the region of Trs65 responsible for TRAPP II stability lies in the N-terminal half of the protein, which is structurally similar to Trs33.

**2. *TRS33* interacts genetically with *TRS120* and *TRS130***

To investigate whether Trs33, like Trs65, plays a functional role in TRAPP II, genetic relationships between *TRS33* and the genes encoding other TRAPP II-specific subunits were

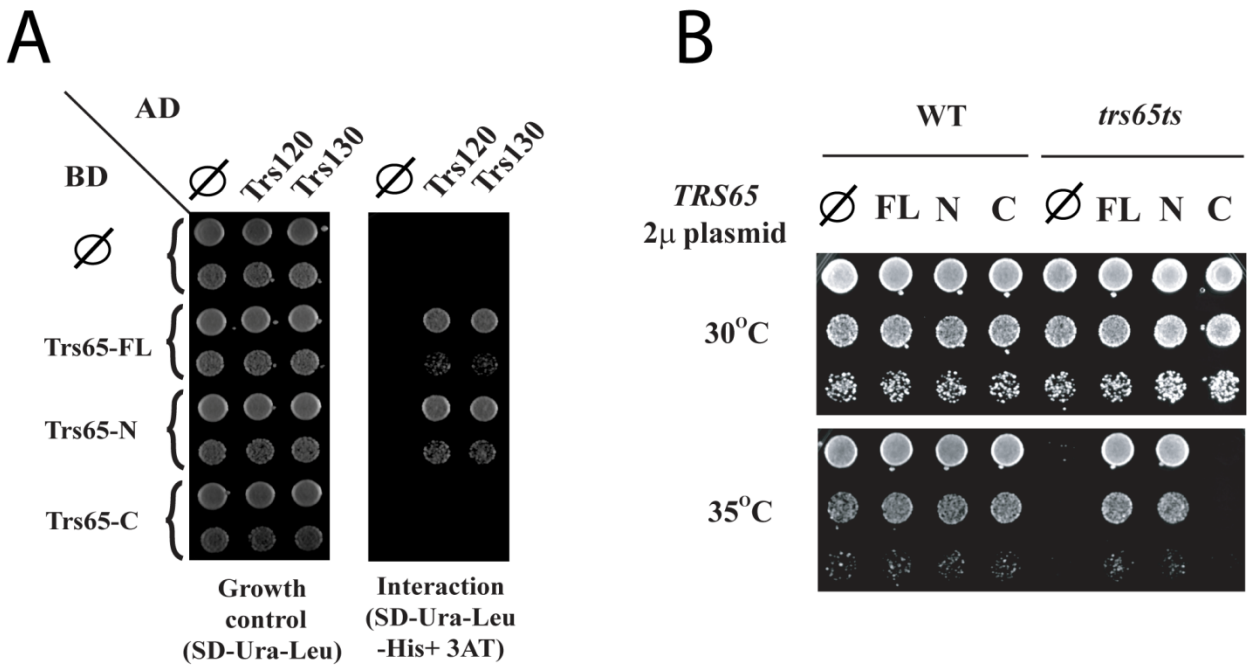


**Figure 6: The amino-terminus of Trs65 is sufficient for its interactions and function.** **A)** Yeast 2-hybrid assay testing interaction between Trs65 full length (FL), N, or C with TRAPP II subunits Trs120 and Trs130. Growth on the interaction plate (right panel) reveals that Trs65FL and Trs65N, but not Trs65C, interact with Trs120 and Trs130 (for A and B, rows represent 10-fold serial dilutions, top to bottom).
**B)** Over-expression of TRS65-N suppresses the temperature sensitive phenotype in *trs65ts*. Empty 2μ plasmid (θ), or plasmid containing TRS65-N, C, or FL, were transformed into wild type (NSY1176) and *trs65ts* (NSY1177) strains, which were plated at permissive (30° C) or restrictive (35° C) temperatures on synthetic dextrose (SD) plates. Growth of the *trs65ts* yeast at 35° C (lower panel, right side), shows that TRS65-N or TRS65-FL, but not TRS65-C over-expression, complements the *trs65ts* growth defect.

explored. *TRS120* and *TRS130* were endogenously tagged with myc and HA epitopes, respectively, either individually or together. As alluded to above, it was previously reported that deletion of *TRS65* causes a temperature sensitive growth phenotype in a *TRS120*-myc/*TRS130*-HA strain (Liang et al. 2007).

Significantly, deletion of *TRS33* from either *TRS120*-myc or *TRS130*-HA yeast strains resulted in a severe temperature sensitive defect (Figure 7A). Furthermore, deletion of *TRS33* from a combined *TRS120*-myc/*TRS130*-HA strain proved lethal, as this strain could survive only with exogenously-expressed wild type *TRS130* (Figure 7B). Thus, *TRS33* deletion is similar to but more severe than deletion of *TRS65*, and genetic interactions of *TRS33* with *TRS130* and *TRS120* implicate Trs33 in a TRAPP II-specific function.

**3. *TRS33* deletion affects secretion and cell morphology**

To further characterize the effect of *TRS33* deletion, we assayed the *TRS130*-HA/*trs33Δ* strain (*trs33ts*) for defects in the secretory pathway. Including *trs65ts* in parallel, the secretion of radio-labeled Hsp150 from wild type and mutant cells was detected and quantified (Figure 8A). The secretion of Hsp150 from *trs33ts* cells was found to be 50% lower than its conjugate wild type. Interestingly, *trs65ts* also showed a significant, but diminished defect in secretion, further suggesting that deletion of *TRS33* results in similar but more severe phenotypes compared with the deletion of *TRS65*.

Defects in intra-cellular transport often cause the accumulation of aberrant structures in the cell. Wild type cells, along with *trs33ts*, were subjected to electron microscopy (EM) in order to analyze cell morphology in each strain. EM analysis revealed abnormal structures in the *trs33ts* cells, when compared with wild type (Figure 8B). These structures slightly accumulated

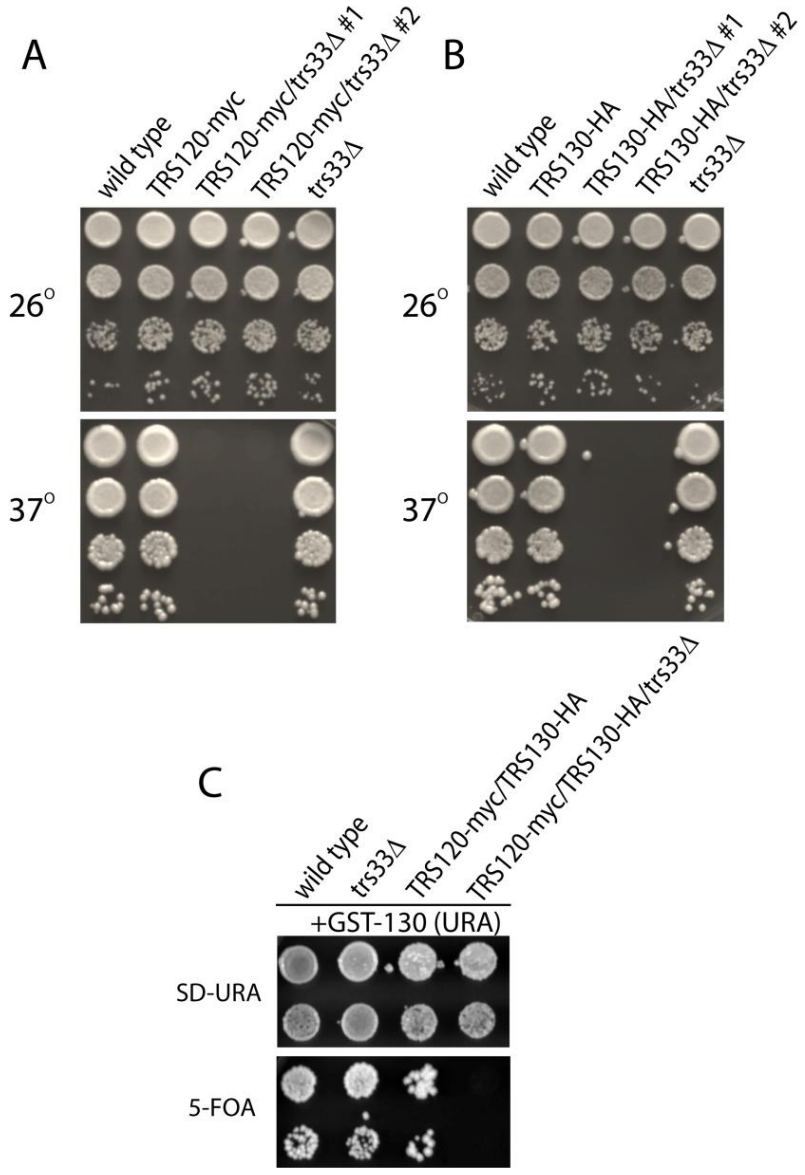


**Figure 7: *TRS33* interacts genetically with TRS120 and TRS130.**

**A)** Growth assay of wild type (NSY825), *TRS120*-myc (NSY1040), *trs33Δ* (NSY1196), or *TRS120*-myc/*trs33Δ* (NSY1429). Cells were plated on rich medium at 26° C and 37° C. While neither *trs33Δ* nor TRS120-myc exhibited a growth defect at 37° C, both independent *TRS120*-myc/*trs33Δ* strains failed to grow at restrictive temperature (bottom panel), indicating genetic interaction between *TRS33* and *TRS120*. For A-C, rows represent 10-fold serial dilutions top to bottom.

**B)** Same as in (A), but *TRS130*-HA instead of *TRS120*-myc. (NSY991 and NSY1430).

**C)** *TRS33* deletion causes lethality in TRS120-myc/TRS130-HA yeast. GST-TRS130, on a URA3 plasmid, was transformed into wild type (NSY825) and *TRS120*-myc/*TRS130*-HA (NSY1176) yeast strains. *TRS33* was then deleted in each strain, and the resulting *trs33Δ* strains were plated, alongside the original yeast, on SD-URA or 5-FOA-containing medium. While wild type, *trs33Δ*, and TRS120-myc/TRS130-HA grew in the presence of 5-FOA, TRS120-myc/TRS130-HA/*trs33Δ* (NSY1431) failed to grow, indicating lethality in the absence of GST-TRS130.

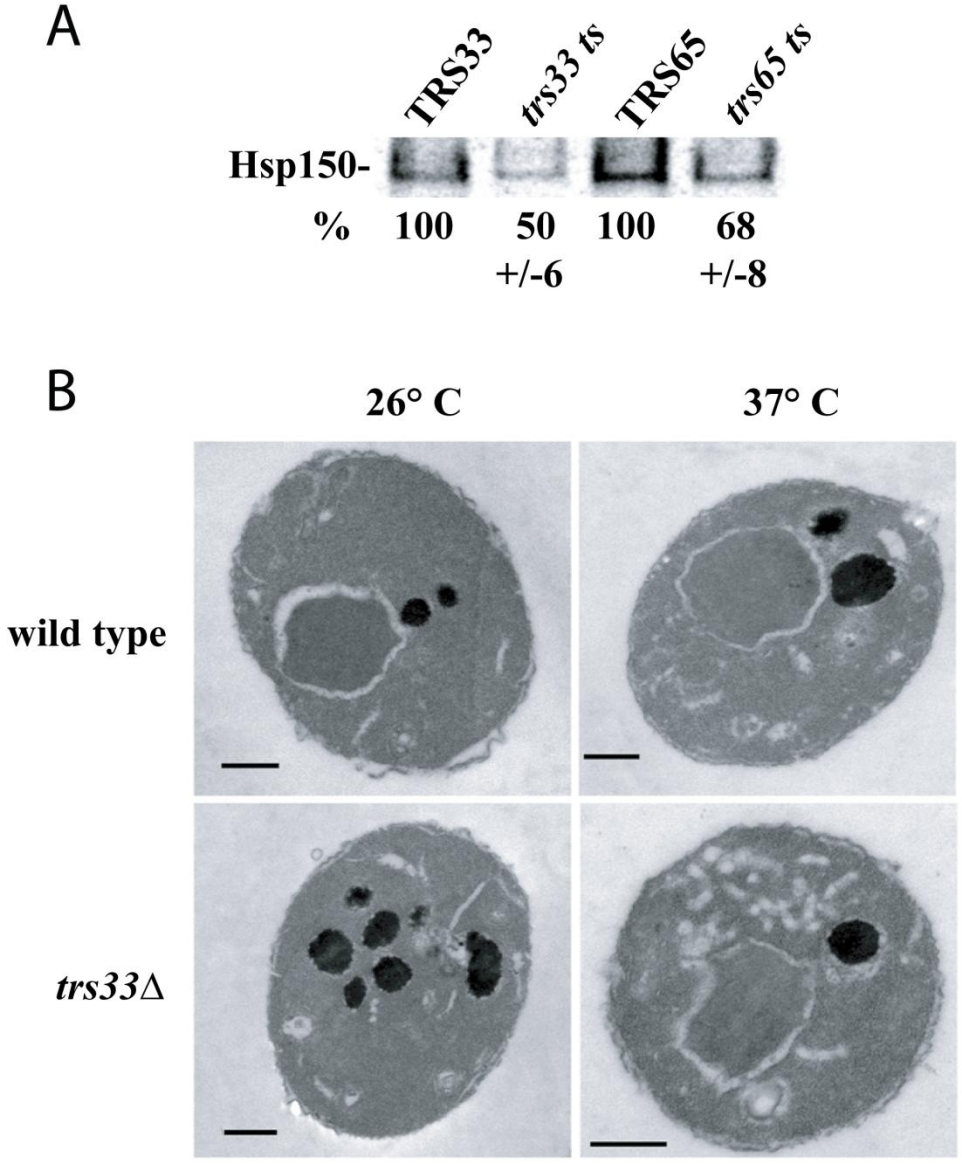


**Figure 8: *TRS33* deletion causes secretory defects and aberrant cellular morphology. A)** Secretion assay in *trs33ts* (NSY1430), *trs65ts* (NSY1177), and their conjugate wild type strains (NSY991 and 1176, respectively). Cells were incubated in $^{35}$S-containing medium, followed by collection of secreted proteins. The levels of Hsp150 secreted into the medium from each strain were quantified, and are shown beneath the radio-blot as percentages relative to the wild type strains. **B)** Electron micrographs (EM) showing vesicle accumulation in *trs33ts* cells, even at the permissive temperature. Wild type and *trs33ts* cells (designated on the left) were incubated at the indicated temperature for 90 minutes, followed by fixation and processing for EM. Representative cells are shown. Scale bar, 1 μm.

at the permissive temperature, but much more after shifting to restrictive temperature, implying that these structures are indeed the result of the *TRS33* deletion, which causes temperature sensitivity. Moreover, these structures are reminiscent of those reported to accumulate in *trs65ts* (Liang et al. 2007) and *ypt31Δ/32ts* (Jedd et al. 1997) yeast cells, suggesting that like Trs65 and the Rab GTPases activated by TRAPP II, Trs33 also plays an important role in trans-Golgi associated traffic.

**4. Deletion of *TRS33* compromises TRAPP II integrity**

It has been previously shown that GST-Bet5, over expressed in wild type yeast lysates, efficiently co-precipitates endogenously tagged Trs130-HA and Trs120-myc (Morozova et al. 2006). To determine if deletion of *TRS33*, as was previously shown for *TRS65* (Liang et al. 2007), affects the co-precipitation of Trs130 or Trs120 with Bet5, the assay was conducted in *trs33ts*, *TRS120*-myc/*trs33Δ*, and their conjugate wild type strains (Figure 9).

Strikingly, the amount of Trs130 co-precipitating with GST-Bet5, was significantly lower in *trs33ts* than the wild type strain. Furthermore the steady-state level of Trs130-HA in the *trs33ts* lysate was lower than that of the wild type strain. The reason for this has not been conclusively shown, but it most likely due to an intrinsic instability of unbound Trs130—that is, Trs130 not incorporated into the TRAPP II complex. However, the level of Trs120-myc, both in the lysate and co-precipitating with GST-Bet5, was not affected with the deletion of *TRS33*, indicating that Trs120 can still bind to TRAPP efficiently in the absence of Trs33 (Figure 9).

To further test our hypothesis that the attachment of Trs130 to TRAPP is diminished in the absence of Trs33, the localization of Trs130-GFP in wild type and *trs33Δ* strains was analyzed. Through live-cell deconvolution microscopy, it was determined that while Trs130-GFP

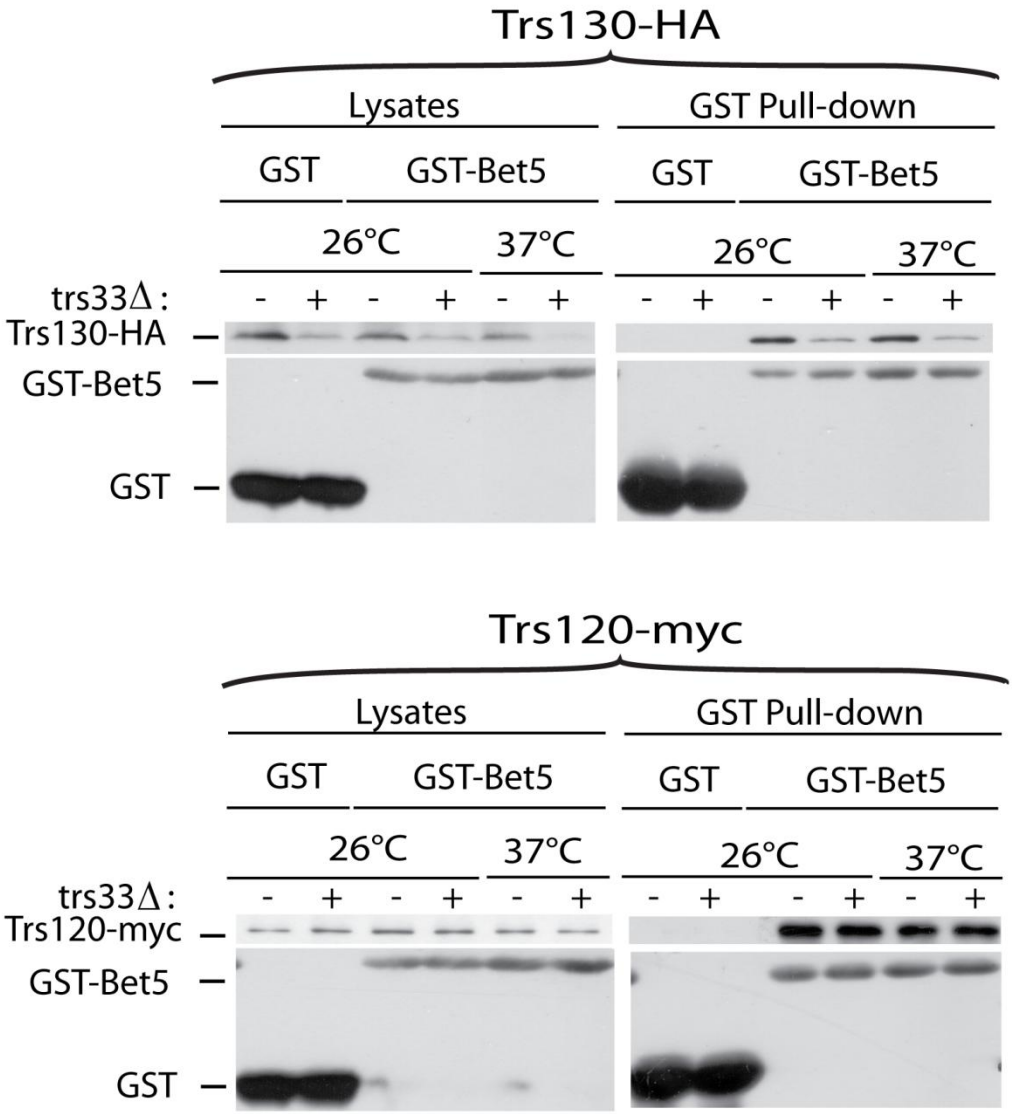


**Figure 9: *TRS33* deletion inhibits binding of Trs130 to TRAPP.** Plasmids encoding GST-Bet5 or GST, as a negative control, were transformed into TRS130-HA (NSY991, upper panels), TRS120-myc (NSY1040, lower panels), and each of these with *trs33Δ* (NSY1430, NSY1429, respectively), as indicated. Cells were grown continually at 26° C, or shifted to 37° C for 2 hours, after which they were harvested and lysed using physical disruption. Lysates were applied to glutathione resin to precipitate GST-Bet5-containing complexes. Lysate samples (left panels) and pull-downs (right panels) were analyzed by Western blotting using α-GST, α-myc, or α-HA antibodies. The lysate levels of Trs130-HA, as well as its co-precipitation with GST-Bet5, were significantly lower in *trs33Δ*, at both 26° C and 37° C temperatures. In contrast, the lysate and co-precipitation levels of Trs120-myc (lower panels) were not affected by *TRS33* deletion.

appears as puncta in wild type cells, largely co-localizing with the trans-Golgi marker Sec7, the appearance of Trs130-GFP in *trs33Δ* was markedly diffuse compared with the wild type pattern (Figure 10). However, the localization of the trans-Golgi marker Sec7 was unaffected, indicating that the defect caused by *TRS33* deletion lies in TRAPP II structure, and not overall Golgi morphology.

**5. Trs33 is associated with Ypt31/32 function**

As described above, TRAPP II functions as a GEF on Ypt31/32 (Jones et al. 2000), and the TRAPP II-specific subunit Trs130 is required for this activity (Morozova et al. 2006). Since TRAPP purified from *trs33ts* contains a lower amount of Trs130 (Figure 9), we postulated that this TRAPP will also have diminished GEF activity on Ypt32. To test this hypothesis, we purified complexes bound to GST-Bet5, or GST alone as a negative control, from wild type and *trs33ts*, and used these products in a GDP-release assay on Ypt32 and Ypt1. Indeed, the Ypt32 GEF activity, measured by the rate GDP-release, of TRAPP purified from *trs33ts* was significantly lower than that purified from the wild type strain (Figure 11A), demonstrating a defect in the GEF function of TRAPP II in *trs33ts*. As expected, the GEF activity of TRAPP on Ypt1 was unaffected in *trs33ts*, consistent with the idea that neither Trs33 nor Trs130 plays a role in Ypt1 GEF activity.

The growth phenotypes of mutant strains deficient in TRAPP II GEF activity, including *trs130ts* and *trs120Δ*, can be suppressed by the over-expression of Ypt31 from a 2 μ plasmid (Morozova et al. 2006). To further explore the relationship between Trs33 and Ypt31/32, we tested whether Ypt31 over-expression could suppress the temperature sensitive growth phenotype observed in *trs33ts*. As shown in Figure 11B, over-expression of Ypt31, but not Ypt1,

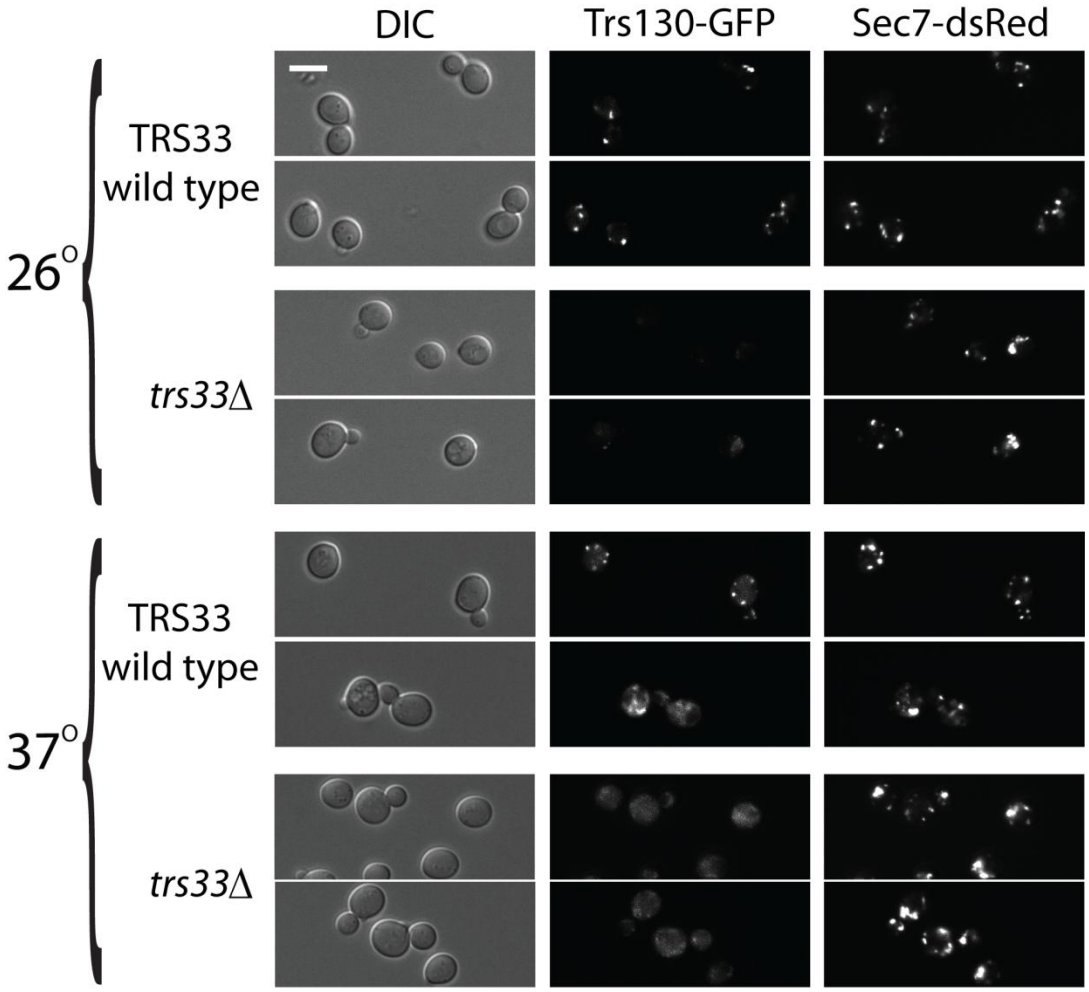


**Figure 10: Trs130-GFP is diffuse in *trs33Δ*.** A yeast strain with endogenously-tagged Trs130-GFP and Sec7-dsRed (NSY1316), or this strain with *TRS33* deleted (NSY1432), was grown at 26° C, or shifted to 37° C for 90 minutes, followed by live-cell deconvolution microscopy. The left panels show DIC images, the right panels the trans-Golgi marker Sec7-dsRed, and the middle show Trs130-GFP. Like other TRAPP II subunits (Cai et al. 2005), Trs130-GFP in wild type cells appears as discrete puncta, which co-localize largely with Sec7-dsRed. In contrast, the Trs130-GFP, but not the Sec7-dsRed, appears strikingly diffuse at both temperatures in *trs33Δ*. Scale bar, 5 μm.

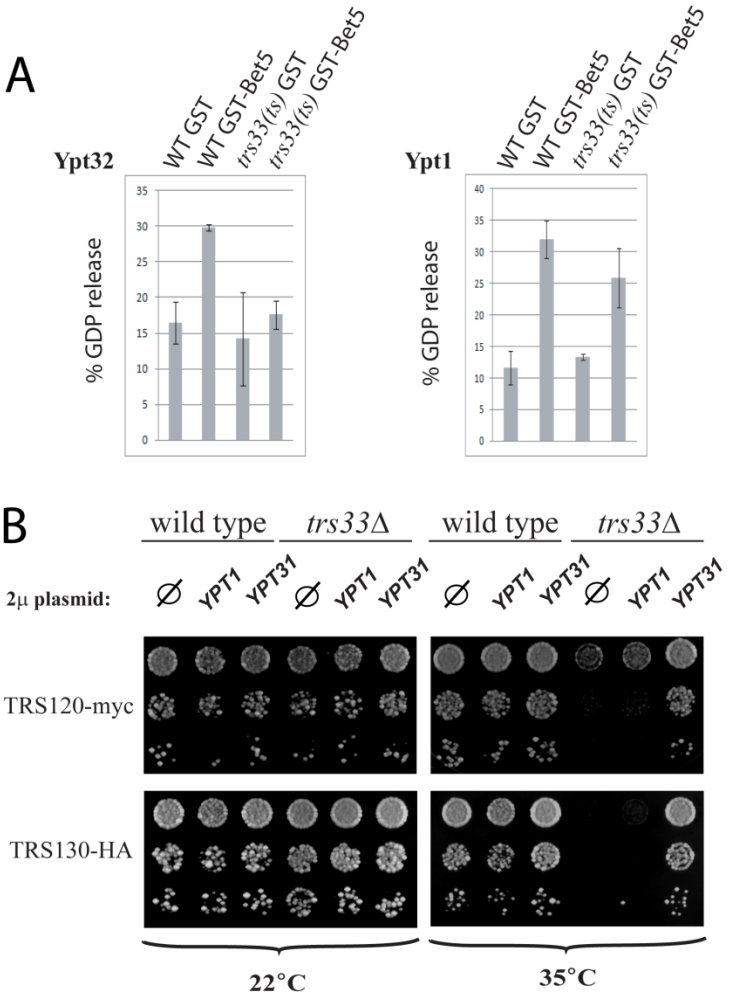


**Figure 11: Trs33 contributes to Ypt31/32 function. A)** TRAPP purified from *trs33Δ* cells demonstrate reduced GEF activity on Ypt32, but not Ypt1. GST-Bet5-containing complexes, or GST as a negative control, were purified from *TRS130*-HA (NSY991) or TRS130-HA/*trs33Δ* (*trs33ts*, NSY1430), after shifting cells to 37° C for 90 minutes. The purified TRAPP complexes were then subjected to GDP-release assays on purified, recombinant Ypt32 (left), or Ypt1 (right). The percent of radio-labeled GDP released from each Ypt after 40 minutes was calculated, and designated in the corresponding graph. Error bars represent standard deviation. **B)** Ypt31, but not Ypt1, complements the temperature sensitive growth defect in *trs33Δ* cells. 2 μ plasmids encoding Ypt1, Ypt31, or empty vector (θ), as a negative control, were transformed into *TRS120*-myc upper panels) or *TRS130*-HA (lower panels) wild type (NSY1040, 991, respectively) and *trs33Δ* (NSY1429, 1430, respectively) cells. Strains were then spotted on synthetic media at 22° C (left panels), for growth control, or 35° C (right panels). Rows represent 10-fold serial dilutions, top to bottom.

dramatically restores growth of *trs33ts* at 35° C, providing evidence that Trs33 functions primarily in a Ypt31/32-dependent pathway.

**6. Trs33 and Trs65 are present on the same complex**

Since *trs33ts* and *trs65ts* exhibit similar phenotypes, and are individually non-essential in yeast, we considered the possibility that Trs65 and Trs33 are functionally redundant. In other words, a TRAPP complex may need either Trs33 or Trs65, but have no use for both. While Trs33 and Trs65 both co-precipitated with Bet3 from yeast lysates (Sacher et al. 2000), it remained possible these proteins never exist on the same TRAPP complex.

To address this hypothesis a co-precipitation analysis was carried out from yeast cells expressing Trs65-YFP from the chromosome, and GST-Trs33, GST-Bet5, GST-Sec2, or GST alone on a plasmid. After binding the lysates to glutathione resin, Trs65-YFP was found to co-precipitate specifically with GST-Trs33, as well as positive control GST-Bet5, but not GST or GST-Sec2, used as negative controls (Figure 12).

**7. Trs33 interacts directly with Trs120**

Having established that Trs33 is important for TRAPP II stability, we next investigated whether Trs33 interacts directly with any TRAPP II-specific subunits. A yeast 2-hybrid assay revealed interaction between Trs33 and Trs120 (Figure 13A). However, Trs33 did not interact with Trs65 or Trs130 in this assay, suggesting that its contribution to TRAPP II structure occurs through its interaction with Trs120.

To confirm this interaction, recombinant GST-Trs33 and $His_6$-Trs120 were cloned into bacterial expression vectors, for pull-down analysis. Indeed, Trs120, but not Calmodulin-HA,

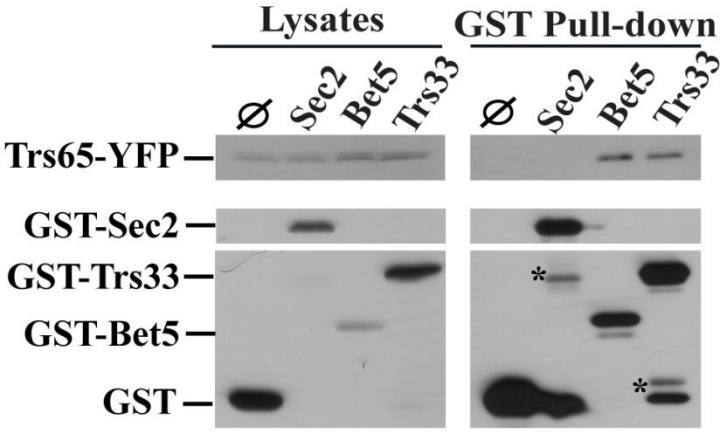


**Figure 12: Trs33 and Trs65 co-precipitate from yeast lysates.**
Vectors expressing GST-Trs33, GST-Bet5, GST-Sec2, or GST alone were transformed into a yeast strain with endogenously-tagged *TRS65*-YFP (NSY1179). After induction of GST-protein expression, cells were harvested and lysed. Cell lysates were applied to glutathione resin to precipitate GST-containing complexes. Lysate (left panels) and pull-down (right panels) samples were probed with α-GFP or α-GST antibodies by Western blotting. As seen in the upper right panel, Trs65-YFP co-precipitates with GST-Trs33 as well as positive control GST-Bet5, but not with negative controls GST-Sec2 or GST alone. Asterisks designate bands caused by mild degradation of GST-Sec2 and GST-Trs33.

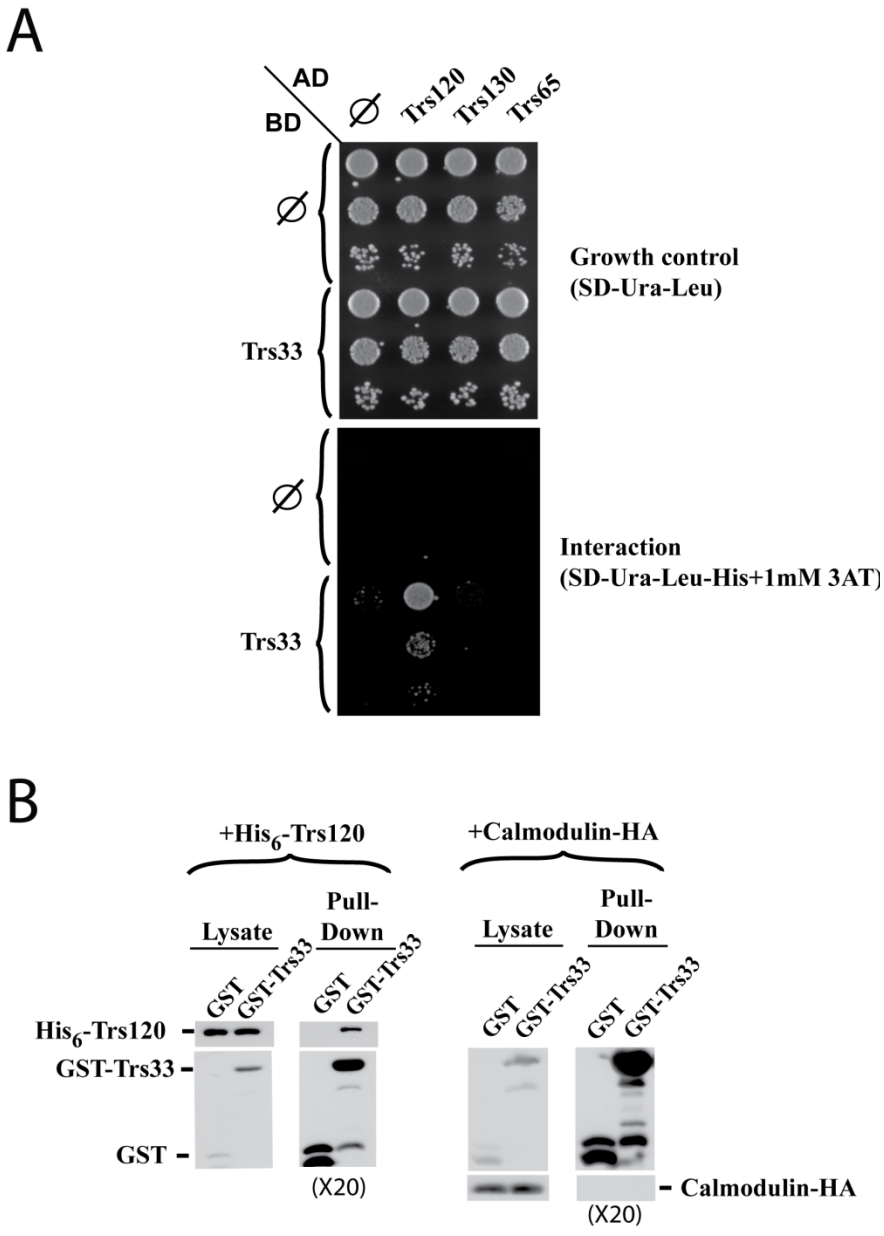


**Figure 13: Trs33 interacts directly with Trs120. A)** Trs33 was cloned into a GAL4 binding domain (BD) vector, and co-transformed with either Trs120, Trs130, or Trs65 fused to the activation domain (AD). As demonstrated by growth on the interaction plate (lower panel), Trs33, but not empty binding domain (θ), interacts specifically with Trs120.

**B)** Plasmids encoding recombinant GST-Trs33 or GST alone were co-transformed with either $His_6$-Trs120 or Calmodulin-HA, as indicated, into *E. coli* for protein expression. Lysates were applied to glutathione resin to precipitate GST-Trs33 and its interacting partners. After washing, bound proteins were detected by Western blotting using α-GST, α-$His_6$, and α-HA antibodies. Lysate samples (5%) are shown to the left of pull-down samples. As seen in the GST-Trs33 pull-down lanes, GST-Trs33 co-precipitated $His_6$-Trs120 but not Calmodulin-HA

used as a negative control, pulled down with GST-Trs33 on glutathione resin (Figure 13B), further supporting a claim of direct interaction between Trs33 and Trs120.

**C. Conclusions**

Together, these results strongly implicate Trs33 in TRAPP II structure and function. This is based upon genetic interactions of *TRS33* with TRAPP II-specific subunits (Figure 7), the defective attachment of Trs130 in *trs33ts* (Figures 9, 10), and the relationship established between Trs33 and Ypt31/32, for which TRAPP II acts as a GEF (Figure 11). Significantly, Trs33 deletion had no effect upon Ypt1 function, despite being considered as a TRAPP I subunit.

Interestingly, while Trs33 primarily affects the attachment of Trs130 to the TRAPP II complex, it interacts directly with Trs120, not Trs130 (Figure 13). Thus, two conclusions can be made. First, Trs120 has a separate point of attachment to the TRAPP complex, as its binding to TRAPP is retained upon *TRS33* deletion. Second, the folding or orientation of Trs120 on TRAPP II is altered in the absence of Trs33, such that the binding of Trs130 to TRAPP is diminished.

Finally, Trs33 is structurally similar to the N-terminal portion of Trs65 (Figures 5, 6). Reflective of this observation, the phenotypes of *trs33ts* are similar to those observed in *trs65ts* (Liang et al. 2007). However, their contributions to TRAPP structure and function are distinct, as Trs33 and Trs65 exist together on the TRAPP II complex (Figure 12), and do not directly interact (Figure 13).

## CHAPTER III: TRS20

The data presented in this chapter were recently published (Taussig et al. 2013). I am the first of five authors of the manuscript. The following list is a report of each individual's contributions to the results shown in this chapter:

Figure 14 (A-B): David Taussig

Figure 15 (A-B): David Taussig

Figure 16: David Taussig

Figure 17 (A-B): David Taussig

Figure 18

A: n/a

B: XiuQi Zhang

Figure 19:

A: XiuQi Zhang

B: David Taussig

Figure 20:

A: n/a

B: Zhanna Lipatova

C: David Taussig

D: David Taussig

E: Jane Kim

## A. Introduction

Like Trs33, Trs20 was identified as a TRAPP subunit through co-precipitation with Bet3 (Sacher et al. 1998), and is considered a member of all three TRAPP complexes (Sacher et al. 2001; Choi et al. 2011). Also like Trs33, though it is considered a TRAPP I subunit, Trs20 is not required for the GEF activity of TRAPP I (Kim et al. 2006).

However, there are several significant differences between Trs33 and Trs20. One important difference is that while *TRS33* can be deleted in wild type yeast yielding no apparent growth defect, *TRS20* is essential to viability. Furthermore, based on a composite of crystal structures of TRAPP I subunits, Trs20 and Trs33 are found on opposite ends of the TRAPP I complex (Figure 4). Thirdly, the mammalian homolog of Trs20, Sedlin, is associated with a human disease. Lastly, Sedlin has been reported to interact with several proteins outside of TRAPP I. Each of these differences will be discussed in more detail here.

Firstly, Trs20 is essential. The highly conserved Sedlin can replace Trs20 in yeast (Gecz et al. 2003), suggesting functional similarity from yeast to humans. A temperature sensitive allele of *TRS20* (*trs20ts*) was constructed in yeast (Scrivens et al. 2009), which can be used to study the function of this protein *in vivo*. Among the TRAPP subunits, only over-expression of Trs120 was found to significantly suppress the growth defect of *trs20ts*. The *trs20ts* allele, in a strain provided by M. Sacher (Concordia University), was a tool used for many of the experiments presented in this chapter.

Crystal structures of mammalian Sedlin have been solved both individually (Jang et al. 2002) and in complex with Bet3 and Trs31, its neighbors in TRAPP I (Kim et al. 2006). Sedlin, 140 amino acids in length, is composed of an anti-parallel β-sheet surrounded by 3 α-helices. One important feature of its structure is the presence of several hydrophobic grooves along the

solvent-accessible region of the protein, suggested as likely binding sites for protein-protein interactions (Jang et al. 2002). Beyond this, Sedlin possesses no strongly conserved domains assigned to any known function. Among TRAPP subunits, its structure is most similar to Bet5, Trs23, and Tca17. Bet3, Trs31, and Trs33 form the other structurally similar group (Kim et al. 2006).

Another key characteristic of Trs20/Sedlin is its direct association with human disease. As briefly alluded to in Chapter 1, mutations in Sedlin have been linked to the cartilage-specific disorder SEDT (Gedeon et al. 1999). The majority of these are nonsense or splicing-site mutations, resulting in truncated protein. However, there are four Sedlin missense mutations reported to cause SEDT: S73L, F83S, V130D, and D47Y (Gedeon et al. 2001; Grunebaum et al. 2001; Fiedler et al. 2004). Of these, the first three residues lie within the internal region of Sedlin, and are thought to disrupt proper folding of the protein. The fourth, D47Y, lies on the surface and likely impairs a specific protein-protein interaction (Jang et al. 2002).

Due to its role in human disease, Sedlin has been the subject of much investigation. As a TRAPP I subunit, Sedlin has been suggested to function in ER-Golgi transport, the accepted function of TRAPP I. However, Sedlin has also been localized to the nucleus (Jeyabalan et al. 2010), and most recently, to ER exit sites (Venditti et al. 2012), where it was shown to play a role in the export of large cargo, including collagen, from the ER.

In addition to its TRAPP I partners TRAPPC3 and TRAPPC5, the human orthologs of Bet3 and Trs31, Sedlin has been shown to interact with several partners acting in pathways not typically associated with TRAPP. These including transcription factor MBP-1 (Ghosh et al. 2001), cytoplasmic chloride channels CLIC1 and CLIC2 (Fan et al. 2003), and resident nuclear protein PAM14 (Liu et al. 2010). The study associating Sedlin with ER exit, mentioned above,

reported that Sedlin acts in this pathway through interactions with the trans-membrane collagen receptor TANGO1 and the Sar1 GTPase, which controls vesicle budding from the ER (Venditti et al. 2012).

Based on the variety of reports connecting Sedlin, but not other TRAPP subunits, with pathways which to date have not been associated with TRAPP, it is possible that Sedlin has functions beyond that of the TRAPP complex. While it is clear that SEDT symptoms arise from compromised Sedlin function, it remains unknown precisely which Sedlin-associated pathway is connected with the SEDT disease.

In this chapter, I present evidence that Trs20 plays a crucial role in TRAPP II assembly, through interaction with Trs120. Furthermore, a mutation analogous to the disease-causing D47Y mutation results in a loss of interaction between Trs20 and Trs120, suggesting that impaired TRAPP structure may be a root cause of SEDT.

## B. Results

### 1. Binding of recombinant Trs120 to TRAPP requires Trs20

It was previously reported that Trs120 was required for the interaction of Trs130 with TRAPP (Morozova et al. 2006). Based on this, as well as interaction of Trs33 with Trs120, demonstrated in Chapter 2, it follows that Trs120 must be the bridge between TRAPP I and Trs130, and interact closely with TRAPP I. However, while recombinant core TRAPP I (GST-Bet5, Trs23-S, Trs31-myc, and Bet3-MBP), co-precipitates efficiently on glutathione resin, this complex fails to recruit recombinant $His_6$-Trs120 (Figure 14A, lane 6).

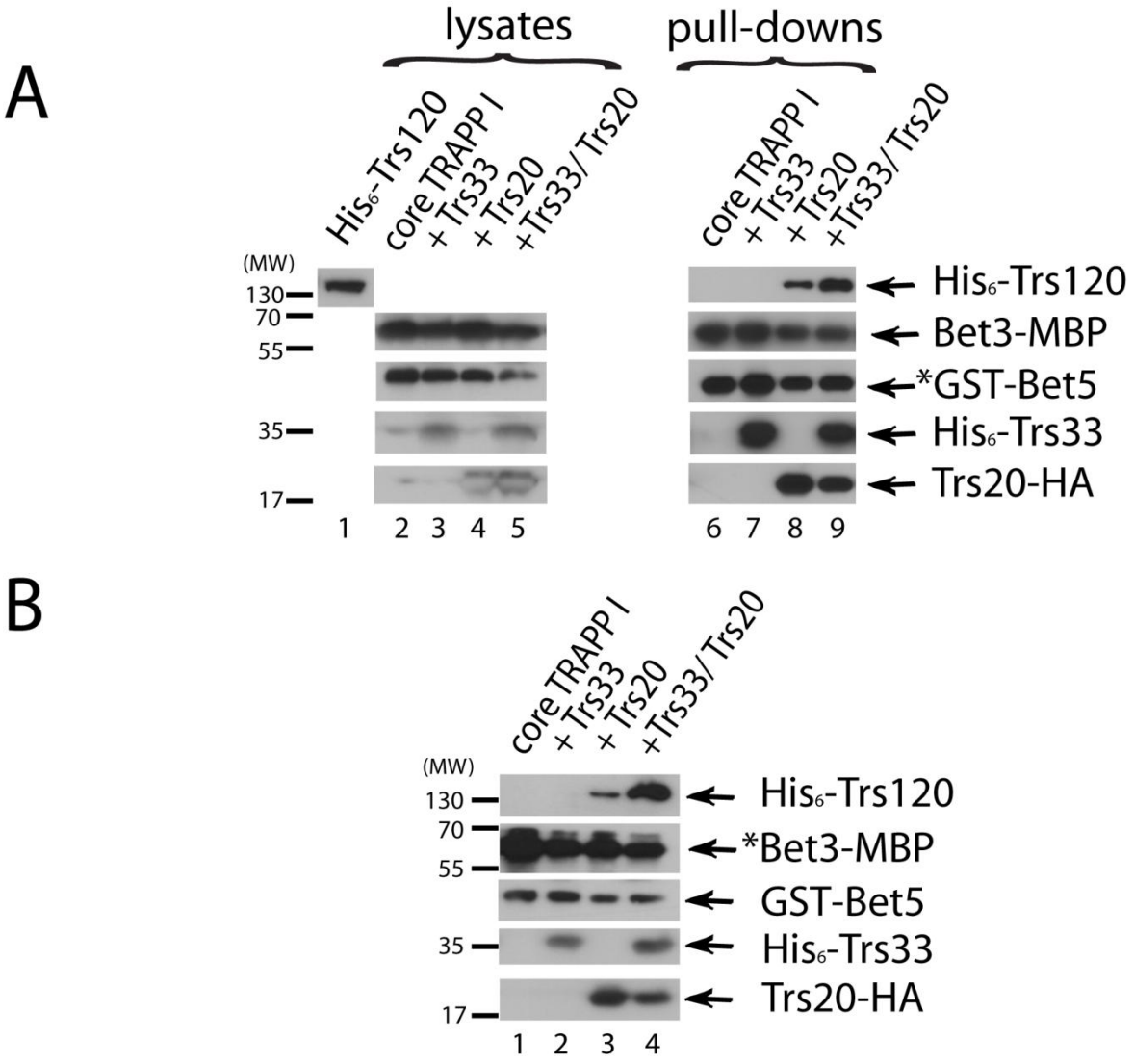


**Figure 14: Trs20 is required for the interaction of $His_6$-Trs120 with recombinant TRAPP I.** **A)** Recombinant core TRAPP I subunits (GST-Bet5, Bet3-MBP, Trs23-S, Trs31-myc) were co-expressed alone or with $His_6$-Trs33, Trs20-HA, or both. Following precipitation of these sub-complexes onto glutathione resin via GST-Bet5, lysate containing $His_6$-Trs120 was incubated with each, to measure co-precipitation of Trs120 with TRAPP I. Western blotting revealed that Trs120 was pulled down by TRAPP I only in the presence of Trs20 (≈5% - lane 8), while the addition of Trs33 along with Trs20 increased co-precipitation 2-fold (≈10% - lane 9).
**B)** Same as in A, but TRAPP I was precipitated onto amylose resin, through the MBP tag fused to Bet3. Lysates were the same for both experiments, and shown in the left panels of part A. Asterisks designate for each experiment the protein being directly pulled down onto the affinity resin.

To circumvent this problem, we first attempted adding recombinant $His_6$-Trs33 to the core TRAPP I subunits. Even though Trs33 alone interacts directly with Trs120 when co-expressed (Figure 13B), the addition of Trs33 to core TRAPP I was not sufficient to co-precipitate Trs120 (Figure 14A, lane 7). Next we tried adding Trs20-HA to core TRAPP I, with or without Trs33. Surprisingly, the addition of Trs20 to the experiment promoted binding of Trs120 to TRAPP I, even without Trs33 (lane 8). Moreover, the precipitation of Trs120 increased ≈2-fold when both Trs20 and Trs33 were present (lane 9), consistent with the earlier reported interaction between Trs33 and Trs120. To approach the same experiment in a different way, the MBP tag on Bet3 was utilized to precipitate the TRAPP subunits onto amylose resin, with the same results (Figure 14B).

**2. TRAPP II integrity is impaired in *trs20ts***

With the ambition of studying the role of Trs20 *in vivo*, we obtained a strain carrying a temperature sensitive allele of *TRS20* (*trs20ts*) from M. Sacher (Scrivens et al. 2009). In order to analyze the effects of defective Trs20 on TRAPP II structure, this allele was combined with strains expressing endogenously-tagged *TRS130*-HA or *TRS120*-myc. Similar to the experiment described earlier for *trs33ts* (Figure 10), TRAPP was precipitated from these strains, along with their wild type counterparts, via over-expression of GST-Bet5 and glutathione resin.

Significantly, both Trs120-myc (Figure 15A) and Trs130-HA (Figure 15B) demonstrate severely impaired binding (<20%) in *trs20ts*, at both permissive temperature and after shifting the cells to 37º C. This result is in contrast to the pull-downs from *trs33ts*, in which only Trs130-HA, and not Trs120-myc, exhibited diminished attachment to GST-Bet5. Consistent with the results seen in *trs33ts* and *trs65ts*, the lysate level of Trs130-HA is lower in *trs20ts*, strongly

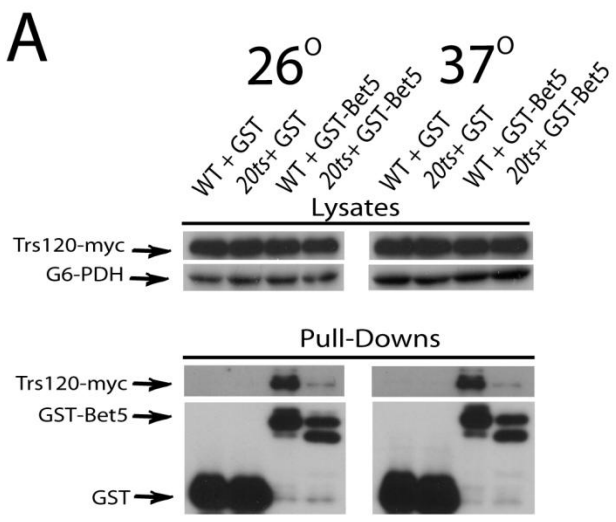


| | | | % of wild-type | $P_{value}$ |
|---|---|---|---|---|
| Trs120-myc (in *trs20ts*) | lysates | 26° | 93.4 ± 3.0 | >0.05 |
| | | 37° | 80.5 ± 10.9 | >0.05 |
| | pull-downs | 26° | 19.7 ± 6.9 | <0.0001 |
| | | 37° | 15.8 ± 10.0 | <0.0001 |

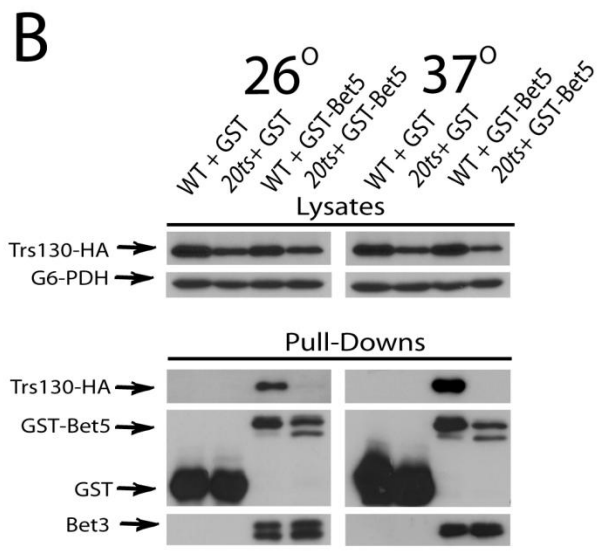


| | | | % of wild-type | $P_{value}$ |
|---|---|---|---|---|
| Trs130-HA (in *trs20ts*) | lysates | 26° | 49.2 ± 20.2 | <0.0001 |
| | | 37° | 44.9 ± 0.3 | <0.0001 |
| | pull-downs | 26° | 17.9 ± 5.0 | <0.0001 |
| | | 37° | 14.9 ± 7.0 | <0.0001 |

**Figure 15: Trs120-myc and Trs130-HA do not efficiently attach to TRAPP in *trs20ts*.**
**A)** GST-Bet5, or GST, as a negative control, was over-expressed in TRS120-myc wild type (NSY1519) and *trs20ts* (NSY1520) cells. Where indicated, cells were shifted to 37º C for 70 minutes prior to lysis. TRAPP was purified from yeast lysates onto glutathione resin. The presence of Trs120-myc in each sample was determined by Western blotting. **B)** Same as in (A), except using Trs130-HA (NSY1521, 1522) instead of Trs120-myc cells, and pull-downs samples were probed for the presence of Bet3 using α-Bet3 antibodies, along with Trs130-HA. For parts A and B, Trs120-myc and Trs130-HA bands were quantified, with absolute values corrected for G6PDH in the lysates or full-length GST-Bet5 in the pull-downs, and are shown as charts beneath the Western images. +/- represents SEM. Both parts demonstrate significantly (P value <0.001) lower Trs120-myc and Trs130-HA levels in the pull-downs. The level of Bet3 was not affected, indicating that TRAPP I remains intact in *trs20ts* cells.

suggesting an inherent instability of Trs130-HA isolated from the TRAPP complex. The co-precipitation of TRAPP I subunit Bet3 was not affected in *trs20ts*, suggesting that Trs20 does not affect TRAPP I assembly.

To confirm the functional relevance of the above result, TRAPP was purified from *TRS130*-HA/*trs20ts* cells, along with its wild type, and subjected to GDP-release assays on Ypt1 and Ypt32. As expected, TRAPP purified from *trs20ts* retained full activity on Ypt1 (Figure 16), confirming that core TRAPP I remained functionally sound. However, the GEF activity of *trs20ts* TRAPP was completely abolished on Ypt32. This result is reminiscent of the impaired Ypt31/32 GEF activity seen using TRAPP purified from several other strains containing defective TRAPP II, including *trs130ts*, *trs120Δ*, *trs65ts*, and *trs33ts* (Morozova et al. 2006; Liang et al. 2007).

While TRAPP purified from *trs20ts* yeast lysates clearly contains lower amounts of Trs120 and Trs130, it remained possible that the dissociation of these subunits occurred during the lysis or purification, due to a minor instability of the complex. To test this hypothesis, *TRS130*, *TRS120*, and *BET3* were tagged on the chromosome with GFP, in wild type and *trs20ts* cells, followed by live-cell deconvolution microscopy. In wild type cells all three TRAPP subunits are found in multiple discrete puncta. However, the TRAPP II-specific subunits Trs130 and Trs120, but not TRAPP I subunit Bet3, are noticeably diffuse in *trs20ts*, even at the permissive temperature (Figure 17A). This was not due to a difference in expression levels, as Western blotting of yeast lysates revealed equal levels of each protein between the wild type and *trs20ts* strains (Figure 17B).

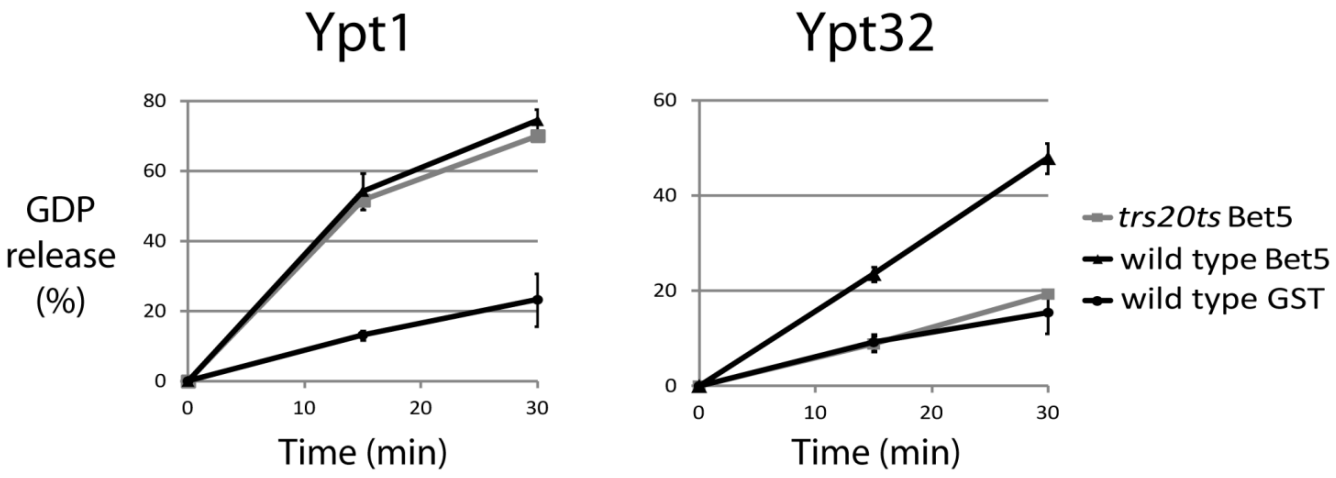


**Figure 16: TRAPP purified from *trs20ts* cells lacks Ypt32 GEF activity.** TRAPP was purified from TRS130-HA wild type (NSY1521) or *trs20ts* (NSY1522) cells using over-expressed GST-Bet5, as in Figure 17B. TRAPP was eluted from the glutathione beads, and subjected to GDP-release assays on Ypt1 (left graph) and Ypt32 (right). In each graph, the solid black line marked with triangles represents the wild type TRAPP, the grey line represents TRAPP purified from *trs20ts*, and the black line marked with circles (at the bottom of each graph) represents the background GDP release. Whereas TRAPP from wild type and *trs20ts* cells had similar activity on Ypt1, the activity of *trs20ts* TRAPP on Ypt32 was completely abolished. Error bars represent standard deviation.

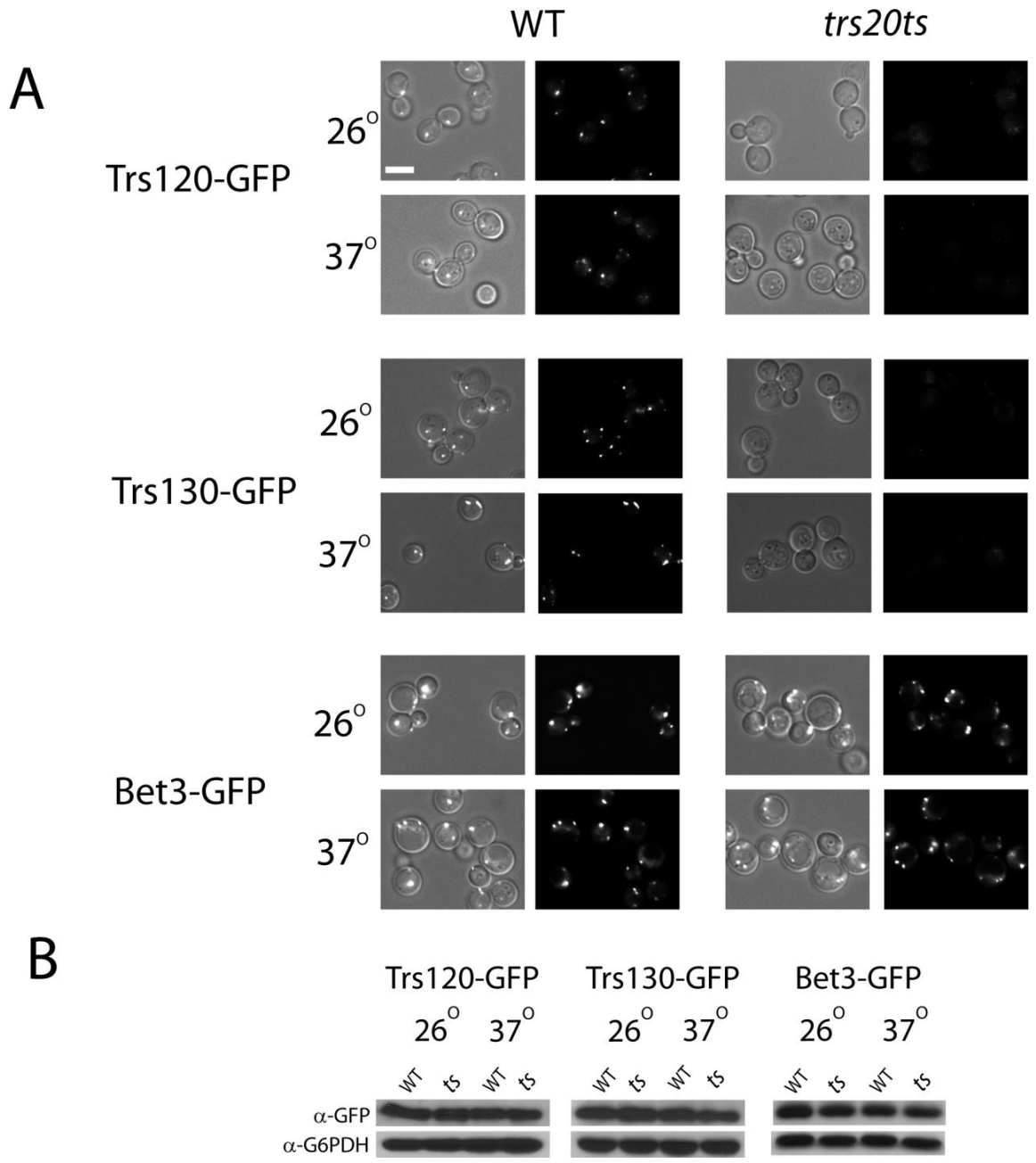


**Figure 17: Trs120 and Trs130 localization is diffuse in *trs20ts* cells. A)** Trs120 (top panels), Trs130 (middle), or Bet3 (lower) were tagged on the chromosome with GFP in wild type and *trs20ts* cells (NSY1513-1518). Cells were grown at 26º C, or shifted to 37º C for 70 minutes where indicated, and subjected to live-cell deconvolution microscopy. For each image, the GFP fluorescence is shown on the right, and merge with DIC on the left. While all three TRAPP subunits appear as distinct puncta in wild type cells, the localization of Trs120-GFP and Trs130-GFP, but not Bet3-GFP, are noticeably diffuse in *trs20ts* cells. **B)** Western blot showing equal expression of TRAPP subunits visualized in part A. G6PDH is used as a loading control.

**3. Mutation of Trs20 abolishes its interaction with Trs120**

As stated above, of the four missense mutations known to cause SEDT, three affect internal residues, and are thought to affect folding, based on the observation that they non-specifically affect Sedlin's protein interactions. These residues, along with F98 and V64, the amino acids corresponding to the mutations in *trs20ts*, are indicated with arrows in a space-filling model of Sedlin (Figure 18A). The only SEDT-associated mutation lying on the surface of Sedlin, and thought to disturb binding with a specific partner, is D47Y. Of the known Sedlin interacting partners, the interaction of MBP1, PITX1, and SF1 with SedlinD46Y were measured, and shown not to be affected by the D47Y mutation (Jayabalan et. al., 2010).

To characterize this mutation in yeast, the analogous Trs20 mutation, D46Y, was cloned into vectors for yeast and bacterial expression. For comparison, vectors containing the *trs20ts* mutations were analyzed alongside Trs20D46Y. The ability of Trs20D46Y to function as a sole copy in yeast was tested by transforming *trs20D46Y* into cells deleted for endogenous *TRS20*. Indeed, the D46Y cells were viable, but exhibited a temperature sensitive phenotype (Figure 18B).

Having confirmed that the D46Y mutation impairs Trs20 function in yeast, we hypothesized that this mutation may disrupt binding between Trs20 and other TRAPP subunits. To test this hypothesis, a yeast 2-hybrid assay was carried out, comparing interaction of Trs20 wild type, Trs20ts, Trs20D46Y, or Bet3 as a negative control, with Trs120 and Bet3 (Figure 19A). Importantly, Trs20 wild type, but not Bet3, interacted with Trs120. Furthermore, both Trs20 mutations abolished interaction with Trs120. However, whereas Trs20ts interacted with neither Trs120 nor Bet3, indicating severe misfolding, Trs20D46Y retained interaction with Bet3. Thus, the D46Y mutation specifically abolishes interaction with Trs120.

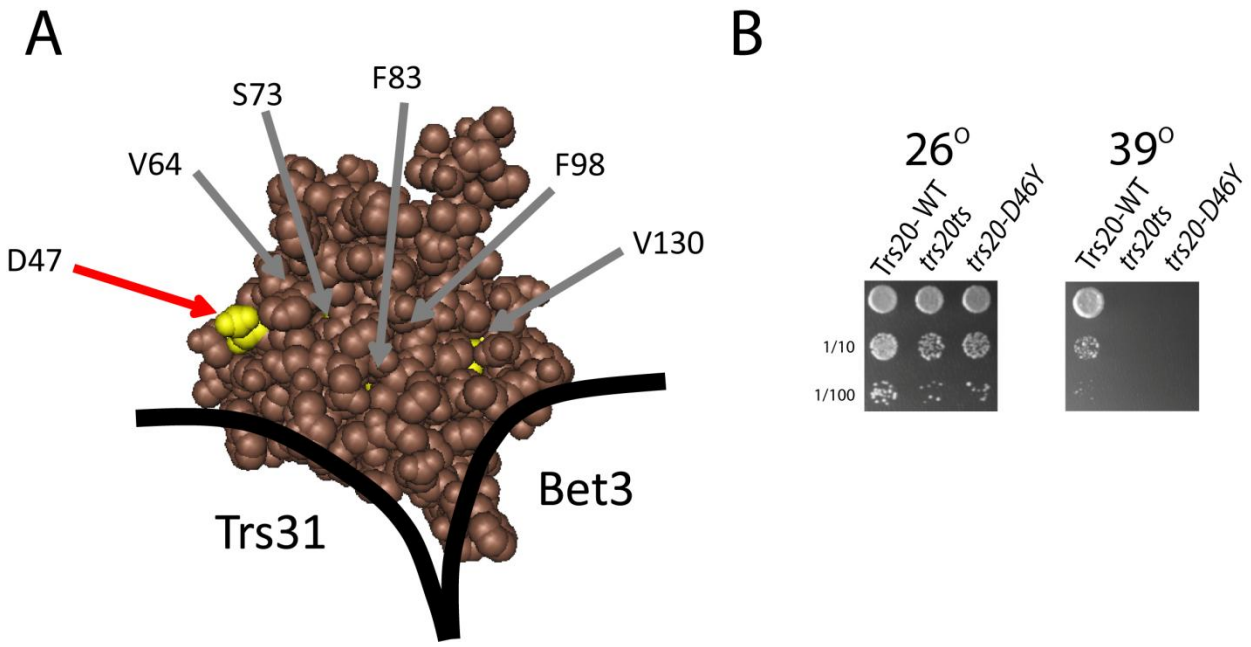


**Figure 18: The Trs20D46Y mutation causes temperature sensitivity in yeast. A)** Space-filling model of Trs20, taken from the crystal structure of a Trs20-Bet3-Trs31 complex (Kim et al. 2006). The general locations of Bet3 and Trs31 with respect to this orientation of Trs20 are indicated. The following residues appear yellow in the Sedlin structure, and are indicated with arrows: F98 and V64 correspond to the mutations in *trs20ts*; S73, F83, V130, and D47 are residues whose mutation is known to cause SEDT. Of the six residues highlighted, only D47 (indicated with red arrow) is clearly visible. V64, one of the *trs20ts* mutations, lies on the surface behind; the others lie within the Sedlin interior. **B)** A Trs20 construct containing the mutation analogous to D47Y, *trs20-D46Y* (NSY1523), was created as a sole copy in yeast. Similar constructs containing the wild type Trs20 (NSY1524) or the two *trs20ts* mutations (NSY1525) were included for comparison. Growth assay at 39º C (right panel) reveals that both *trs20-D46Y* and *trs20ts*, but not wild type, exhibit temperature sensitivity, indicating a partial loss of function caused by the mutations. Rows represent 10-fold serial dilutions, top to bottom.

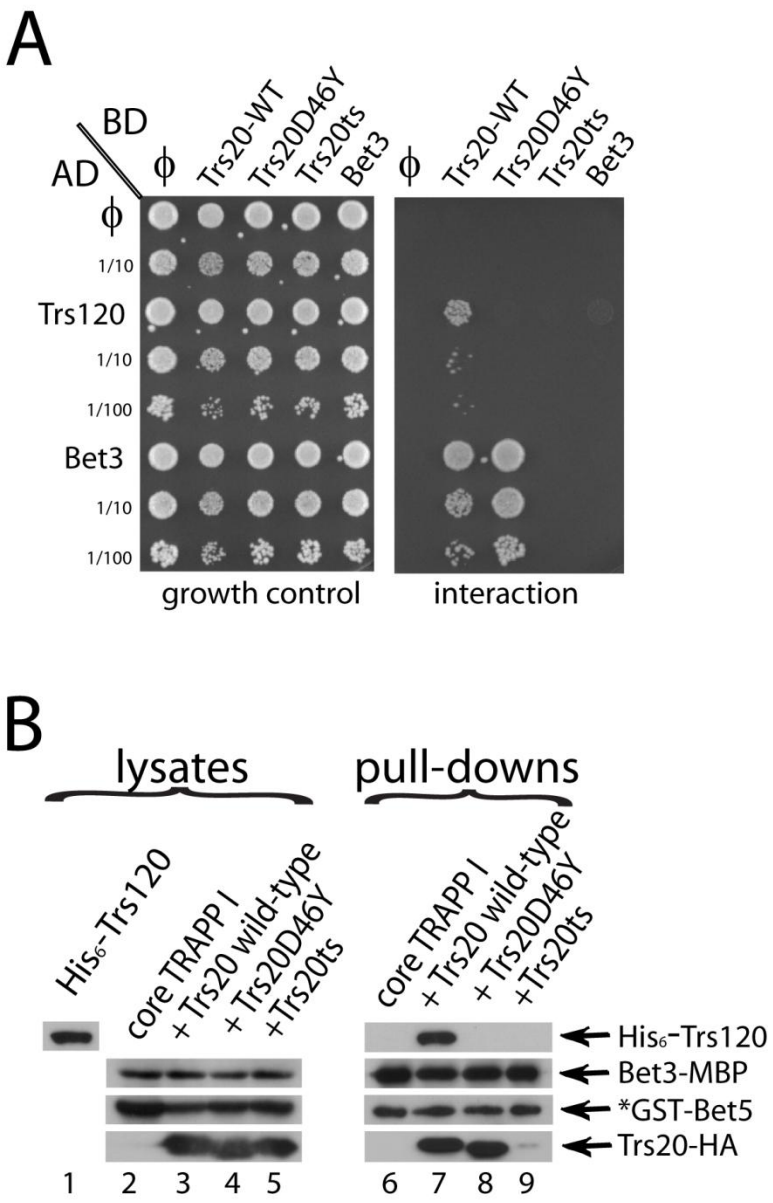


**Figure 19: The Trs20D46Y mutation prevents interaction with Trs120. A)** Yeast 2-hybrid assay to detect direct interaction of Trs120 or Bet3, fused to the GAL4 activation domain (AD), with Trs20 wild type (WT), Trs20D46Y, Trs20ts, or Bet3, fused to the GAL4 binding domain (BD). θ represents empty AD or BD, used as negative controls. Rows represent 10-fold serial dilutions top to bottom. As seen on the interaction plate (right), Trs120 interacts with only wild type Trs20, and not the Trs20 mutants or Bet3. Bet3 in AD interacts with Trs20 wild type and Trs20D46Y, but not Trs20ts.

**B)** Similar to the experiment shown in Figure 14, recombinant core TRAPP I was expressed alone or together with Trs20 wild type, D46Y, or Trs20ts in *E. coli*. After precipitation onto glutathione resin via GST-Bet5, lysate containing $His_6$-Trs120 was incubated with each sample. Co-precipitation was determined by Western blotting, which revealed that Trs20 wild type and D46Y co-precipitated with core TRAPP I, but not Trs20ts. However, Trs120 co-precipitated only with core TRAPP I together with wild type Trs20, and not with core TRAPP I alone or with either Trs20 mutant.

To investigate this hypothesis using a different approach, recombinant Trs20D46Y, Trs20ts, and wild type Trs20 were expressed in *E. coli* along with the core TRAPP I subunits, and tested for their ability to co-precipitate $His_6$-Trs120 onto glutathione resin, in an experiment similar to that shown in Figure 14A. Consistent with the yeast 2-hybrid results, both mutants failed to recruit Trs120 to the TRAPP I complex (Figure 19B). Furthermore, Trs20D46Y, but not Trs20ts, co-precipitated with the TRAPP I complex, further indicating that the D46Y mutation does not affect interaction with TRAPP I.

While interaction between Trs20 and Trs120, and loss of this interaction in the D46Y mutant, was shown by yeast 2-hybrid and recombinant proteins, it remained possible that this interaction does not occur within the context of the yeast TRAPP complex. To confront this idea, the bi-molecular fluorescence complementation (BiFC) technique was utilized. As illustrated in Figure 20A, BiFC involves fusing the two halves of a fluorescent protein to two proteins of interest, and transforming these sequences into living cells. If the two proteins of interest interact inside the cell, the fluorescent protein will be reconstituted and can be visualized through fluorescent microscopy (Kerppola 2008).

To apply the BiFC technique to the Trs20-Trs120 interaction, Trs120 was fused to the amino terminus of YFP, and either Trs20 wild type (WT) or D46Y was fused to the carboxy terminus. Live-cell microscopy revealed discrete puncta within the cells expressing Trs120 together with wild type Trs20, but not with Trs20D46Y (Figure 20C). Western blotting confirmed equal expression of Trs20 wild type and D46Y proteins (Figure 20D). Bet3-Trs20 interaction was then tested by fusing Bet3 to the amino terminus of CFP, and transforming into yeast along with the Trs20 wild type or D46Y fused to the carboxyl terminus. As expected,

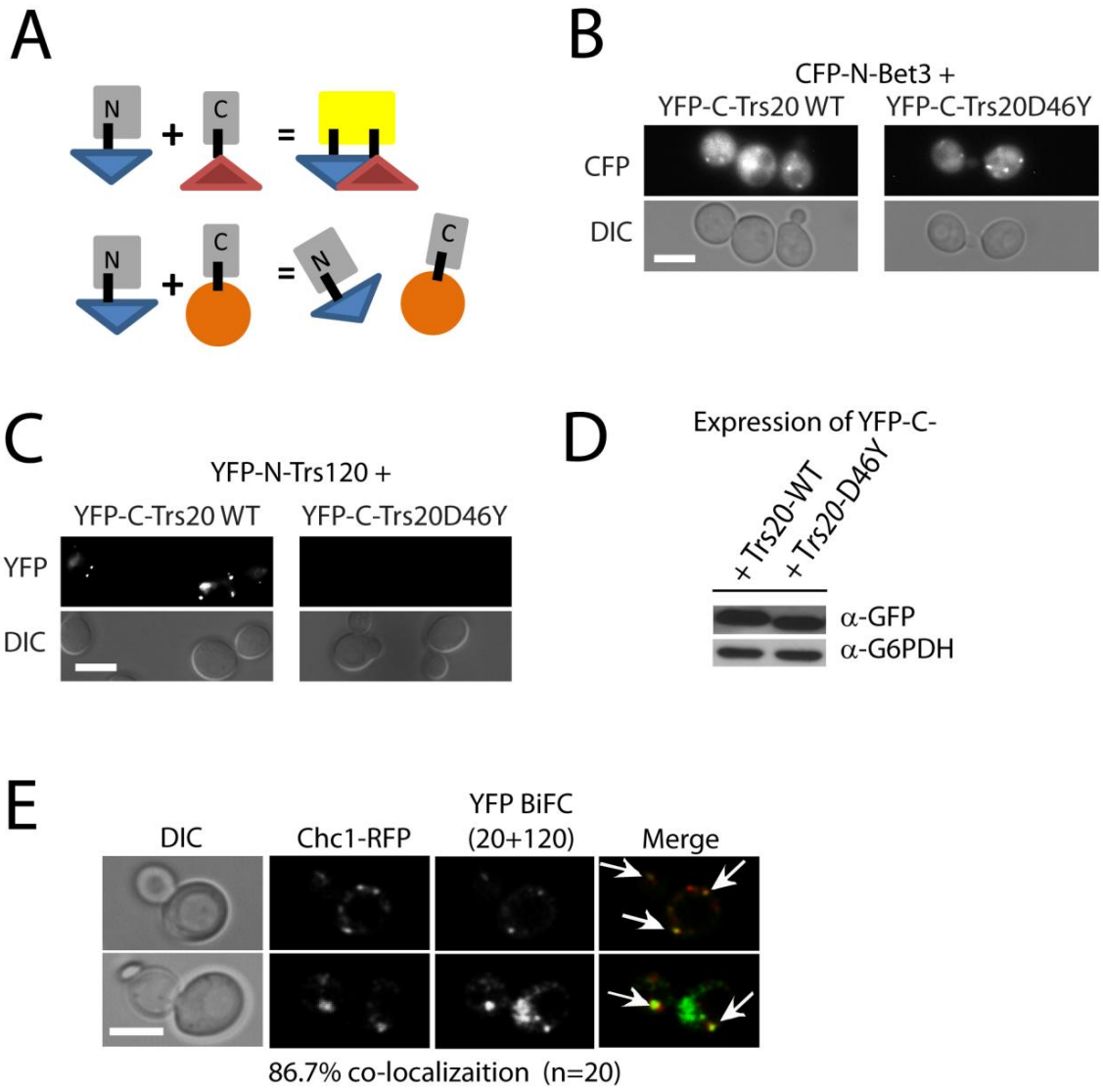


**Figure 20: Trs20 and Trs120 interact in living cells at the trans-Golgi. A)** Schematic of the BiFC assay: One protein of interest (blue) is fused to the N-terminus of YFP, and another (red or orange) is fused to the C-terminus of YFP. If the two proteins of interest interact (top), the YFP components come together, and fluorescence is seen (yellow). If the two proteins do not interact (bottom), fluorescence is not detected. **B)** BiFC fluorescence of Trs20 interaction with Bet3. Bet3 was fused to the N-terminus of CFP (CFP-N), and co-transformed with either Trs20 wild type or D46Y fused to the C-terminus of YFP (YFP-C—the C-terminus is identical between CFP and YFP) into wild type cells (NSY128). Live-cell fluorescence microscopy reveals clear puncta in both strains, indicating that both Trs20 wild type and Trs20 D46Y interact with Bet3. **C)** Same as in B, except co-transforming Trs20 wild type and D46Y constructs with Trs120 fused to the N-terminus of YFP (YFP-N). The presence of visible puncta in the Trs120-Trs20 wild type cells indicate direct interaction. The absence of such puncta in the Trs120-Trs20D46Y cells indicate a loss of interaction caused by the D46Y mutation. **D)** Expression, determined by Western blotting, of YFP-C-Trs20 wild type and D46Y in the transformants visualized in part C. **E)** Trs20 and Trs120 interact at the trans-Golgi. YFP-C-Trs120 and YFP-N-Trs20 wild type were co-transformed into cells expressing Chc1-RFP (NSY863). Co-localization between Chc1 and Trs20-Trs120 BiFC (indicated with arrows) was quantified, with results shown. Scale bars, 5μm.

puncta were observed in both Trs20WT-Bet3 and Trs20D46Y-Bet3 strains (Figure 20B). To confirm that the BiFC interaction represents the TRAPP complex, plasmids encoding wild type Trs20 and Trs120 fused to YFP halves were transformed into yeast expressing trans-Golgi marker Chc1-RFP. Importantly, the BiFC puncta co-localized largely (86%) with Chc1 (Figure 20E), consistent with the accepted trans-Golgi localization of TRAPP II.

**C. Conclusions**

The results in this chapter demonstrate that Trs20 serves as the primary attachment point for Trs120 to the TRAPP complex. Recombinant core TRAPP I failed to bind Trs120 *in vitro*, but the addition of Trs20 to the reaction facilitated the recruitment of Trs120 (Figure 14). Consistent with the results of Chapter 2, the inclusion of Trs33 in this experiment increased the amount of co-precipitating Trs120, although alone could not recruit Trs120.

Further evidence supporting dependence of Trs120 attachment on Trs20 was obtained through TRAPP pull-down from yeast lysates, where Trs120 failed to co-precipitate with a GST-Bet5 complex from *trs20ts* lysates. (Figure 15). In agreement with the dependency of Trs130 binding on Trs120, the former also failed to co-precipitate with GST-Bet5 from *trs20ts* lysates. Moreover, the *trs20ts* mutations abolished GEF activity of purified TRAPP on Ypt31/32, implicating Trs20 in TRAPP II function (Figure 16). The relationship between Trs20 and TRAPP II subunits was confirmed *in vivo* through fluorescence microscopy, where it was shown that Trs130-GFP and Trs120-GFP appear diffuse in *trs20ts* cells (Figure 17).

The contribution of Trs20 toward TRAPP II integrity lies in direct interaction between Trs20 and Trs120, in the basis of yeast 2-hybrid and BiFC results. Moreover, this interaction was specifically disrupted by the SEDT-associated D46Y mutation (Figures 19, 20), which partially

blocked Trs20 function, due to the temperature sensitive phenotype observed when Trs20D46Y was present as a sole copy (Figure 18). Taken together, these data provide strong evidence that Trs20 plays an essential role in TRAPP II structure and function, and suggests a possible link between Trs20-Trs120 interaction and the SEDT disease in humans.

# CHAPTER IV: DISCUSSION

In this Chapter I restate the major conclusions based on the results of the data shown in this dissertation, and discuss the implications of these findings for our understanding of TRAPP structure and function. Furthermore, I discuss several topics regarding the function of yeast and mammalian TRAPP which I consider to be open questions in the field. Finally, to address some of these questions, I recommend experiments for further research.

## A. Summary of conclusions

Based on the genetic interactions, microscopy, and biochemical results shown in Chapter 2, Trs33 plays a significant role in the structure of TRAPP II. Through interaction of Trs33 with Trs120, Trs33 helps to stabilize Trs130, an essential TRAPP subunit required for GEF activity on Ypt31/32 (Morozova et al. 2006).

In Chapter 3, I demonstrate that Trs20 is similarly involved in TRAPP II structure. Trs120 cannot bind to the TRAPP complex in the absence of functional Trs20, which further affects the attachment of Trs130. This occurs through direct interaction of Trs20 with Trs120, based on *in vitro* as well as *in vivo* evidence. Furthermore, this interaction is disrupted by the D46Y mutation in Trs20, which causes the SEDT disease in humans.

## B. Implications of results

### 1. Implications for TRAPP II structure

The novel direct interactions reported in this dissertation, of Trs120 with Trs33 and Trs20, are not accurately reflected in the existing models of TRAPP II organization. Of the three most recent published models of TRAPP II, none show interaction of Trs120 with both Trs20 and Trs33. Two of these models, based on images of TRAPP II visualized through electron microscopy, indicate that Trs120 is found on the Trs33 side of TRAPP, but separated from Trs20 (Yip et al. 2010; Yu and Liang 2012). The third model illustrates Trs120 distant from all TRAPP I subunits, and connected to them via interaction with Trs130 (Choi et al. 2011) This arrangement was based upon the dual interactions of Tca17 with Trs130 and Trs31/Bet3, of which the latter I judge as extremely questionable (see **Open Questions**, Tca17). I consider these models inadequate on the basis of two important points, not reflected in the existing models: Trs120 directly contacts both Trs20 and Trs33, and Trs130 interacts with TRAPP in a manner dependent upon the attachment of Trs120.

The interaction of Trs120 with both Trs33 and Trs20 were shown conclusively in Chapters 2 and 3 (Figures 13, 19, 20). The dependency of Trs130 attachment on Trs120 was previously published (Morozova et al. 2006), and is consistent with my results. I show that both Trs33 and Trs20 impact the attachment of Trs130, but their direct interactions are with Trs120, indicating that the impacts on Trs130 attachment is an indirect effect mediated by the binding or orientation of Trs120 (Figures 9, 15).

To resolve these issues, I propose two refined models of TRAPP II architecture (Figure 21A and B). Both models illustrate TRAPP as being composed of two anti-parallel TRAPP I complexes combined through interactions with TRAPP II-specific subunits. They incorporate the micro-structure of TRAPP I, which is broadly accepted in the field. In the figure, TRAPP I is shown as space filling models of composite crystal structures. These models also illustrate TRAPP II as a dimer, which was shown to exist *in vitro*, in a manner dependent upon the non-essential subunit Trs65 (Yip et al. 2010; Choi et al. 2011). Trs130 and Trs65, for which no crystal structure data is available, are indicated in positions consistent with the known direct interactions of each protein. However, their shape and orientation remain completely unknown, and as such were not fitted to specific shapes in the models. In addition, Tca17 was left out of these models, as further information regarding its interacting partners is required to position it in the TRAPP II structure with confidence.

The difference between the two models proposed here lies in the orientation of Trs120 with respect to the TRAPP I subunits. In Figure 21A, Trs120 is depicted as lying flat across each TRAPP I complex, with one end contacting Trs20 and the other Trs33. Physical contact between Trs120 and other TRAPP I subunits may occur, but such interactions are not strong enough to recruit Trs120 to TRAPP I in the absence of Trs20, at least under the conditions used for the *in vitro* pull-downs using recombinant subunits. In contrast, Figure 21B illustrates Trs120 as being oriented perpendicular to the TRAPP complexes—binding to Trs20 on one complex and Trs33 on the other. In both models, Trs130 and Trs65 are positioned in between the two Trs120 subunits.

I consider the first model to be more likely, for two reasons. First, recombinant Trs120 binds to TRAPP I ≈2-fold more efficiently in the presence of Trs33 than with Trs20 alone

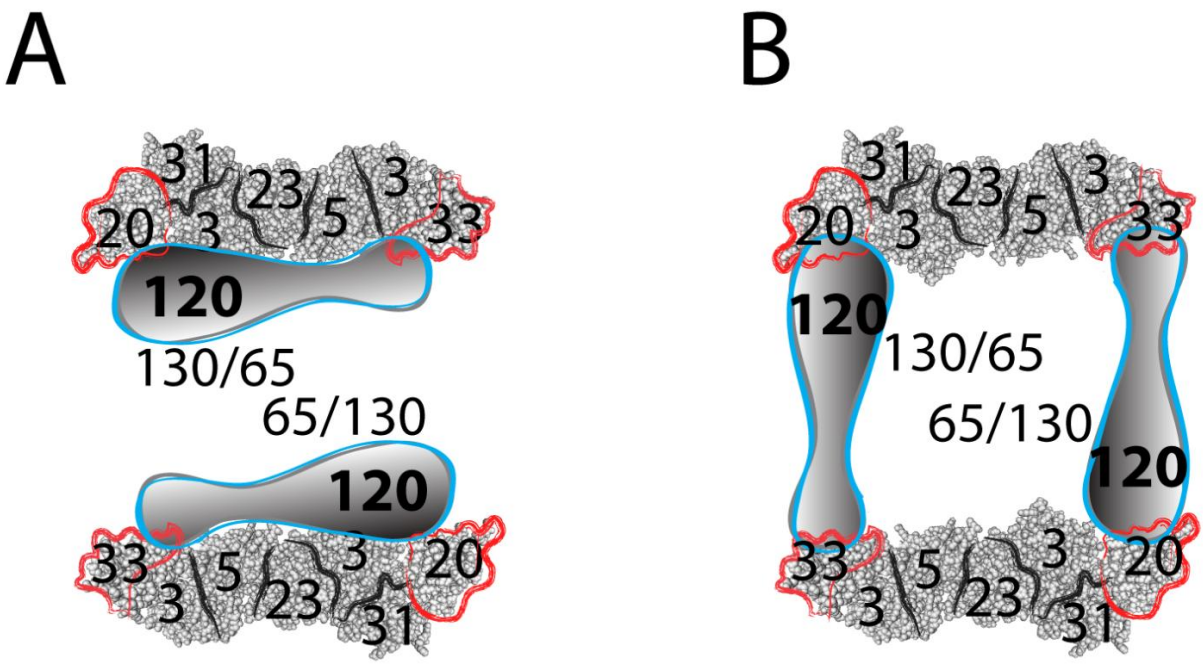


**Figure 21: Two possible models of TRAPP II architecture. A)** TRAPP II is composed of two anti-parallel TRAPP I complexes linked by TRAPP II-specific subunits Trs120, Trs130, and Trs65. In this model, Trs120 lies flat across each TRAPP I sub-complex, contacting Trs20 and Trs33 on each end. Two each of Trs130 and Trs65 locate to the region between Trs120 subunits, and interact with Trs120 and each other. Dimerization is dependent upon Trs65 self-interaction. **B)** Similar to (A), except that Trs120 interacts with Trs33 and Trs20 on opposing TRAPP I sub-complexes.

(Figure 16), suggesting that Trs120 is contacting both Trs33 and Trs20 in this context. Therefore, if the second model were correct, this would indicate that the recombinant TRAPP I is pulled down as a dimer—that is possible but unlikely in the absence of Trs65, shown to be required for dimerization in yeast lysates (see **Future Experiments**, TRAPP II structure). The second reason is that neither Trs130 nor Trs65 have been shown to interact with TRAPP I subunits. With reference to the model in Figure 21B, it is unlikely that two copies each of Trs130 and Trs65 could fit in the space allotted without contacting TRAPP I. However, it is possible that undiscovered interactions exist, or that the non-essential Tca17 localizes to this region (see **Future Experiments**).

**2. Implications for TRAPP II assembly**

As discussed in Chapter 1, one possible mechanism by which TRAPP may coordinate the Ypt1 and Ypt31/32-dependent transport steps is through the assembly of TRAPP II. Since TRAPP II contains all of the TRAPP I subunits, presumably in the same arrangement as in TRAPP I, it is possible that TRAPP II is formed by adding its four specific subunits to pre-existing TRAPP I. As such, it may ensure that post-Golgi transport is dependent upon the completion of ER-Golgi transport, an intriguing hypothesis.

While direct evidence to support this claim has not been reported, the results shown in this dissertation suggest a possible chronology for TRAPP II assembly which could be used to facilitate coordination. Illustrated in Figure 22, TRAPP II assembly may begin with the formation of core TRAPP I, which is necessary and sufficient for GEF activity on Ypt1 (Kim et al. 2006). Assembly progresses through the attachment of Trs20 and Trs33, which are also considered TRAPP I subunits, to the complex. The presence of these two subunits results in the

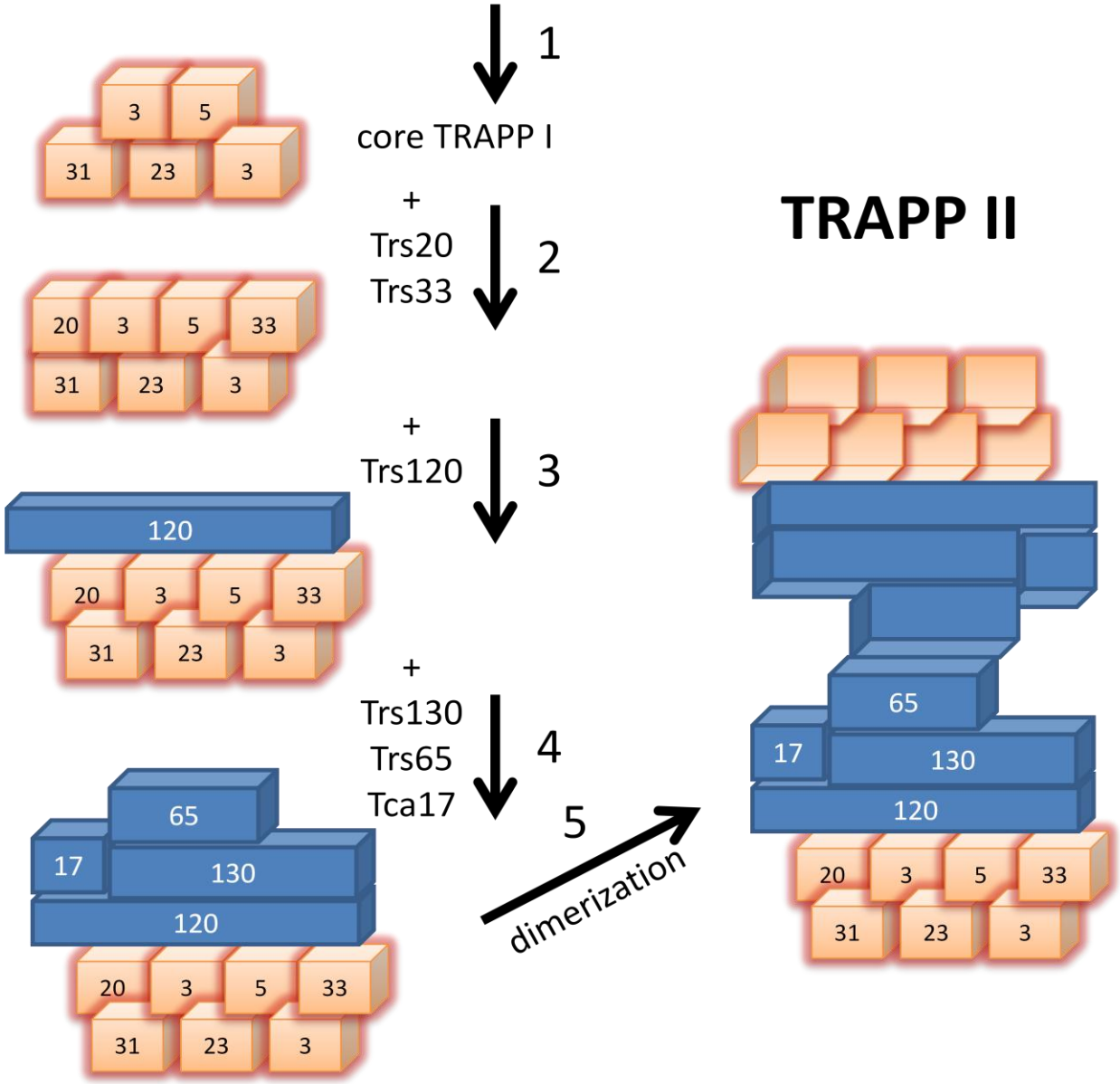


**Figure 22: Hypothetical chronology for TRAPP II assembly.** The first step (indicated as 1) in assembly of TRAPP II is the formation of the core TRAPP I complex, composed of Bet3, Trs31, Trs23, and Bet5. Next (2), Trs33 and Trs20 are added, through interaction with core TRAPP I subunits. After this (3), Trs120 can be recruited to the complex by interaction with Trs20 and Trs33. Subsequently (4), the remaining subunits Trs65, Tca17, and Trs130 attach, through interactions with Trs120 and each other. Finally (5), the complex dimerizes, a process dependent upon the self-interaction of Trs65, to form the final TRAPP II structure.

recruitment of Trs120 to the complex, through direct interaction. This recruitment, which likely occurs at the trans-Golgi in yeast, could be affected by factors in the molecular environment, such as trans-Golgi resident proteins or the absence of ER-Golgi transport-specific components. The last essential component to be added is Trs130, through interaction with Trs120 (Figure 24A, Appendix). The non-essential subunits Trs65 and Tca17 may arrive before Trs130, or come after but interact with Trs130 to stabilize the complex; both have been shown to play a role in TRAPP II structure (Liang et al. 2007; Montpetit and Conibear 2009). The final step for TRAPP II assembly would be dimerization through the self-interactions of Trs120 (Figure 24A, appendix) and Trs65 (Choi et al. 2011), if indeed dimerization occurs *in vivo* (see open questions).

A modification to the above chronology for TRAPP II assembly is that a sub-complex composed of Trs120, Trs130, Trs65, and Tca17, or one of Trs120 and Trs130 alone, form first, followed by binding of this complex to TRAPP I, advancing TRAPP II assembly. However, the observation that Trs130 stability is lower in strains preventing its attachment to a Bet5-containing complex (Figures 9A, 15B) makes the existence of a TRAPP II sub-complex less likely. In either case, further research is necessary to establish the precise nature of TRAPP II assembly.

**3. Implications for TRAPP II function**

The function of the TRAPP II complex remains open to discussion. As previously mentioned, it has been suggested to act as a tethering factor as well as a GEF for Ypt31/32. However, the latter role is not universally accepted in the field. My results strongly connect TRAPP II with Ypt31/32 function, and provide additional support to the claim that it acts as a

Ypt31/32 GEF. These results include the phenotype suppression of *trs33ts* by over-expression of Ypt31, the secretion phenotype of *trs33ts,* and the aberrant structures accumulating in *trs33ts,* which are reminiscent of those which accumulate in *ypt31Δ/32ts* (Jedd et al. 1997). Each of these implicates TRAPP II as a regulator of a pathway under the control of Ypt31/32.

Moreover, TRAPP purified from multiple wild type strains efficiently released nucleotide from Ypt32, the hallmark of a GEF. This was previously shown (Jones et al. 2000; Morozova et al. 2006), but has been challenged by others in the field who were unable to reproduce the result, attributing the activity to impure TRAPP preparations or faulty GEF assays (Wang and Ferro-Novick 2002). However, the fact that my results (Figures 11, 16) demonstrate GDP release on Ypt32 by TRAPP preparations further support the claim that TRAPP acts as a Ypt31/32 GEF. Furthermore, the disruption of this activity through deletion of *TRS33,* or mutation of *TRS20,* strongly indicate that the GEF activity is a function of the TRAPP complex, and not a non-specific factor co-precipitating with TRAPP in the experiment.

**4. Implications for SEDT**

The SEDT disorder in humans is caused by mutation of Sedlin, the human ortholog of Trs20. However, the precise molecular mechanism underlying SEDT symptoms remains unclear The only SEDT-associated mutation thought to disrupt a particular protein-protein interaction, rather than causing severe misfolding of Sedlin, is the D47Y mutation (Jang et al. 2002). In Chapter 3, I clearly demonstrate that the analogous yeast mutation caused a temperature sensitivity phenotype, indicating a partial, but not complete, block in protein function. This block was not caused by major misfolding or instability, as protein expression was equivalent to wild type, and retained interaction with Bet3. Rather, the mutation specifically abolished interaction

with Trs120 (Figures 19, 20). In a report published simultaneously with my research, it was shown that the D47Y mutation in Sedlin impairs co-precipitation of Sedlin with the orthologs of both Trs120 and Trs85 (Zong et al. 2011). These results implicate intra-molecular TRAPP interactions as a possible SEDT-causing defect. However, the precise transport step blocked in humans by the unnatural dissociation of their mammalian orthologs remains unclear.

## C. Open questions

### 1. What *is* the function of TRAPP II in yeast?

As previously stated, the precise function of the TRAPP II complex in yeast remains unclear. One possibility, mentioned above, is that TRAPP II acts as a GEF on Ypt31/32. Support for this claim, beyond this dissertation, includes the catalytic GEF activity of TRAPP observed *in vitro* (Morozova et al. 2006) and the effect of mutations in TRAPP II subunits on Ypt31 localization (Liang et al. 2007; Montpetit and Conibear 2009). While I find this suggested role compelling, it is not universally accepted. Other groups have claimed different functions for TRAPP II-specific subunits, such as in tethering COP I vesicles for endosome-Golgi transport (Cai et al. 2005). While its localization to the trans-Golgi and function in a post-Golgi transport step are broadly accepted, the specific role played by this complex is not. Further research is needed to clarify the function of TRAPP II (see **Future Experiments**).

### 2. Where does Tca17 fit into the TRAPP II structure?

Tca17, a relatively new addition to the TRAPP family, is a non-essential protein with a high degree of structural similarity to Trs20. However, unlike Trs20, it was shown to be present only in TRAPP II (Montpetit and Conibear 2009). The interactions of Tca17, and its

relationships with other TRAPP subunits, paint a confusing picture. Direct interactions have been reported for Tca17 with Trs130 (Choi et al. 2011) and a Trs31/Bet3 sub-complex (Scrivens et al. 2009), which I consider likely to be relatively distant in the TRAPP II complex from Trs130 (Figure 21A). Moreover, its attachment to TRAPP is dependent upon Trs33, but deletion of *TCA17* results in defective attachment of Trs65, likely distant from Trs33, to the complex.

I consider it likely that the reported interaction of Tca17 with Trs31/Bet3 is a misleading artifact due to its structural similarity to Trs20, which interacts with Trs31/Bet3 in TRAPP I. Furthermore, while the evidence that Tca17 can interact with TRAPP is compelling, based on co-precipitation with other TRAPP subunits from yeast lysates (Choi et al. 2011), it remains an open question whether all TRAPP II complexes contain Tca17, or whether it perhaps replaces another subunit in a subset of complexes.

**3. Does TRAPP II exist as a dimer *in vivo*?**

Two independent groups have provided evidence that TRAPP II exists as a dimer *in vitro*. This is based upon electron microscopy of purified TRAPP II (Yip et al. 2010), and the observation that myc-tagged TRAPP II subunits can co-precipitate HA-tagged versions of the same subunit (Choi et al. 2011). Furthermore, different groups have carried out gel filtration of purified TRAPP complexes; the apparent molecular weight corresponding to the peak assigned to TRAPP II far exceeds the expected size of monomeric TRAPP II calculated by adding up the masses of each subunit. Together, these data suggest that TRAPP II dimerizes *in vitro*.

Despite this observation, there is as yet no evidence that dimerization occurs *in vivo*. It is generally accepted that Trs65 is required for dimerization, as both groups mentioned above showed that deletion of *TRS65* impaired dimer formation. Therefore, since *TRS65* is a non-

essential gene, the dimerization of TRAPP II, if it occurs *in vivo*, must also be non-essential. Moreover, it remains entirely unclear what advantage dimerization might impart to TRAPP II.

One possibility is that there are two functions of TRAPP II—one non-essential, perhaps a tethering function, and one essential, such as a Ypt31/32 GEF. Trs65, and dimerization, may be required for the non-essential, but not the essential, function of TRAPP II. Another possibility is that the dimerization of TRAPP II occurs only during the lysis and purification of the complex, but no dimer exists in living cells. It has been shown that the complex dynamics of TRAPP are strongly affected by salt concentrations (Brunet et al. 2012), suggesting that the observed dimerization may be an artifact of the biochemical purification. The evidence reported to date is insufficient to determine whether TRAPP II indeed functions as a dimer in living cells, and if so, the advantage provided by the dimerization.

**4. Does coordination exist between yeast TRAPP complexes?**

Illustrated in Figure 1, different combinations of TRAPP subunits are involved in three separate protein trafficking steps in yeast. TRAPP I functions in ER-Golgi transport, TRAPP II in post-Golgi transport, and TRAPP III in ER-vacuole and autophagy. However, while the subunit makeup of each complex has largely been elucidated, no functional relationship between the complexes has been shown in living cells. Certainly one possibility is that no relationship exists—the three complexes are formed and act completely independent of each other. However, an intriguing alternative is that these complexes serve to coordinate the trafficking steps under their control.

An obvious mechanism through which this might be accomplished is through assembly of the TRAPP complexes. Since both TRAPP II and III contain all TRAPP I subunits as part of

their composition, forming these two complexes could simply involve adding additional subunits to pre-functional TRAPP I. For instance, TRAPP I can be combined with Trs85 to form TRAPP III, activating the ER-vacuole pathway, or TRAPP I could travel through the Golgi and combine with TRAPP II-specific subunits to stimulate Golgi exit and secretion. Hypothetically, the ratio of TRAPP II to TRAPP III in the cell could be dependent upon environmental conditions, such as nutrient deprivation or aggregation of mis-folded proteins.

Determining whether coordination exists, through complex assembly or some other mechanism, is an important objective in understanding how TRAPP complexes contribute to protein transport in yeast. Furthermore, it may also illuminate unknown functions of TRAPP in mammalian cells, of which less is currently known.

**5. Where does Trs20/Sedlin function?**

On the basis of the results shown in Chapter 3 of this dissertation, I propose that Trs20 is required for attachment of Trs120, and thereby Trs130, to the TRAPP II complex, which functions at the trans-Golgi. However, this does not rule out other functions of Trs20 in yeast, or Sedlin in humans. Interestingly, over-expression of both Ypt1 and Ypt31 partially suppress the temperature sensitive defect of *trs20ts* (my unpublished data). One possible explanation for this is that Trs20 plays separate roles in transport steps controlled by Ypt1 and Ypt31/32. However, another possibility is that over-expression of Ypt1 transports more TRAPP I to the trans-Golgi, where it subsequently becomes TRAPP II.

Furthermore, the *trs20ts* strain, unlike *trs33ts* (Figure 8A), does not exhibit a noticeable defect in general secretion (Mahfouz et al. 2012) and my unpublished data). The reason for this is unclear, but one possibility is that Trs20 functions only in endosome-Golgi transport, and not

Golgi-exit, both of which are considered roles of TRAPP II. Similarly, it has been reported that mutations in *TRS130* exhibit secretion defects (Sacher et al. 2001), but not mutations in *TRS120* (Cai et al. 2005). Whether these differences are reflective of specific roles of the TRAPP II subunits in different transport steps, or simply that the mutations in the temperature sensitive strains are not severe enough to fully eliminate protein function, is unclear. Thus, whether the function of Trs20 is identical to that of the TRAPP II complex in yeast, or merely overlaps with it, remains an important question.

Sedlin, the human ortholog of Trs20, has been tied to a number of roles throughout the cell. As discussed in the introduction to Chapter 3, Sedlin has been shown to interact with transcription factors (Ghosh et al. 2001), cytoplasmic chloride channels (Fan et al. 2003), and other partners, all on the basis of co-precipitation from cell lysates. Its localization has been reported to include the nucleus (Jeyabalan et al. 2010) and ER exit sites (Venditti et al. 2012). However, these reported characteristics of Sedlin should be accepted cautiously, in consideration of the following issues. Sedlin is structurally similar to a number of other proteins, including TRAPPC2L, the human ortholog of Tca17 (Scrivens et al. 2009). As such, the direct interactions reported based on co-precipitation *in vitro* may not be genuine, but reflect its structural similarity to different proteins. Moreover, the nuclear localization of Sedlin was determined from immuno-fluorescence of over-expressed, tagged Sedlin. Its localization to ER sites was unconvincing until a 3-hour temperature shift from 32° C to 42º C. In either case, such manipulations can drastically alter the localization of any intra-cellular protein. Therefore, additional experiments under normal cellular conditions are needed to substantiate these claims.

The best-characterized role shown for Sedlin was in the ER export of collagen (Venditti et al. 2012). This role is particularly intriguing, since the symptoms of SEDT, the disease caused

by mutations in Sedlin, are primarily skeletal in nature. As such, defective collagen transport is a logical hypothesis for the molecular basis of the disease. However, I find the provided explanation for Sedlin's role in this process to be incomplete.

Sedlin was associated with the ER-export of collagen through abnormal phenotypes caused by siRNA-mediated Sedlin depletion, co-localization of Sedlin with ER exit-site marker Sec31 as well as the trans-membrane collagen receptor TANGO1, and direct interaction of Sedlin with TANGO1 and Sar1, a GTPase which controls vesicle budding from the ER. From their data, the authors suggest a mechanism whereby Sedlin is recruited to ER exit sites by TANGO1, after which it binds to Sar1-GTP, slowing the latter's push towards membrane curvature, thus allowing for larger vesicle size, and thereby collagen incorporation.

While this mechanism agrees well with the data they report, and may be the most straightforward hypothesis, I do not think it is the only way to explain their data. As mentioned above, the claims of direct interactions and localization are not beyond dispute. The most compelling result was the ER-retention of collagen in Sedlin-depleted cells, as well as in chondrocytes taken from SEDT patients. However, these phenotypes can possible arise from defects in later transport steps. For example, a block in ER-Golgi or post-Golgi transport may hypothetically stall ER-export, through pathway coordination. In agreement with this idea, knockdown of TRAPPC3, the ortholog of Bet3, resulted in a similar defect in the ER export of collagen. In a separate study, TRAPPC3 was localized to vesicular tubular clusters (VTCs), which form by homotypic fusion of ER-derived vesicles, and thus downstream of ER exit. Interference with TRAPPC3 function resulted in the accumulation these vesicles (Yu et al. 2006). If Sedlin does indeed function at the ER to facilitate ER exit of large cargo, does it function alone or in complex with other TRAPP components?

**6. What pathways in mammals are regulated by mTRAPP?**

As mentioned in Chapter 1, each of the yeast TRAPP subunits has an identifiable mammalian ortholog (Table I). However, while the yeast subunits have been shown to arrange in three alternative complexes, the arrangements of the mammalian TRAPP subunits are poorly understood. Unlike its yeast counterpart, the mammalian ortholog of Bet3, TRAPPC3, migrates in a single peak on a gel filtration column (Yamasaki et al. 2009). However, this does not rule out the possibility of multiple complexes of similar molecular weight, or complexes containing TRAPP subunits without TRAPPC3. Indeed, the existence of alternative complexes has been suggested based on differences in gel filtration migration of three isoforms of TRAPPC6, the ortholog of Trs33 (Kummel et al. 2008).

As well as the arrangement of mTRAPP complexes, the functions of mammalian TRAPP subunits are still poorly understood. While the yeast complexes are thought to reside stably on membranes, TRAPPC3, the mammalian ortholog of Bet3, was reported to be primarily cytosolic (Loh et al. 2005). This would seem to belie the notion of it possessing a tethering function, suggested for yeast TRAPP. However, TRAPPC3 was later reported to partially localize to peri-nuclear structures and mediate tethering of COPII vesicles in post-ER transport (Yu et al. 2006). Yet another study showed that depletion of Sedlin or TRAPPC2L, the ortholog of Tca17, disrupts the structure of the Golgi apparatus, implicating these subunits in intra-Golgi transport (Scrivens et al. 2009). To further complicate matters, TRAPPC10, the mammalian counterpart of Trs130, was localized to COPI vesicles, which can be derived from VTCs or the Golgi apparatus. Furthermore, depletion of TRAPPC10 accumulates vesicles adjacent to the Golgi (Yamasaki et al. 2009). Interestingly, this study also reported that a TRAPP complex co-precipitating with

TRAPPC10 exhibited GEF activity on Rab1, the human ortholog of Ypt1, suggesting that the GEF function of TRAPP is at least partially conserved.

In yeast, TRAPP exists as multiple complexes, regulating separate transport steps. Although it has yet to be fully elucidated, I expect this complexity to ultimately be found in mammals as well. The primary motivation for studying these processes in yeast is to inform our understanding of how they occur in mammals, while using the faster growth conditions and easier genetic manipulation of yeast. If TRAPP functions entirely different from yeast to humans, the advantage to understanding the yeast complex would be minimal. However, considering the variety of localizations and functions proposed for mammalian TRAPP, it is likely that multiple TRAPP arrangements exist, which function in separate pathways. Further research is needed to clarify the specific roles of TRAPP complexes, and the subunits present in each complex. Another important question regarding the function of mTRAPP is possible GEF activity on a Ypt31/32 ortholog. No such activity has yet been demonstrated, but the GEF activity of yeast TRAPP II on Ypt31/32 makes this a question worth further investigation.

## D. Future experiments

### 1. *In vitro* reconstitution of TRAPP II

In order to address many questions regarding the structure and function of TRAPP II, it would be extremely useful to reconstitute the entire complex using bacterially-expressed and purified components. TRAPP I has been successfully expressed in bacteria, and precipitates efficiently as a complex *in vitro*. However, the larger TRAPP II subunits have proven far more difficult to use as recombinant proteins. Trs130, and to a lesser extent Trs120, degrade extensively when expressed in bacteria. Efforts involving protease-deficient bacteria as well as

co-expression of chaperone proteins have not overcome this problem. The likely reason for degradation, especially in the case of Trs130, is an intrinsic instability of the protein when not part of the TRAPP II complex. This presents a major hurdle, as bacteria do not have the capacity to co-express all of the TRAPP II subunits.

Continued improvements of *in vitro* translation technology make this a legitimate alternative to bacterial expression. If TRAPP II can be successfully expressed *in vitro*, or enough of TRAPP II to stabilize Trs130, it could be used to great advantage in further study of its structure and function.

Another possibility for expression of Trs120 and Trs130 is the use of their orthologs from *Chaetomium thermophilum*. This organism is a filamentous fungus which thrives at high temperatures (50º C), and therefore its proteins have been suggested to be more stable than their budding yeast counterparts. Recently this approach was used to reconstitute part of the nuclear pore complex, a massive 30-subunit structure which, similar to TRAPP II, contains many large proteins whose yeast orthologs are poorly expressed in bacteria (Amlacher et al. 2011). Currently an experiment is in progress to clone the *C. thermophilum* ortholog of *TRS130* into yeast and bacterial-expression vectors, to determine if it demonstrates increased stability but similar functionality to yeast Trs130.

**2. Clarification of TRAPP II structure**

The two major questions I have concerning TRAPP II structure are the orientation of Trs120 with respect to TRAPP I subunits (Figure 21A versus 21B), and the arrangement of Tca17 in the TRAPP II structure. To answer the first question, regarding the orientation of Trs120, I propose using immuno-electron microscopy (EM) on recombinant TRAPP complexes

containing Trs120 bound to TRAPP I subunits. While this approach proved informative when applied to the yeast-purified TRAPP II complex (Yip et al. 2010), the specific positions and orientations of the large TRAPP II subunits could not be identified. By omitting Trs130 and Trs65 from the structure, the position and orientation of Trs120 should be sufficiently clear. As mentioned previously, the orientation of Trs120 is radically different with respect to the TRAPP I subunits between the two models in Figure 21. Furthermore, if the model in Figure 21B is correct, Trs120 bound to core TRAPP I along with both Trs20 and Trs33 should appear, at least in some complexes, as a dimer, while the complex lacking Trs33 would be monomeric. I expect this difference to be discernible using immuno-EM, thus improving our understanding of TRAPP II architecture.

An alternative approach to study the orientation of the large TRAPP II subunits would be to determine the interactions of smaller domains of these proteins with other TRAPP subunits. This could also be used to possibly circumvent the issue of degradation in bacteria, as smaller portions of these proteins may be more stable than the full-length versions. In the Appendix to this dissertation, I show that the amino terminus of Trs120 interacts with Trs20, while its carboxy terminus interacts with Trs65 and Trs130. A further developed study involving the Trs120 domains, or those of Trs130, could improve our understanding of how these subunits are oriented in the TRAPP II complex.

To answer the second question, I propose two experiments. First, precipitate Tca17 from yeast lysates, and use mass spectrometry to identify co-precipitating proteins. This would answer the question of whether Tca17 is present on the complex in addition to all of the other TRAPP II subunits, or whether it replaces one of the subunits. Second, to identify its specific placement within the complex, direct interactors need to be identified. However, as previously stated, close

structural similarity with Trs20 make misleading results an unfortunate probability. To circumvent this problem, I propose adding a chemical crosslinker to the yeast lysate, followed by purification of Tca17 under denaturing conditions. Only subunits crosslinked, directly or indirectly, with Tca17 should co-precipitate with it. Subsequent analysis of the resulting product by mass spectrometry should indicate the proteins directly interacting with Tca17, as these will most efficiently co-purify with it under these conditions.

**3. Clarification of TRAPP II function**

As previously mentioned, roles for TRAPP II have been proposed for tethering as well as GEF activity on Ypt31/32. If *in vitro* reconstitution of TRAPP II is achieved, confirming the latter role, that of a GEF on Ypt31/32, would be relatively straightforward. If recombinant TRAPP II does act as a Ypt31/32 GEF, as I would expect, one could then test individual subunits or sub-complexes to determine the protein(s) necessary and sufficient for this activity.

A separate approach, to provide evidence for this role *in vivo*, would be to analyze the GDP or GTP-bound states of Ypt31 in wild type and TRAPP II mutant strains. If TRAPP II acts as a GEF for Ypt31, the amount of GTP-bound Ypt31, relative to GDP-bound, should be lower in TRAPP II mutants at restrictive temperature. This can currently be tested through *in vivo* nucleotide labeling with P-32, but would be made considerably simpler with antibodies recognizing the nucleotide-specific confirmations of Ypt31.

Addressing the putative tethering function of TRAPP II could be done by analyzing cellular morphology in TRAPP II mutants, such as *trs130ts*, supplemented with over-expressed Ypt31. If aberrant structures, such as secretory vesicles, accumulate in such cells, it would implicate TRAPP II in a role different from that as a Ypt31/32 GEF. However, a negative result

in this case would not be conclusive, as the Ypt31 over-expression could mask defective non-GEF function in the TRAPP II mutant strain.

**4. Investigate possible coordination of TRAPP I and II**

As discussed in the previous section, TRAPP complexes could potentially coordinate the transport pathways under their control, through assembly of the alternate TRAPP complexes. However, no direct evidence to support this conclusion has been reported. To shed light on this topic, two testable hypotheses have been suggested: first, TRAPP II is derived from pre-functional TRAPP I, and second, that TRAPP II assembly and function is dependent upon Ypt1.

To expound on the first hypothesis, one scenario could be that TRAPP I is formed at the cis-Golgi, where it activates Ypt1 to stimulate ER-Golgi transport. This same complex then travels to the trans-Golgi, where it forms the foundation for TRAPP II, the GEF regulating the next step in the secretory pathway. This can be tested using 4D-microscopy.

For example, a TRAPP I subunit such as Bet3 can be tagged with a fluorescent marker such as GFP, in a strain containing cis-, medial-, and trans-Golgi proteins tagged with different fluorescent markers. At steady-state conditions, Bet3 co-localizes with both cis and trans-Golgi markers. But by analyzing co-localization with markers as a function of time, it could be shown that an individual Bet3 punctum localizes first to the cis-Golgi, then medial, and finally trans-Golgi compartment. If this were observed, it would make a compelling case that TRAPP II is formed from TRAPP I. Alternatively, if trans-Golgi puncta are found to arise de novo, it would suggest that TRAPP II is not formed from TRAPP I—also a useful result. A possible improvement to this assay would be characterizing the movement of a punctum arising from the BiFC fluorescence of two TRAPP I subunits, such as Bet3-Trs31, instead of just a single tagged

subunit such as Bet3-GFP. This would help to confirm that the punctum being tracked represents an actual TRAPP complex, and not merely an aggregation of the single tagged subunit.

The second hypothesis is based on the assumption that if TRAPP I moves through the Golgi to form TRAPP II, then this transport is dependent upon the action of Ypt1, which is known to play a role in intra-Golgi transport. This assumption may not be valid, and so a negative result from this experiment would not be a compelling case against TRAPP I/II coordination. However, a positive result showing that TRAPP II structure or function is dependent upon Ypt1 would strongly support the claim that TRAPP II does not form de novo, but from TRAPP I which is transported as cargo through the Golgi.

This can be tested using yeast cells mutant for Ypt1. Multiple temperature sensitive strains have been constructed with compromised Ypt1 function. The integrity of TRAPP II in these strains can be tested in a number of ways, several of which were utilized in this dissertation. Examples include the localization of Trs130-GFP, the co-precipitation of Trs120 or Trs130 with a GST-Bet5 containing complex, the lysate level of Trs130-HA, or the Ypt31/32 GEF activity of TRAPP purified from these cells. If TRAPP II is found to be defective in *ypt1ts* cells, it would suggest that TRAPP is being transported in a manner dependent upon Ypt1, providing evidence for coordination between the Ypt1 and Ypt31/32-controlled pathways.

**5. Further investigate the molecular basis of SEDT**

As discussed at length above, SEDT results from mutations in Sedlin, the human ortholog of Trs20. However, the specific defects in Sedlin which cause SEDT symptoms remain unknown. With reference to the recent report associating Sedlin with the ER export of collagen,

a pathway defective in SEDT patients (Venditti et al. 2012), I propose further investigation into the role of Sedlin in this pathway.

A straightforward experiment toward this end would be to analyze the effects of the SEDT-associated D47Y mutation on the interactions of Sedlin with TANGO1 and Sar1-GTP, the proteins with which Sedlin is thought to partner in the regulation of collagen ER exit. If the mutation is found to disrupt one of these specific interactions, such would be strong evidence that defects in that interaction provides the molecular basis for the disease. If not, however, it may be that the disease arises from defective attachment of Sedlin to other TRAPP components.

Depletion of the TRAPPC3, the Bet3 ortholog, by siRNA inhibited collagen ER exit in a manner similar to Sedlin depletion (Venditti et al. 2012), indicating that Sedlin is likely functioning in this process in complex with TRAPPC3. However, the interaction between their yeast counterparts was not disrupted by the mutation analogous to D47Y. In contrast, the interaction of Trs20 with Trs120 was inhibited by this mutation (Figures 19, 20). Therefore, it would be meaningful to test whether knockdown of the Trs120 ortholog, TRAPPC9, also results in defective ER export of collagen. If so, this would shed light on the molecular basis of SEDT, as well as demonstrate a novel function of the Trs120 ortholog in mammalian cells.

# CHAPTER V: MATERIALS AND METHODS

## A. Antibodies and reagents

All reagents were purchased from Thermo Fisher Scientific unless otherwise noted. Yeast nitrogen base, yeast extract, and 5-fluoroorotic acid (5-FOA) were purchased from US Biological. Amino acids, Triton X-100, and antibiotics were purchased from Sigma. DTT was purchased from Biorad. Protogel for acrylamide gels was purchased from National Diagnostics. EDTA-free Protease Inhibitor Cocktail (PIC) was purchased from Roche. Restrictions enzymes were purchased from New England Biolabs. $^{3}$H-GDP and $^{35}$S trans-label were purchased from Perkin Elmer. PVDF membranes and filter paper were purchased from Whatman.

Primary antibodies used for this study include α-HA (mouse, Cell Signaling), α-myc (mouse, Santa Cruz), α-GFP (mouse, Roche), α-His (mouse, Clontech), α-G6PDH (rabbit, Sigma) α-GST (rabbit, Invitrogen), α-Gal4 binding domain (rabbit, Santa Cruz), α-S tag (mouse, Novagen ) and α-Bet3 (rabbit, provided by M. Sacher). Horseradish peroxidase-conjugated secondary antibodies (α-Rabbit or α-mouse) were purchased from GE healthcare.

## B. Microscopy – Figures 10, 17, 20

For BiFC experiments, strains were transformed with the appropriate plasmids, and grown in synthetic dropout medium to mid-log phase. For the experiment shown in Figure 20C, YFP fluorescence was visualized using a Zeiss Confocal LSM 700microscope. For all other BiFC experiments, fluorescence was visualized using a deconvolution Axioscope microscope (Carl Zeiss). For experiments comparing the fluorescence of endogenously-tagged proteins, cells

were grown to mid-log phase in YPD medium, and shifted to 37º for 70 minutes where indicated. Cells were subsequently washed once in synthetic medium, and visualized using a deconvolution Axioscope microscope (Carl Zeiss) equipped with DIC, FITC (for GFP fluorescence), and Texas red (for dsRed or RFP fluorescence) filters.

**C. GDP-release assays – Figures 12, 18**

GDP-release assays were done in the same way as described previously (Jones et al. 1998), except that the amounts of Ypt1 or Ypt32 were increased ~2 fold. The Ypt1 and Ypt32 were purified from *E. coli* as described previously (Jones et al. 1998). Briefly, 11 pmol purified Ypt1 or Ypt32 was incubated with 11 pmol H3-GDP (specific activity ~10-40 Ci/mmol) for 15 minutes at 30º C in 5 µl preloading buffer (20 mM HEPES pH 7.2, 20 mM KoAc, 5 mM EDTA, 1 mM DTT), followed by the addition of $MgCl_2$ to 12 mM. To begin the assay, the pre-loaded Ypt was added to 45 µl reaction buffer (20 mM HEPES pH 7.2, 5 mM $Mg(oAc)_2$, 1 mM DTT, 0.5 mM GDP, 0.5 mM GTP) containing 10 µg yeast-purified TRAPP, and incubated at 30º C. Samples (10 µl) were taken at the indicated times, added to 200 µl stop buffer (20 mM Tris-HCl pH 8.0, 25 mM $MgCl_2$, 1 mM DTT), and applied to PVDF membrane filters (Whatman, Protran BA85) using a MilliPore vacuum filtration device, and washed two times with 4 ml stop buffer. Filters were dissolved in scintillation fluid (BioSafe II, Research Products International) and protein-bound $^3H$ counted using a scintillation counter (Beckman Coulter).

**D. Recombinant protein pull-down – Figures 13, 14, 19, 24**

Plasmids were transformed into BL21(DE3) *E. coli* (Novagen), and grown at 37° C to $OD_{600}$ ~0.8 in Terrific Broth (Tartof and Hobbs 1987) (1.2 mg/ml tryptone, 2.4 mg/ml yeast

extract, 0.4% glycerol) with appropriate antibiotics. Protein expression was induced with 0.4 mM IPTG for 3 hours at 26º C. 1 liter of cells were harvested by centrifugation at 4° C, and washed with 45 ml ice cold water; cell pellets were frozen at -80º C.

For pull-downs, cells were suspended in lysis buffer (PBS, 10% glycerol, PIC, 1.5 mM DTT) at a concentration of ≈4 g cells per 25 ml buffer, and lysed by French press or sonication. Cell debris and unbroken cells were cleared by centrifugation at 3000 **g**, 4° C. 300 µl lysate was added to 35 µl glutathione or amylose resin, followed by incubation at 4° C and end-over-end rotation for 1 hour. After binding, the resin was washed with 350 µl wash buffer (PBS, 10% glycerol, 1.5 mM DTT), by resuspending resin in wash buffer and manually inverting microfuge tubes 6-7 times, leaving on ice for 2 minutes, and centrifuging resin for 1 minute at 500 **g**, 4° C. For the experiment shown in Figure 13B, resin was washed 3 times in wash buffer by adding and resuspended in 50 µl SDS sample buffer. For all other recombinant protein pull-downs, the resin was washed once after binding TRAPP I subunits, 400 µl lysate containing $His_6$-Trs120 was added, and incubated for 1 hour at 4º by end-over-end rotation. Following this incubation, samples were washed 2-3 times in wash buffer and resuspended in SDS sample buffer, made as described in section 10.2 of (Ausubel et al. 1994).

**E. Yeast TRAPP purification – Figures 9, 11, 12, 15, 16**

To purify TRAPP from yeast, plasmids encoding GST or the indicated GST-tagged protein were transformed into the indicated strain. Transformants were then grown to mid-log phase, and induced for 2 hours with 0.5 mM copper sulfate. Where indicated, cells were shifted to 37º for the last 70 minutes of induction. Cells were harvested by centrifugation at 3000 **g**, 4° C, washed with cold water, and pellets frozen at -80º C.

For the purification, cells were resuspended in lysis buffer (50 mM Tris-HCl pH 7.5, 250 mM NaCl, 5 mM DTT, 10% glycerol, 4 mM $MgCl_2$, 1.5X PIC). For the pull-down experiments shown in figures 9, 12, and 15, 200 ml of cells were harvested and suspended in 1.5 ml lysis buffer. For the purifications required for the GDP-release assays shown in figures 12 and 18, 1 liter of cells was harvested and resuspended in 5 ml of lysis buffer. Cells were broken by agitation with 1/3 volume of 0.5 mm glass beads (Biospec Products) using a Micro BeadBeater (Biospec). Triton X-100 was added to 0.1% and incubated for 10 minutes on ice. Lysates were subsequently cleared of unbroken cells by centrifugation at ≈3000 g for 10 minutes at 4º. Cleared lysates were added to 1/5 volume of glutathione resin (40 µl for pull-downs, 1 ml for GDP-release assays). Proteins were allowed to bind for 90 minutes by end-over-end rotation at 4º. Beads were then washed 2-3X with wash buffer (50 mM Tris-HCl pH 7.5, 250 mM NaCl, 5 mM DTT, 10% glycerol, 4 mM $MgCl_2$). After washing, samples used for co-precipitation experiments were resuspended in 50 µl SDS sample buffer. For purifications used for GDP-release assays, proteins bound to the resin after washing were eluted from the resin in 1 ml elution buffer (wash buffer plus 50 mM glutathione (Sigma) and NaOH to pH 8) for 1 hour at 4º, followed by dialysis of purified protein into B88 buffer (250 mM sorbitol, 20 mM HEPES pH 6.8, 150 mM KoAc, 5 mM $Mg(oAc_2)$), using SpectraPor dialysis tubing, and stirring with 500 ml B88 for 2 hours, changing buffer twice.

**F. Secretion assay – Figure 8**

General secretion assay was performed as described previously (Liang et al. 2007), except media proteins' amounts were quantified using phosphor screen (GE Healthcare) and

phosphor imager STORM860 (Molecular Dynamics) and were normalized to the amounts of labeled proteins.

**G. Electron microscopy – Figure 8**

Cells were grown to mid-log phase in YPD medium, and incubated at the indicated temperature for 90 minutes. Cells were then fixed in 0.2M sodium cacodylate buffer, pH 6.7, and 4% glutaraldehyde (both reagents are from Ted Pella, Redding, CA) and processed for EM as described previously (Byers and Goetsch 1975).

**H. Yeast 2-hybrid assays – Figures 6, 13, 19, 23**

For yeast 2-hybrid experiments, plasmids containing the indicated protein fused to the GAL4 activation domain (in pACT2) or binding domain (in pGBDU-C2) were transformed into PJ469-a or PJ469-α, respectively. Haploid strains were mated on YPD and diploids selected on SD –ura –leu plates. Transformants were grown overnight in synthetic medium, and 3 μl spotted onto SD-ura –leu (for growth control), SD –ura –leu –his (for interaction), or SD –ura –leu –his containing 1-3 mM 3AT (for higher stringency interaction), along with 10-fold serial dilutions. Pictures of plates were taken after 2 or 3 days.

**I. Growth assays – Figures 8, 12, 20**

Yeast were grown overnight in YPD medium; 3 μl of each were spotted onto YPD plates along with 10-fold serial dilutions, and placed in incubators set to the indicated temperature. Pictures were taken after 1-2 days.

**J. Western blotting – Figures 9, 12, 13, 14, 15, 17, 19, 20, 24**

Western blotting to compare protein levels was carried out by running samples on 10% SDS-PAGE gels, as described in section 10.2 of (Ausubel et al. 1994). Proteins were transferred to PVDF membranes at 100 mV for 2 hours, or 25 mV overnight, at 4º C, in transfer buffer (20 mM Tris-HCl, 20% methanol, 15 mM glycine). Membranes were blocked with 5% milk in PBST (PBS with 0.2% Tween-20) for one hour at room temperature or overnight at 4° C. Primary antibodies were bound for 1 hour at room temperature in PBST, or overnight at 4º C, followed by 3 washes in PBST. Secondary antibodies were bound for 1 hour at room temperature, followed by 3 washes in PBST. Proteins were detected using ECL (regular or plus, GE), according to the manufacturer's protocols, followed by developing onto autoradiography film. For the quantification shown in figure 15, protein levels, exposed in the range determined to be linear, were calculated using band density as determined by ImageJ software. The indicated values for percent co-precipitation were the averages from the results of three independent experiments.

**K. Amino acid sequence alignment – Figure 6**

Multiple sequence alignment was done using the CLUSTALW2 program (Larkin et al. 2007) with default values (gap opening penalty 10, and gap extension penalty 0.2, using the Gonnet250 matrix, no end gaps, and gap separation penalty 4).

**L. Protein structure illustrations – Figures 18, 21**

The illustration of Sedlin in Figure 18 was copied from the crystal structure of that protein in complex with mBet3 and mTrs31, viewed using Cn3D software (NCBI). The corresponding Protein Database (PDB) ID number is 2J3W (Kim et al. 2006).

The TRAPP I portion of Figure 21 was generated by orienting three structures with respect to overlapping portions, using Cn3D software (NCBI). The PDB ID numbers are: 2J3W, 2J3T (Kim et al. 2006), and 3CUE (Cai et al. 2008).

**M. Yeast transformation**

Transformation of plasmids or PCR products into yeast was done using the lithium acetate (LiAc) method described previously (Ito et al. 1983). Throughout the transformation procedures, each step took place at room temperature unless otherwise indicated. For transformation of plasmids into yeast, 3 ml of cells were grown overnight in YPD. 10 $OD_{600}$ units of cells were harvested by centrifugation, and washed in 400 µl 100 mM (LiAc). Cells were then resuspended in 500 µl transformation buffer (80% PEG, 100 mM LiAc, 100 mM tris-HCl, 10 mM EDTA, 2% salmon testes DNA). 5 µl plasmid DNA was added to the cells in transformation buffer, and samples vortexed vigorously for 60 seconds. Transformation reactions were left overnight at room temperature, and cells plated the following day onto synthetic dropout medium.

For transformation of PCR products, used for chromosomal tagging or deletion, 10 ml of cells were grown to mid-log phase in YPD, and 5 $OD_{600}$ units of cells were harvested by centrifugation. Cells were washed with 400 µl LiAc, and subsequently resuspended in 360 µl transformation buffer (67% PEG, 100 mM LiAc, 2% salmon testes DNA, and 21% PCR product). Reactions were incubated at 26º C for 30 minutes, followed by a heat shock at 42º for 20 minutes. Cells were collected and resuspended in 1.5 ml YPD medium, and incubated overnight at 26º. Transformants were plated onto selective medium and grown at 26º for 3-4 days. Single colonies (usually among 50-200 transformants) were selected for verification of

tagging or deletion, which was accomplished by genomic DNA extraction and PCR. Genomic DNA extraction was done as described previously (Holm et al. 1986).

**N. Bacterial transformation**

For expression of recombinant proteins, 2 µl of plasmid were added to electrocompetent BL21(DE3) *E. coli* (Novagen). Transformation was accomplished through electroporation (Bio-Rad *E. coli* Pulser and with Bio-Rad electroporation cuvettes, used according to the manufacturer's instructions), followed by incubation at 37º C for 1 hour, and plating onto LB plates containing appropriate antibiotics. Transformants were grown overnight at 37° C, pooled, and inoculated into media for recombinant protein expression (see **Recombinant Protein Pull-down**).

**O. Construction of plasmids**

The plasmids used in this dissertation are listed in Table II. Plasmids pNS1015, 981, 1000, 1043, 1385-1387, 1436-1440, and 1180 were used for bacterial expression. The remaining plasmids were transformed into yeast. All plasmids constructed for this study were made through ligation of yeast genes into commercially available, or previously published, vector backbones. Maps of these vectors are given in the original publications or manufacturers' websites. All pRS vectors used in this study were previously published (Sikorski and Hieter 1989). pETDuet-1, pRSFDuet-1, and pCDFDuet-1 are available from Novagen. pACT2 is available from Clontech Laboratories, Inc. pGBDU-C2 was published by (James et al. 1996). The pRS vectors containing BiFC fragments were published by (Lipatova et al. 2012).

The yeast genes inserted during plasmid construction were amplified from yeast genomic DNA, extracted as described previously (Holm et al. 1986), by PCR. Primers were designed in each case to amplify the yeast gene ORF, while adding restriction sites to each end of the product, which were then used for cloning into the multiple cloning sites of destination vectors. The genomic DNA sequences of all genes used for this study are available from the Saccharomyces Genome Database (www.yeastgenome.org) The restriction sites used for each cloning are listed along with the insert in Table II.

Inserts were cloned in frame with the designated epitope tag, already present the destination vector, unless indicated otherwise. pNS1015 was generated by subcloning the GST tag from pET41a (Novagen) into pETDuet-1 (Novagen). pNS1000 and pNS1180 were then cloned into pNS1015 by insertion of Bet5 or Trs33, respectively, into multiple cloning site 1 (MCS1) in frame with the GST tag. For pNS1043, MBP was subcloned from pMAL-C2X (New England BioLabs) into MCS1 of pRSFDuet-1 (Novagen), and then inserting Bet3 in frame with the MBP tag. The epitopes in Trs31-myc, Trs20-HA, or Calmodulin-HA constructs were added by engineering the sequence into the reverse primer during cloning. For cloning *TRS20* into pRS vectors, *TRS20,* along with 400 base pairs upstream and 200 downstream, was sub-cloned, using SacI, from *TRS20* in pRS425, provided by M. Sacher (Concordia University). To generate *trs20D46Y* and *trs20ts* mutants in pRS and pCDF vectors, PCR-based mutagenesis was utilized to mutate T276C and T398C (for the V92A and F133S amino acid substitutions in the *trs20ts* constructs) or G136T (for D46Y) from the plasmids containing wild type *TRS20*. To construct the BiFC plasmids, *TRS120, TRS20, trs20D46Y*, or *BET3* were cloned in frame with the indicated portion of YFP or CFP using pNS1426 (YFP-C in pRS413), pNS1425 (YFP-N in pRS416), or pNS1431 (CFP-N in pRS415). (Lipatova et al. 2012).

**Table II: plasmids used in this study**

| Name | Backbone (source) | Insert(s) (restriction enzymes used for cloning) | Figure(s) | reference |
|---|---|---|---|---|
| pNS981 | pCDFDuet-1 (Novagen) | $His_6$-*TRS120* (SacI/SalI) | 13, 14, 19 | (Tokarev et al. 2009) |
| pNS1000 | pETDuet-1 (Novagen) | GST-*Bet5* (SpeI/BglII) *TRS23*-S (NdeI/XhoI) | 14, 19, 24 | (Taussig et al. 2013) |
| pNS1043 | pRSFDuet-1 (Novagen) | *BET3*-MBP (BamHI/AvrII) | | (Taussig et al. 2013) |
| pNS1436 | pCDFDuet-1 | $His_6$-*TRS33* (BamHI/SacI) | 14 | (Taussig et al. 2013) |
| pNS1385 | pCDFDuet-1 | *TRS20*-HA (NdeI/XhoI) | 14, 19 | (Taussig et al. 2013) |
| pNS1437 | pCDFDuet-1 | $His_6$-*TRS33* (BamHI/SacI) *TRS20*-HA (NdeI/XhoI) | 14, 24 | (Taussig et al. 2013) |
| pNS1386 | pCDFDuet-1 | *trs20ts*-HA (NdeI/XhoI) | 19 | (Taussig et al. 2013) |
| pNS1387 | pCDFDuet-1 | *trs20D46Y*-HA (NdeI/XhoI) | 19 | (Taussig et al. 2013) |
| pNS1015 | pETDuet-1 | GST (Xba/BglII) | 13 | (Tokarev et al. 2009) |
| pNS1180 | pETDuet-1 | GST-*TRS33* (BamHI/SalI) | 13 | (Tokarev et al. 2009) |
| pNS1438 | pCDFDuet-1 | *CALMODULIN*-HA (NdeI/XhoI) | 13 | (Tokarev et al. 2009) |
| pNS422 | pYEX4T-1 | GST | 9, 11, 12, 15 | (Martzen et al. 1999) |
| pNS424 | pYEX4T-1 | GST-*BET5* | 9, 11, 12, 15 | (Martzen et al. 1999) |
| pNS549 | pYEX4T-1 | GST-*TRS33* | 12 | (Martzen et al. 1999) |
| pNS412 | pYEX4T-1 | GST-*SEC2* | 12 | (Martzen et al. 1999) |
| pNS196 | pACT2 (Clontech) | GAL4-activation domain | 6, 13, 19, 23 | Clontech Laboratories, Inc |
| pNS1152 | pACT2 | AD-*TRS20* (BamHI/SacI) | 19 | (Taussig et al. 2013) |
| pNS1395 | pACT2 | AD-*trs20D46Y* (BamHI/SacI) | 19 | (Taussig et al. 2013) |
| pNS1096 | pACT2 | AD-*BET3* (BamHI/XhoI) | 19 | (Taussig et al. 2013) |
| pNS1394 | pACT2 | AD-*trs20ts* (BamHI/SacI) | 19 | (Taussig et al. 2013) |
| pNS989 | pACT2 | AD-*TRS120* (NcoI/SacI) | 6, 13, 23 | (Tokarev et al. 2009) |
| pNS990 | pACT2 | AD-*TRS130* (SmaI/XhoI) | 6, 13 | (Tokarev et al. 2009) |

**Table II (continued): Plasmids used in this study**

| Name | Backbone | Insert(s) (restriction enzymes used for cloning) | Figure(s) | Reference |
|---|---|---|---|---|
| pNS206 | pGBDU-C2 | GAL4-binding domain | 6, 13, 19, 23 | (James et al. 1996) |
| pNS1115 | pGBDU-C2 | BD-*TRS120* (SmaI/SalI) | 19 | (Taussig et al. 2013) |
| pNS1106 | pGBDU-C2 | BD-*BET3* (BamHI/SalI) | 19 | (Taussig et al. 2013) |
| pNS1156 | pGBDU-C2 | BD-*TRS33* (BamHI/SalI) | 13, 23 | (Tokarev et al 2009) |
| pNS1110 | pGBDU-C2 | BD-*TRS65* (SalI/PstI) | 6, 23 | (Tokarev et al 2009) |
| pNS1111 | pGBDU-C2 | BD-*TRS65N* (SalI/PstI) | 6 | (Tokarev et al 2009) |
| pNS1112 | pGBDU-C2 | BD-*TRS65C* (SalI/PstI) | 6 | (Tokarev et al 2009) |
| pNS1396 | pRS316 | *TRS20* (SacI) | | |
| pNS1397 | pRS315 | *TRS20* (SacI) | 18 | (Taussig et al 2013) |
| pNS1398 | pRS315 | *trs20D46Y* | 18 | (Taussig et al 2013) |
| pNS1399 | pRS315 | *trs20ts* | 18 | (Taussig et al 2013) |
| pNS1432 | pRS416 | CFP-N-*BET3* (BspEI/XhoI) | 20 | (Taussig et al 2013) |
| pNS1428 | pRS413 | YFP-C-*TRS20* (SpeI/BamHI) | 20 | (Taussig et al 2013) |
| pNS1427 | pRS416 | YFP-N-*TRS120* (BspEI/XhoI) | 20 | (Taussig et al 2013) |
| pNS1429 | pRS413 | YFP-C-*trs20D46Y* (SpeI/BamHI) | 20 | (Taussig et al 2013) |
| pNS1433 | pRS416 | YFP-N-*TRS20* (BamHI/XhoI) | 20 | (Taussig et al 2013) |
| pNS1435 | pRS413 | YFP-C-*TRS120* (SpeI/BamHI) | 20 | (Taussig et al 2013) |
| pNS552 | pYEX4T-1 | GST-*TRS130* | 7 | (Martzen et al. 1999) |
| pNS489 | yEP24 | *YPT1* | 11 | (Morozova et al 2006) |
| pNS229 | yEP24 | *YPT31* | 11 | (Jones et al. 1999) |
| pNS274 | yEP24 | θ | 11 | D. Botstein |
| pNS1439 | pCDFDuet-1 | $His_6$-*TRS120*-N (SacI/SalI) | 24 | |

**Table II (continued): plasmids used for this study.**

| Name | Backbone (source) | Insert(s) (restriction enzymes used for cloning) | Figure(s) | Reference |
|---|---|---|---|---|
| pNS1116 | pGBDU-C2 | BD-*TRS130* (EcoRI/SalI) | 23 | |
| pNS1441 | pACT2 | AD-*TRS120*-C (BamHI/SacI) | 23 | |
| pNS1442 | pGBDU-C2 | BD-*TRS120*-C (SmaI/SacI) | 23 | |
| pNS1443 | pACT2 | AD-*TRS120*-N (BamHI/SacI) | 23 | |
| pNS1444 | pGBDU-C2 | BD-*TRS120*-N (SmaI/SacI) | 23 | |
| pNS1107 | pGBDU-C2 | BD-*BET5* (EcoRI/BamHI) | 23 | |
| pNS1155 | pGBDU-C2 | BD-*TRS20* (BamHI/PstI) | 23 | |
| pNS1108 | pGBDU-C2 | BD-*TRS23* (EcoRI/BamHI) | 23 | |
| pNS1109 | pGBDU-C2 | BD-*TRS31* (SmaI/PstI) | 23 | |
| pNS1101 | pACT2 | AD-*TRS65* (BamHI/SacI) | 13 | (Tokarev et al. 2009) |
| pNS1440 | pCDFDuet-1 | $His_6$-*TRS120*-C (SacI/SalI) | 24 | |

**P. Construction of yeast strains**

The yeast strains used in this dissertation are listed in Table III. Strains deleted for *TRS33* were constructed by transformation and homologous recombination of a PCR product containing a KanMX4 cassette (from pAG29, Yeast Resource Center) flanked by regions homologous to the region directly upstream and downstream of the *TRS33* open reading frame, in its corresponding wild type strain. The *trs20ts* strain and its cognate wild type (NSY1471 and 1472) were provided by M. Sacher. Strains expressing Trs120-myc and Trs130-HA in *trs20ts* (NSY1520, 1522, respectively) were constructed by mating NSY1471 with NSY1176 (Trs130-HA::HIS3/Trs120-myc::TRP1), followed by sporulation and tetrad dissection. Trs120 was tagged on the C-terminus with GFP in NSY1471 and NSY1472 to create NSY1513-1514, by PCR and homologous recombination of GFP::KanMX4 cassette (from pKT128, Euroscarf). In a similar manner, Bet3 was tagged with GFP in NSY1472 and 1471 to create strains NSY1517 and 1518, respectively. Strains expressing Trs130-GFP in *trs20ts* and its wild type (NSY1516 and 1515) were generated by mating NSY1471 with NSY1316, followed by tetrad dissection. Strains expressing Trs20 wild type, Trs20-D46Y, or Trs20ts on plasmids covering *trs20Δ* were created by transforming *TRS20* in pRS316 into NSY1472, deleting *TRS20* from the chromosome via PCR and homologous recombination using Hygromycin B resistance (from pAG32, Yeast Resource Center), transforming the resulting strain with Trs20 wild type, trs20-D46Y, or trs20ts expressed from pRS315 (pNS1397-1399), and selecting the final strains from 5-FOA plates.

**Table III: Yeast strains used for this study.**

| Name | Genotype | Figure(s) | Reference |
|---|---|---|---|
| NSY752 | PJ469-α (for yeast 2-hybrid)<br>MATα, trp1, leu2, ura3-52, his3, lys2, gal4Δ | 6, 13, 19, 23 | (James et al. 1996) |
| NSY468 | PJ469-a (for yeast 2-hybrid)<br>MATa, trp1, ura3-52, leu2, his3, lys2, gal4Δ | 6, 13, 19, 23 | (James et al. 1996) |
| NSY1176 | *TRS120*-myc/*TRS130*-HA<br>MATα, leu2, ura3-52, lys2 | 6, 7 | (Liang et al. 2007) |
| NSY1177 | *trs65ts*<br>NSY1176, but with *trs65Δ* | 6, 8 | (Liang et al. 2007) |
| NSY825 | "wild type"<br>MATa, his3, leu2, met15, ura3 | 7 | (Brachmann et al. 1998) |
| NSY1196 | *trs33Δ* (::KanMX4)<br>NSY825, but with *trs33Δ* | 7 | (Brachmann et al. 1998) |
| NSY1040 | *TRS120*-myc<br>MATa, leu2, ura3-52, his3, lys2 | 7, 9 | (Morozova et al. 2006) |
| NSY1429 | *TRS120*-myc/*trs33Δ* (::KanMX4)<br>NSY1040, but with *trs33Δ* | 7, 9 | (Tokarev et al. 2009) |
| NSY991 | *TRS130*-HA<br>MATα, leu2, ura3-52, lys2, trp1 | 7, 8, 9, 11 | (Sciorra et al. 2005) |
| NSY1430 | *TRS130*-HA/*trs33Δ* (::KanMX4) – *trs33ts*<br>NSY991, but with *trs33Δ* | 7, 8, 9, 11 | (Tokarev et al. 2009) |
| NSY1431 | *TRS120*-myc/*TRS130*-HA/*trs33Δ* + pNS552<br>NSY1176, but with *trs33Δ* and adding pNS552 | 7 | (Tokarev et al 2009) |
| NSY1316 | *TRS130*-GFP/*SEC7*-dsRed<br>MATα, lys2 | 10 | (Tokarev et al. 2009) |
| NSY1432 | *TRS130*-GFP/*SEC7*-dsRed/*trs33Δ*<br>NSY1316, but with *trs33Δ* | 10 | (Tokarev et al. 2009) |
| NSY1179 | *TRS65*-YFP<br>MATa, ura3, leu2, his3, met15 | 12 | (Liang et al. 2007) |
| NSY1472 | "wild type"<br>MATa, his3, ura3, leu2-3, | | (Scrivens et al. 2009) |
| NSY1471 | *trs20ts*<br>MATa, lys2, his3, leu2, | | (Scrivens et al. 2009) |
| NSY1519[1] | *TRS120*-myc<br>MATa, ura3, leu2-3, lys2-801 | 15 | (Taussig et al. 2013) |
| NSY1520[1] | *TRS120*-myc/*trs20ts*<br>MATa, leu2-3, lys2-801 | 15 | (Taussig et al. 2013) |
| NSY1521[1] | *TRS130*-HA<br>MATα, leu2-3, ura3 | 15, 16 | (Taussig et al. 2013) |
| NSY1522[1] | *TRS130*-HA/*trs20ts*<br>MATα, leu2-3, lys2-801 | 15, 16 | (Taussig et al. 2013) |

[1] These strains were derived from tetrad dissection of a diploid strain generated by mating NSY1176 with NSY1471

**Table III (continued): Yeast strains used in this study**

| Name | Genotype | Figure(s) | Reference |
|---|---|---|---|
| NSY1513 | *TRS120*-GFP<br>NSY1471, but *TRS120* tagged with GFP | 17 | (Taussig et al. 2013) |
| NSY1514 | *TRS120*-GFP/*trs20ts*<br>NSY1472, but *TRS120* tagged with GFP | 17 | (Taussig et al. 2013) |
| NSY1515[2] | *TRS130-GFP*<br>MATa, ura3, lys2 | 17 | (Taussig et al. 2013) |
| NSY1516[2] | *TRS130-GFP*/*trs20ts*<br>MATa, lys2 | 17 | (Taussig et al. 2013) |
| NSY1517 | *BET3*-GFP<br>NSY1471, but *BET3* tagged with GFP | 17 | (Taussig et al. 2013) |
| NSY1518 | *BET3*-GFP/*trs20ts*<br>NSY1472, but *BET3* tagged with GFP | 17 | (Taussig et al. 2013) |
| NSY1523 | *trs20Δ +* pNS1397<br>NSY1471, but with *trs20Δ* and adding pNS1397 | 18 | (Taussig et al. 2013) |
| NSY1524 | *trs20Δ +* pNS1398<br>NSY1471, but with *trs20Δ* and adding pNS1398 | 18 | (Taussig et al. 2013) |
| NSY1525 | *trs20Δ +* pNS1399<br>NSY1471, but with *trs20Δ* and adding pNS1399 | 18 | (Taussig et al. 2013) |
| NSY128 | "wild type"<br>MATα ade2 his3 leu2-3 lys2 ura3-52 | 20 | D. Botstein, DBY4975 |
| NSY863 | CHC1-RFP (::KanMX6)<br>MATα his3 leu2 lys2 ura3 | 20 | (Huh et al. 2003) |

[2] These strains were derived from tetrad dissection of a diploid strain generated by mating NSY1316 with NSY1472

# APPENDIX

Despite a thorough understanding of TRAPP I structure, the full architecture of TRAPP II is still poorly understood. In this dissertation I have shown that Trs120, the largest TRAPP subunit, binds to TRAPP I through its interactions with Trs33 and Trs20. It has previously been shown that Trs120 is required for the attachment of Trs130 to the complex (Morozova et al. 2006). Thus, Trs120 was positioned between TRAPP I and Trs130 in Figure 21A.

While this position of Trs120 is well-founded, there has been no evidence reported to suggest a particular orientation of this protein. To address this issue I separated Trs120 into two roughly equal parts: the first 626 amino acids are referred to as Trs120N, and the last 663 as Trs120C. Based on an amino-acid sequence alignment between Trs120 and TRAPPC9, its human ortholog, Trs120N encompasses 3 small conserved domains, and Trs120C 2 larger conserved domains (Cox et al. 2007).

In order to discover whether these portions of Trs120 interacted specifically with other TRAPP subunits, *TRS120N* and *TRS120C* were cloned into vectors for yeast 2-hybrid analysis. The subsequent assay revealed a notable result: the amino terminus of Trs120 (Trs120N) interacts specifically with TRAPP I subunits, including Trs20, Trs23, and Trs31. Weaker interaction was detected between Trs120N and other TRAPP I subunits Bet3 and Bet5. However, this domain of Trs120 did not interact at all with Trs130 or Trs65. On the other hand, the carboxy terminus of Trs120 (Trs120C) interacted specifically with Trs130, Trs65, itself, and the full-length Trs120 protein (Figure 23, Appendix).

These results suggest that within TRAPP II, Trs120 is oriented in a way such that its N-terminal portion contacts TRAPP I subunits, and its C-terminus is buried within the middle of the

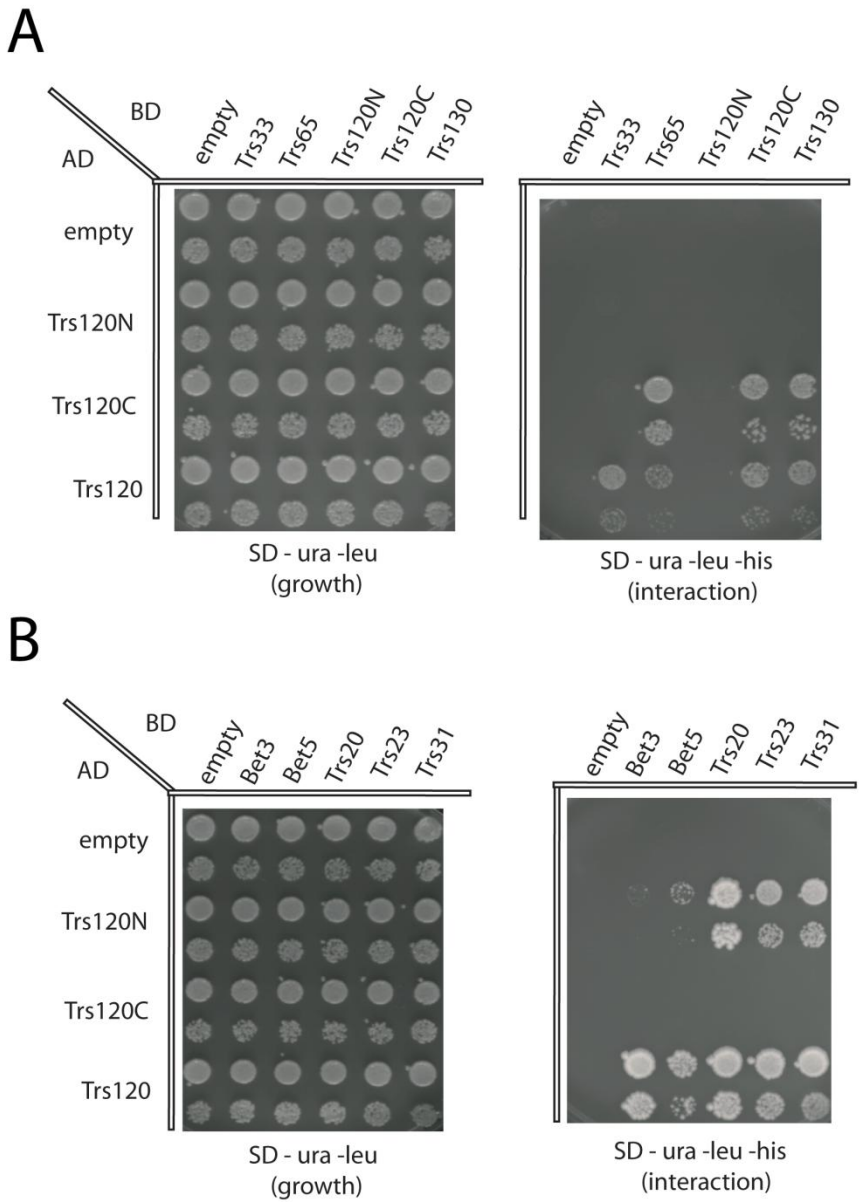


**Figure 23: Interactions of Trs120 N or C-terminal halves with TRAPP subunits. A and B)** Trs120N, Trs120C, and Trs120 full length were fused to the GAL4 activation domain (AD), and the indicated TRAPP subunits were fused to GAL4 binding domain (BD). Growth on the interaction plate (left panels) indicate interaction. Empty BD and AD were included as negative controls. The lower row for each strain represents a 10-fold dilution.

complex, in contact with Trs130 and Trs65. Surprisingly, Trs33 did not interact with either piece of Trs120, although it did interact with the full-length protein. One possible reason for this may be that Trs33 interacts with the middle of the protein, where the protein was cut for this assay, likely changing the protein's tertiary structure in this region. Furthermore, the interaction of Trs120C with itself as well as full-length Trs120 implies that this subunit, along with previously reported Trs65 (Yip et al. 2010), may contribute to the dimerization of TRAPP II.

To confirm the specific interaction of Trs120N with TRAPP subunits, the *TRS120N* and *TRS120C* regions were cloned into vectors for bacterial expression and recombinant protein pull-down. This experiment, done in a manner similar to that shown in Figure 14A, corroborated the yeast 2-hybrid result. Shown previously, the core TRAPP I subunits did not co-precipitate the full-length Trs120. Not surprisingly, neither Trs120N nor Trs120C co-precipitated with core TRAPP I. However, the addition of Trs20, or Trs20 along with Trs33, to core TRAPP I resulted in substantial co-precipitation of Trs120N, but not Trs120C (Figure 24, Appendix). Importantly, the addition of Trs33 did not increase the co-precipitation of Trs120N, in contrast to the full-length Trs120 (Figure 14). Therefore, both yeast 2-hybrid and co-precipitation results suggest that Trs33 does not bind to Trs120 through its amino-terminal half.

Without a crystal structure available for Trs120, these results do not entirely elucidate the orientation of Trs120. However, they do help to shed light on how Trs120 might be oriented with respect to other TRAPP subunits. Additional experiments using these domains, or possibly those of Trs130, can further clarify how these proteins fit into the TRAPP II structure.

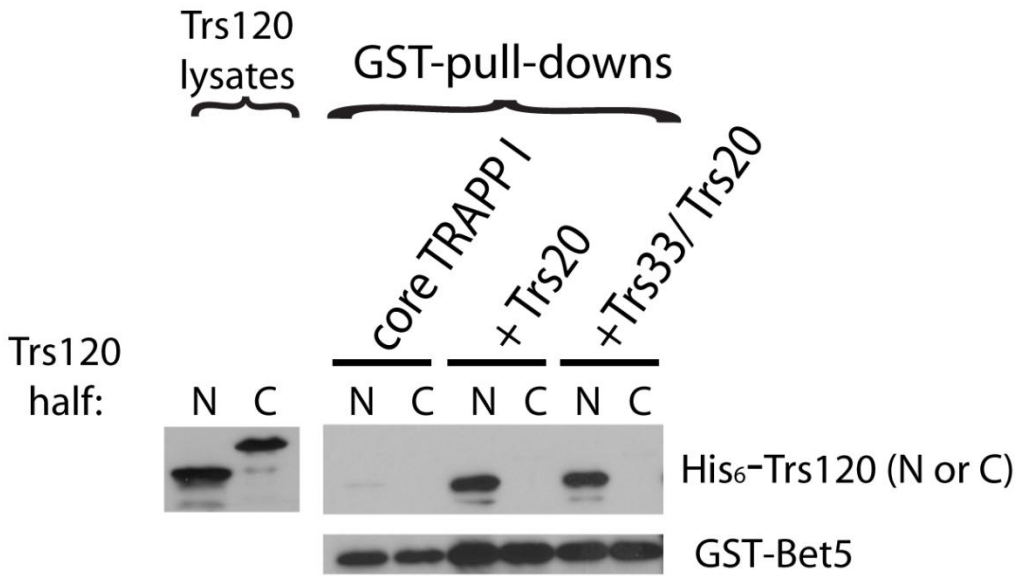


**Figure 24: The N-terminal half of Trs120 binds specifically to TRAPP containing Trs20.** Similar to the experiment shown for Figure 14A, groups of recombinant TRAPP I containing Trs23-Trs31-Bet5-Bet3 (core TRAPP I), core TRAPP I plus Trs20, or core TRAPP I plus Trs20 and Trs33 were co-expressed in bacteria and precipitated onto glutathione resin. The resin was subsequently incubated with lysate containing either the N-terminal or C-terminal half of Trs120. After washing, co-precipitation of the Trs120 piece with GST-Bet5 was determined by Western blotting. The left two lanes show the levels of Trs120N and Trs120C in their respective lysates, and the right lanes show the Trs120N, Trs120C, or GST-Bet5 bound to the glutathione resin after GST pull-down.

## CITED LITERATURE


Albert, S. and D. Gallwitz (1999). "Two new members of a family of Ypt/Rab GTPase activating proteins. Promiscuity of substrate recognition." J Biol Chem **274**(47): 33186-9.

Allan, B. B., B. D. Moyer and W. E. Balch (2000). "Rab1 recruitment of p115 into a cis-SNARE complex: programming budding COPII vesicles for fusion." Science **289**(5478): 444-8.

Amlacher, S., P. Sarges, D. Flemming, V. van Noort, R. Kunze, D. P. Devos, M. Arumugam, P. Bork and E. Hurt (2011). "Insight into structure and assembly of the nuclear pore complex by utilizing the genome of a eukaryotic thermophile." Cell **146**(2): 277-89.

Anant, J. S., L. Desnoyers, M. Machius, B. Demeler, J. C. Hansen, K. D. Westover, J. Deisenhofer and M. C. Seabra (1998). "Mechanism of Rab geranylgeranylation: formation of the catalytic ternary complex." Biochemistry **37**(36): 12559-68.

Araki, K. and K. Nagata (2011). "Protein folding and quality control in the ER." Cold Spring Harb Perspect Biol **3**(11): a007526.

Ausubel, F. M., R. Brent, R. E. Kingston, D. D. Moore, J. G. Seidman, J. A. Smith and K. Struhl, Eds. (1994). Current Protocols in Molecular Biology, John Wiley & Sons, Inc.

Benli, M., F. Doring, D. G. Robinson, X. Yang and D. Gallwitz (1996). "Two GTPase isoforms, Ypt31p and Ypt32p, are essential for Golgi function in yeast." Embo J **15**(23): 6460-75.

Bonifacino, J. S. and B. S. Glick (2004). "The mechanisms of vesicle budding and fusion." Cell **116**(2): 153-66.

Bonifacino, J. S. and J. Lippincott-Schwartz (2003). "Coat proteins: shaping membrane transport." Nat Rev Mol Cell Biol **4**(5): 409-14.

Brachmann, C. B., A. Davies, G. J. Cost, E. Caputo, J. Li, P. Hieter and J. D. Boeke (1998). "Designer deletion strains derived from Saccharomyces cerevisiae S288C: a useful set of strains and plasmids for PCR-mediated gene disruption and other applications." Yeast **14**(2): 115-32.

Brown, J. L. and H. Bussey (1993). "The yeast KRE9 gene encodes an O glycoprotein involved in cell surface beta-glucan assembly." Mol Cell Biol **13**(10): 6346-56.

Brunet, S., B. Noueihed, N. Shahrzad, D. Saint-Dic, B. Hasaj, T. L. Guan, A. Moores, C. Barlowe and M. Sacher (2012). "The SMS domain of Trs23p is responsible for the in vitro appearance of the TRAPP I complex in Saccharomyces cerevisiae." Cell Logist **2**(1): 28-42.

Byers, B. and L. Goetsch (1975). "Electron microscopic observations on the meiotic karyotype of diploid and tetraploid Saccharomyces cerevisiae." Proc Natl Acad Sci U S A **72**(12): 5056-60.

Cai, H., S. Yu, S. Menon, Y. Cai, D. Lazarova, C. Fu, K. Reinisch, J. C. Hay and S. Ferro-Novick (2007). "TRAPPI tethers COPII vesicles by binding the coat subunit Sec23." Nature **445**(7130): 941-4.

Cai, H., Y. Zhang, M. Pypaert, L. Walker and S. Ferro-Novick (2005). "Mutants in trs120 disrupt traffic from the early endosome to the late Golgi." J Cell Biol **171**(5): 823-33.

Cai, Y., H. F. Chin, D. Lazarova, S. Menon, C. Fu, H. Cai, A. Sclafani, D. W. Rodgers, E. M. De La Cruz, S. Ferro-Novick and K. M. Reinisch (2008). "The structural basis for activation of the Rab Ypt1p by the TRAPP membrane-tethering complexes." Cell **133**(7): 1202-13.

Calero, M., C. Z. Chen, W. Zhu, N. Winand, K. A. Havas, P. M. Gilbert, C. G. Burd and R. N. Collins (2003). "Dual prenylation is required for Rab protein localization and function." Mol Biol Cell **14**(5): 1852-67.

Caro, L. G. and G. E. Palade (1964). "Protein Synthesis, Storage, and Discharge in the Pancreatic Exocrine Cell. an Autoradiographic Study." J Cell Biol **20**: 473-95.

Carroll, K. S., J. Hanna, I. Simon, J. Krise, P. Barbero and S. R. Pfeffer (2001). "Role of Rab9 GTPase in facilitating receptor recruitment by TIP47." Science **292**(5520): 1373-6.

Chavrier, P., J. P. Gorvel, E. Stelzer, K. Simons, J. Gruenberg and M. Zerial (1991). "Hypervariable C-terminal domain of rab proteins acts as a targeting signal." Nature **353**(6346): 769-72.

Chen, S., H. Cai, S. K. Park, S. Menon, C. L. Jackson and S. Ferro-Novick (2011). "Trs65p, a subunit of the Ypt1p GEF TRAPPII, interacts with the Arf1p exchange factor Gea2p to facilitate COPI-mediated vesicle traffic." Mol Biol Cell **22**(19): 3634-44.

Chen, S. H., S. Chen, A. A. Tokarev, F. Liu, G. Jedd and N. Segev (2005). "Ypt31/32 GTPases and their novel F-box effector protein Rcy1 regulate protein recycling." Mol Biol Cell **16**(1): 178-92.

Choi, C., M. Davey, C. Schluter, P. Pandher, Y. Fang, L. J. Foster and E. Conibear (2011). "Organization and assembly of the TRAPPII complex." Traffic **12**(6): 715-25.

Ciechanover, A. (2012). "Intracellular protein degradation: from a vague idea thru the lysosome and the ubiquitin-proteasome system and onto human diseases and drug targeting." Biochim Biophys Acta **1824**(1): 3-13.

Conibear, E. and T. H. Stevens (2000). "Vps52p, Vps53p, and Vps54p form a novel multisubunit complex required for protein sorting at the yeast late Golgi." Mol Biol Cell **11**(1): 305-23.

Cooper, A. A., A. D. Gitler, A. Cashikar, C. M. Haynes, K. J. Hill, B. Bhullar, K. Liu, K. Xu, K. E. Strathearn, F. Liu, S. Cao, K. A. Caldwell, G. A. Caldwell, G. Marsischky, R. D. Kolodner, J. Labaer, J. C. Rochet, N. M. Bonini and S. Lindquist (2006). "Alpha-synuclein blocks ER-Golgi traffic and Rab1 rescues neuron loss in Parkinson's models." Science **313**(5785): 324-8.

Cox, R., S. H. Chen, E. Yoo and N. Segev (2007). "Conservation of the TRAPPII-specific subunits of a Ypt/Rab exchanger complex." BMC Evol Biol **7**: 12.

Dumas, J. J., Z. Zhu, J. L. Connolly and D. G. Lambright (1999). "Structural basis of activation and GTP hydrolysis in Rab proteins." Structure **7**(4): 413-23.

Fan, L., W. Yu and X. Zhu (2003). "Interaction of Sedlin with chloride intracellular channel proteins." FEBS Lett **540**(1-3): 77-80.

Fiedler, J., M. Le Merrer, G. Mortier, S. Heuertz, L. Faivre and R. E. Brenner (2004). "X-linked spondyloepiphyseal dysplasia tarda: Novel and recurrent mutations in 13 European families." Hum Mutat **24**(1): 103.

Gallwitz, D., C. Donath and C. Sander (1983). "A yeast gene encoding a protein homologous to the human c-has/bas proto-oncogene product." Nature **306**(5944): 704-7.

Garrett, M. D., J. E. Zahner, C. M. Cheney and P. J. Novick (1994). "GDI1 encodes a GDP dissociation inhibitor that plays an essential role in the yeast secretory pathway." Embo J **13**(7): 1718-28.

Gecz, J., M. A. Shaw, J. R. Bellon and M. de Barros Lopes (2003). "Human wild-type SEDL protein functionally complements yeast Trs20p but some naturally occurring SEDL mutants do not." Gene **320**: 137-44.

Gedeon, A. K., A. Colley, R. Jamieson, E. M. Thompson, J. Rogers, D. Sillence, G. E. Tiller, J. C. Mulley and J. Gecz (1999). "Identification of the gene (SEDL) causing X-linked spondyloepiphyseal dysplasia tarda." Nat Genet **22**(4): 400-4.

Gedeon, A. K., G. E. Tiller, M. Le Merrer, S. Heuertz, L. Tranebjaerg, D. Chitayat, S. Robertson, I. A. Glass, R. Savarirayan, W. G. Cole, D. L. Rimoin, B. G. Kousseff, H. Ohashi, B. Zabel, A. Munnich, J. Gecz and J. C. Mulley (2001). "The molecular basis of X-linked spondyloepiphyseal dysplasia tarda." Am J Hum Genet **68**(6): 1386-97.

Gentzsch, M., X. B. Chang, L. Cui, Y. Wu, V. V. Ozols, A. Choudhury, R. E. Pagano and J. R. Riordan (2004). "Endocytic trafficking routes of wild type and DeltaF508 cystic fibrosis transmembrane conductance regulator." Mol Biol Cell **15**(6): 2684-96.

Ghosh, A. K., M. Majumder, R. Steele, R. A. White and R. B. Ray (2001). "A novel 16-kilodalton cellular protein physically interacts with and antagonizes the functional activity of c-myc promoter-binding protein 1." Mol Cell Biol **21**(2): 655-62.

Gourraud, P. A., M. Sdika, P. Khankhanian, R. G. Henry, A. Beheshtian, P. M. Matthews, S. L. Hauser, J. R. Oksenberg, D. Pelletier and S. E. Baranzini (2013). "A genome-wide association study of brain lesion distribution in multiple sclerosis." Brain.

Grunebaum, E., E. Arpaia, J. J. MacKenzie, J. Fitzpatrick, P. N. Ray and C. M. Roifman (2001). "A missense mutation in the SEDL gene results in delayed onset of X linked spondyloepiphyseal dysplasia in a large pedigree." J Med Genet **38**(6): 409-11.

Guo, W., D. Roth, C. Walch-Solimena and P. Novick (1999). "The exocyst is an effector for Sec4p, targeting secretory vesicles to sites of exocytosis." Embo J **18**(4): 1071-80.

He, H., F. Dai, L. Yu, X. She, Y. Zhao, J. Jiang, X. Chen and S. Zhao (2002). "Identification and characterization of nine novel human small GTPases showing variable expressions in liver cancer tissues." Gene Expr **10**(5-6): 231-42.

Holm, C., D. W. Meeks-Wagner, W. L. Fangman and D. Botstein (1986). "A rapid, efficient method for isolating DNA from yeast." Gene **42**(2): 169-73.

Hu, W. H., J. S. Pendergast, X. M. Mo, R. Brambilla, V. Bracchi-Ricard, F. Li, W. M. Walters, B. Blits, L. He, S. M. Schaal and J. R. Bethea (2005). "NIBP, a novel NIK and IKK(beta)-binding protein that enhances NF-(kappa)B activation." J Biol Chem **280**(32): 29233-41.

Huh, W. K., J. V. Falvo, L. C. Gerke, A. S. Carroll, R. W. Howson, J. S. Weissman and E. K. O'Shea (2003). "Global analysis of protein localization in budding yeast." Nature **425**(6959): 686-91.

Hutagalung, A. H. and P. J. Novick (2011). "Role of Rab GTPases in membrane traffic and cell physiology." Physiol Rev **91**(1): 119-49.

Ito, H., Y. Fukuda, K. Murata and A. Kimura (1983). "Transformation of intact yeast cells treated with alkali cations." J Bacteriol **153**(1): 163-8.

James, P., J. Halladay and E. A. Craig (1996). "Genomic libraries and a host strain designed for highly efficient two-hybrid selection in yeast." Genetics **144**(4): 1425-36.

Jang, S. B., Y. S. Cho, S. J. Eom, E. J. Choi, K. H. Kim, P. G. Suh and B. H. Oh (2002). "Crystallization and preliminary X-ray crystallographic analysis of SEDL." Acta Crystallogr D Biol Crystallogr **58**(Pt 3): 564-6.

Jedd, G., J. Mulholland and N. Segev (1997). "Two new Ypt GTPases are required for exit from the yeast trans-Golgi compartment." J Cell Biol **137**(3): 563-80.

Jeyabalan, J., M. A. Nesbit, J. Galvanovskis, R. Callaghan, P. Rorsman and R. V. Thakker (2010). "SEDLIN forms homodimers: characterisation of SEDLIN mutations and their interactions with transcription factors MBP1, PITX1 and SF1." PLoS One **5**(5): e10646.

Jiang, Y., A. Scarpa, L. Zhang, S. Stone, E. Feliciano and S. Ferro-Novick (1998). "A high copy suppressor screen reveals genetic interactions between BET3 and a new gene. Evidence for a novel complex in ER-to-Golgi transport." Genetics **149**(2): 833-41.

Jones, S., C. Newman, F. Liu and N. Segev (2000). "The TRAPP complex is a nucleotide exchanger for Ypt1 and Ypt31/32." Mol Biol Cell **11**(12): 4403-11.

Jones, S., C. J. Richardson, R. J. Litt and N. Segev (1998). "Identification of regulators for Ypt1 GTPase nucleotide cycling." Mol Biol Cell **9**(10): 2819-37.

Kerppola, T. K. (2008). "Bimolecular fluorescence complementation: visualization of molecular interactions in living cells." Methods Cell Biol **85**: 431-70.

Kim, M. S., M. J. Yi, K. H. Lee, J. Wagner, C. Munger, Y. G. Kim, M. Whiteway, M. Cygler, B. H. Oh and M. Sacher (2005). "Biochemical and crystallographic studies reveal a specific interaction between TRAPP subunits Trs33p and Bet3p." Traffic **6**(12): 1183-95.

Kim, Y. G., S. Raunser, C. Munger, J. Wagner, Y. L. Song, M. Cygler, T. Walz, B. H. Oh and M. Sacher (2006). "The architecture of the multisubunit TRAPP I complex suggests a model for vesicle tethering." Cell **127**(4): 817-30.

Kim, Y. G., E. J. Sohn, J. Seo, K. J. Lee, H. S. Lee, I. Hwang, M. Whiteway, M. Sacher and B. H. Oh (2005). "Crystal structure of bet3 reveals a novel mechanism for Golgi localization of tethering factor TRAPP." Nat Struct Mol Biol **12**(1): 38-45.

Kummel, D., A. Oeckinghaus, C. Wang, D. Krappmann and U. Heinemann (2008). "Distinct isocomplexes of the TRAPP trafficking factor coexist inside human cells." FEBS Lett **582**(27): 3729-33.

Larkin, M. A., G. Blackshields, N. P. Brown, R. Chenna, P. A. McGettigan, H. McWilliam, F. Valentin, I. M. Wallace, A. Wilm, R. Lopez, J. D. Thompson, T. J. Gibson and D. G. Higgins (2007). "Clustal W and Clustal X version 2.0." Bioinformatics **23**(21): 2947-8.

Lee, M. T., A. Mishra and D. G. Lambright (2009). "Structural mechanisms for regulation of membrane traffic by rab GTPases." Traffic **10**(10): 1377-89.

Liang, Y., N. Morozova, A. A. Tokarev, J. W. Mulholland and N. Segev (2007). "The role of Trs65 in the Ypt/Rab guanine nucleotide exchange factor function of the TRAPP II complex." Mol Biol Cell **18**(7): 2533-41.

Lipatova, Z., N. Belogortseva, X. Q. Zhang, J. Kim, D. Taussig and N. Segev (2012). "Regulation of selective autophagy onset by a Ypt/Rab GTPase module." Proc Natl Acad Sci U S A **109**(18): 6981-6.

Lipatova, Z., A. A. Tokarev, Y. Jin, J. Mulholland, L. S. Weisman and N. Segev (2008). "Direct interaction between a myosin V motor and the Rab GTPases Ypt31/32 is required for polarized secretion." Mol Biol Cell **19**(10): 4177-87.

Liu, X., Y. Wang, H. Zhu, Q. Zhang, X. Xing, B. Wu, L. Song and L. Fan (2010). "Interaction of Sedlin with PAM14." J Cell Biochem **109**(6): 1129-33.

Loh, E., F. Peter, V. N. Subramaniam and W. Hong (2005). "Mammalian Bet3 functions as a cytosolic factor participating in transport from the ER to the Golgi apparatus." J Cell Sci **118**(Pt 6): 1209-22.

Lynch-Day, M. A., D. Bhandari, S. Menon, J. Huang, H. Cai, C. R. Bartholomew, J. H. Brumell, S. Ferro-Novick and D. J. Klionsky (2010). "Trs85 directs a Ypt1 GEF, TRAPPIII, to the phagophore to promote autophagy." Proc Natl Acad Sci U S A **107**(17): 7811-6.

Mahfouz, H., A. Ragnini-Wilson, R. Venditti, M. A. De Matteis and C. Wilson (2012). "Mutational analysis of the yeast TRAPP subunit Trs20p identifies roles in endocytic recycling and sporulation." PLoS One **7**(9): e41408.

Marangi, G., V. Leuzzi, F. Manti, S. Lattante, D. Orteschi, V. Pecile, G. Neri and M. Zollino (2013). "TRAPPC9-related autosomal recessive intellectual disability: report of a new mutation and clinical phenotype." Eur J Hum Genet **21**(2): 229-32.

Martzen, M. R., S. M. McCraith, S. L. Spinelli, F. M. Torres, S. Fields, E. J. Grayhack and E. M. Phizicky (1999). "A biochemical genomics approach for identifying genes by the activity of their products." Science **286**(5442): 1153-5.

Meiling-Wesse, K., U. D. Epple, R. Krick, H. Barth, A. Appelles, C. Voss, E. L. Eskelinen and M. Thumm (2005). "Trs85 (Gsg1), a component of the TRAPP complexes, is required for the organization of the preautophagosomal structure during selective autophagy via the Cvt pathway." J Biol Chem **280**(39): 33669-78.

Mir, A., L. Kaufman, A. Noor, M. M. Motazacker, T. Jamil, M. Azam, K. Kahrizi, M. A. Rafiq, R. Weksberg, T. Nasr, F. Naeem, A. Tzschach, A. W. Kuss, G. E. Ishak, D. Doherty, H. H. Ropers, A. J. Barkovich, H. Najmabadi, M. Ayub and J. B. Vincent (2009). "Identification of mutations in TRAPPC9, which encodes the NIK- and IKK-beta-binding protein, in nonsyndromic autosomal-recessive mental retardation." Am J Hum Genet **85**(6): 909-15.

Mizuno-Yamasaki, E., F. Rivera-Molina and P. Novick (2012). "GTPase networks in membrane traffic." Annu Rev Biochem **81**: 637-59.

Montpetit, B. and E. Conibear (2009). "Identification of the novel TRAPP associated protein Tca17." Traffic **10**(6): 713-23.

Morozova, N., Y. Liang, A. A. Tokarev, S. H. Chen, R. Cox, J. Andrejic, Z. Lipatova, V. A. Sciorra, S. D. Emr and N. Segev (2006). "TRAPPII subunits are required for the specificity switch of a Ypt-Rab GEF." Nat Cell Biol **8**(11): 1263-9.

Moyer, B. D., B. B. Allan and W. E. Balch (2001). "Rab1 interaction with a GM130 effector complex regulates COPII vesicle cis--Golgi tethering." Traffic **2**(4): 268-76.

Nazarko, T. Y., J. Huang, J. M. Nicaud, D. J. Klionsky and A. A. Sibirny (2005). "Trs85 is required for macroautophagy, pexophagy and cytoplasm to vacuole targeting in Yarrowia lipolytica and Saccharomyces cerevisiae." Autophagy **1**(1): 37-45.

Nordmann, M., M. Cabrera, A. Perz, C. Brocker, C. Ostrowicz, S. Engelbrecht-Vandre and C. Ungermann (2010). "The Mon1-Ccz1 complex is the GEF of the late endosomal Rab7 homolog Ypt7." Curr Biol **20**(18): 1654-9.

Ortiz, D., M. Medkova, C. Walch-Solimena and P. Novick (2002). "Ypt32 recruits the Sec4p guanine nucleotide exchange factor, Sec2p, to secretory vesicles; evidence for a Rab cascade in yeast." J Cell Biol **157**(6): 1005-15.

Palade, G. (1975). "Intracellular aspects of the process of protein synthesis." Science **189**(4200): 347-58.

Qi, X., M. Kaneda, J. Chen, A. Geitmann and H. Zheng (2011). "A specific role for Arabidopsis TRAPPII in post-Golgi trafficking that is crucial for cytokinesis and cell polarity." Plant J **68**(2): 234-48.

Rivera-Molina, F. E. and P. J. Novick (2009). "A Rab GAP cascade defines the boundary between two Rab GTPases on the secretory pathway." Proc Natl Acad Sci U S A **106**(34): 14408-13.

Rossi, G., K. Kolstad, S. Stone, F. Palluault and S. Ferro-Novick (1995). "BET3 encodes a novel hydrophilic protein that acts in conjunction with yeast SNAREs." Mol Biol Cell **6**(12): 1769-80.

Sacher, M., J. Barrowman, D. Schieltz, J. R. Yates, 3rd and S. Ferro-Novick (2000). "Identification and characterization of five new subunits of TRAPP." Eur J Cell Biol **79**(2): 71-80.

Sacher, M., J. Barrowman, W. Wang, J. Horecka, Y. Zhang, M. Pypaert and S. Ferro-Novick (2001). "TRAPP I implicated in the specificity of tethering in ER-to-Golgi transport." Mol Cell **7**(2): 433-42.

Sacher, M., Y. Jiang, J. Barrowman, A. Scarpa, J. Burston, L. Zhang, D. Schieltz, J. R. Yates, 3rd, H. Abeliovich and S. Ferro-Novick (1998). "TRAPP, a highly conserved novel complex on the cis-Golgi that mediates vesicle docking and fusion." Embo J **17**(9): 2494-503.

Salminen, A. and P. J. Novick (1987). "A ras-like protein is required for a post-Golgi event in yeast secretion." Cell **49**(4): 527-38.

Sato, T. K., P. Rehling, M. R. Peterson and S. D. Emr (2000). "Class C Vps protein complex regulates vacuolar SNARE pairing and is required for vesicle docking/fusion." Mol Cell **6**(3): 661-71.

Schimmoller, F. and H. Riezman (1993). "Involvement of Ypt7p, a small GTPase, in traffic from late endosome to the vacuole in yeast." J Cell Sci **106 ( Pt 3)**: 823-30.

Schwenk, R. W., J. J. Luiken and J. Eckel (2007). "FIP2 and Rip11 specify Rab11a-mediated cellular distribution of GLUT4 and FAT/CD36 in H9c2-hIR cells." Biochem Biophys Res Commun **363**(1): 119-25.

Sciorra, V. A., A. Audhya, A. B. Parsons, N. Segev, C. Boone and S. D. Emr (2005). "Synthetic genetic array analysis of the PtdIns 4-kinase Pik1p identifies components in a Golgi-specific Ypt31/rab-GTPase signaling pathway." Mol Biol Cell **16**(2): 776-93.

Scrivens, P. J., B. Noueihed, N. Shahrzad, S. Hul, S. Brunet and M. Sacher (2011). "C4orf41 and TTC-15 are mammalian TRAPP components with a role at an early stage in ER-to-Golgi trafficking." Mol Biol Cell **22**(12): 2083-93.

Scrivens, P. J., N. Shahrzad, A. Moores, A. Morin, S. Brunet and M. Sacher (2009). "TRAPPC2L is a novel, highly conserved TRAPP-interacting protein." Traffic **10**(6): 724-36.

Seabra, M. C. (1998). "Membrane association and targeting of prenylated Ras-like GTPases." Cell Signal **10**(3): 167-72.

Segev, N. (2001). "Ypt/rab gtpases: regulators of protein trafficking." Sci STKE **2001**(100): RE11.

Segev, N. and D. Botstein (1987). "The ras-like yeast YPT1 gene is itself essential for growth, sporulation, and starvation response." Mol Cell Biol **7**(7): 2367-77.

Segev, N., J. Mulholland and D. Botstein (1988). "The yeast GTP-binding YPT1 protein and a mammalian counterpart are associated with the secretion machinery." Cell **52**(6): 915-24.

Shimada, K., K. Uzawa, M. Kato, Y. Endo, M. Shiiba, H. Bukawa, H. Yokoe, N. Seki and H. Tanzawa (2005). "Aberrant expression of RAB1A in human tongue cancer." Br J Cancer **92**(10): 1915-21.

Sikorski, R. S. and P. Hieter (1989). "A system of shuttle vectors and yeast host strains designed for efficient manipulation of DNA in Saccharomyces cerevisiae." Genetics **122**(1): 19-27.

Siniossoglou, S., S. Y. Peak-Chew and H. R. Pelham (2000). "Ric1p and Rgp1p form a complex that catalyses nucleotide exchange on Ypt6p." Embo J **19**(18): 4885-94.

Stroupe, C. and A. T. Brunger (2000). "Crystal structures of a Rab protein in its inactive and active conformations." J Mol Biol **304**(4): 585-98.

Suvorova, E. S., R. Duden and V. V. Lupashin (2002). "The Sec34/Sec35p complex, a Ypt1p effector required for retrograde intra-Golgi trafficking, interacts with Golgi SNAREs and COPI vesicle coat proteins." J Cell Biol **157**(4): 631-43.

Tartof, K. and C. Hobbs (1987). "Improved media for growing plasmids and cosmid clones." Bethesda Research Laboratories **9**.

Taussig, D., Z. Lipatova, K. Jane, Z. Xuiqi and N. Segev (2013). "Trs20 is Required for TRAPP II Assembly." Traffic.

Tiller, G. E., V. L. Hannig, D. Dozier, L. Carrel, K. C. Trevarthen, W. R. Wilcox, S. Mundlos, J. L. Haines, A. K. Gedeon and J. Gecz (2001). "A recurrent RNA-splicing mutation in the SEDL gene causes X-linked spondyloepiphyseal dysplasia tarda." Am J Hum Genet **68**(6): 1398-407.

Tokarev, A. A., D. Taussig, G. Sundaram, Z. Lipatova, Y. Liang, J. W. Mulholland and N. Segev (2009). "TRAPP II complex assembly requires Trs33 or Trs65." Traffic **10**(12): 1831-44.

Touchot, N., P. Chardin and A. Tavitian (1987). "Four additional members of the ras gene superfamily isolated by an oligonucleotide strategy: molecular cloning of YPT-related cDNAs from a rat brain library." Proc Natl Acad Sci U S A **84**(23): 8210-4.

Turnbull, A. P., D. Kummel, B. Prinz, C. Holz, J. Schultchen, C. Lang, F. H. Niesen, K. P. Hofmann, H. Delbruck, J. Behlke, E. C. Muller, E. Jarosch, T. Sommer and U. Heinemann (2005). "Structure of palmitoylated BET3: insights into TRAPP complex assembly and membrane localization." Embo J **24**(5): 875-84.

Venditti, R., T. Scanu, M. Santoro, G. Di Tullio, A. Spaar, R. Gaibisso, G. V. Beznoussenko, A. A. Mironov, A. Mironov, Jr., L. Zelante, M. R. Piemontese, A. Notarangelo, V. Malhotra, B. M. Vertel, C. Wilson and M. A. De Matteis (2012). "Sedlin controls the ER export of procollagen by regulating the Sar1 cycle." Science **337**(6102): 1668-72.

Walch-Solimena, C., R. N. Collins and P. J. Novick (1997). "Sec2p mediates nucleotide exchange on Sec4p and is involved in polarized delivery of post-Golgi vesicles." J Cell Biol **137**(7): 1495-509.

Wang, W. and S. Ferro-Novick (2002). "A Ypt32p exchange factor is a putative effector of Ypt1p." Mol Biol Cell **13**(9): 3336-43.

Wang, W., M. Sacher and S. Ferro-Novick (2000). "TRAPP stimulates guanine nucleotide exchange on Ypt1p." J Cell Biol **151**(2): 289-96.

Weide, T., M. Bayer, M. Koster, J. P. Siebrasse, R. Peters and A. Barnekow (2001). "The Golgi matrix protein GM130: a specific interacting partner of the small GTPase rab1b." EMBO Rep **2**(4): 336-41.

Westlake, C. J., J. R. Junutula, G. C. Simon, M. Pilli, R. Prekeris, R. H. Scheller, P. K. Jackson and A. G. Eldridge (2007). "Identification of Rab11 as a small GTPase binding protein for the Evi5 oncogene." Proc Natl Acad Sci U S A **104**(4): 1236-41.

Wiederkehr, A., J. O. De Craene, S. Ferro-Novick and P. Novick (2004). "Functional specialization within a vesicle tethering complex: bypass of a subset of exocyst deletion mutants by Sec1p or Sec4p." J Cell Biol **167**(5): 875-87.

Yamamoto, K. and Y. Jigami (2002). "Mutation of TRS130, which encodes a component of the TRAPP II complex, activates transcription of OCH1 in Saccharomyces cerevisiae." Curr Genet **42**(2): 85-93.

Yamasaki, A., S. Menon, S. Yu, J. Barrowman, T. Meerloo, V. Oorschot, J. Klumperman, A. Satoh and S. Ferro-Novick (2009). "mTrs130 is a component of a mammalian TRAPPII complex, a Rab1 GEF that binds to COPI-coated vesicles." Mol Biol Cell **20**(19): 4205-15.

Yip, C. K., J. Berscheminski and T. Walz (2010). "Molecular architecture of the TRAPPII complex and implications for vesicle tethering." Nat Struct Mol Biol **17**(11): 1298-304.

Yu, S. and Y. Liang (2012). "A trapper keeper for TRAPP, its structures and functions." Cell Mol Life Sci.

Yu, S., A. Satoh, M. Pypaert, K. Mullen, J. C. Hay and S. Ferro-Novick (2006). "mBet3p is required for homotypic COPII vesicle tethering in mammalian cells." J Cell Biol **174**(3): 359-68.

Zeigerer, A., M. A. Lampson, O. Karylowski, D. D. Sabatini, M. Adesnik, M. Ren and T. E. McGraw (2002). "GLUT4 retention in adipocytes requires two intracellular insulin-regulated transport steps." Mol Biol Cell **13**(7): 2421-35.

Zhu, H., Z. Liang and G. Li (2009). "Rabex-5 is a Rab22 effector and mediates a Rab22-Rab5 signaling cascade in endocytosis." Mol Biol Cell **20**(22): 4720-9.

Zong, M., A. Satoh, M. K. Yu, K. Y. Siu, W. Y. Ng, H. C. Chan, J. A. Tanner and S. Yu (2012). "TRAPPC9 mediates the interaction between p150 and COPII vesicles at the target membrane." PLoS One **7**(1): e29995.

Zong, M., X. G. Wu, C. W. Chan, M. Y. Choi, H. C. Chan, J. A. Tanner and S. Yu (2011). "The adaptor function of TRAPPC2 in mammalian TRAPPs explains TRAPPC2-associated SEDT and TRAPPC9-associated congenital intellectual disability." PLoS One **6**(8): e23350.

Zou, S., Y. Chen, Y. Liu, N. Segev, S. Yu, Y. Liu, G. Min, M. Ye, Y. Zeng, X. Zhu, B. Hong, L. O. Bjorn, Y. Liang, S. Li and Z. Xie (2013). "Trs130 participates in autophagy through GTPases Ypt31/32 in Saccharomyces cerevisiae." Traffic **14**(2): 233-46.

# VITA

NAME David Taussig

EDUCATION B.S, Biology, Wheaton College,
Wheaton, IL, 2006

(currently pursuing) Ph.D., Biological Sciences, University of Illinois at Chicago
Chicago, IL, 2013

TEACHING EXPERIENCE

Teaching Assistant for Molecular and Mendelian Genetics, UIC (12 times)
Led a 50-minute discussion section each week, and an additional office hour (optional for students) to help with concepts and homework problems.

Teaching Assistant for Genetics Laboratory, UIC (one semester)
Led two 3-hour laboratory exercises each week to convey genetics concepts.

Teaching Assistant for Biology of Cells and Organisms, UIC (one semester)
Led two 3-hour laboratory exercises each week to convey biology concepts.

Teaching Assistant for Microbiology, Wheaton College (one semester)
Preparatory work for laboratory exercises.

PUBLICATIONS

first author: Taussig, D., Lipatova, Z., Kim, J., Zhang, X.Z., and N. Segev (2013). "Trs20 is Required for TRAPP II Assembly." Traffic.

Taussig, D., Chen, S.H., and N. Segev (2011). The Golgi Gatekeepers: Ypt1 Rab1 and Ypt31/32-Rab11 – Chapter of e-book: Rab GTPases and Membrane Trafficking. – Editors Guangpu Li and Nava Segev. Published by *Bentham eBooks*. DOI: 10.2174/978160805365011201010018

co-first author: Tokarev, A. A., D. Taussig, G. Sundaram, Z. Lipatova, Y. Liang, J. W. Mulholland and N. Segev (2009). "TRAPP II complex assembly requires Trs33 or Trs65." Traffic 10(12): 1831-44.

co-author: Lipatova, Z., N. Belogortseva, X. Q. Zhang, J. Kim, D. Taussig and N. Segev (2012). "Regulation of selective autophagy onset by a Ypt/Rab GTPase module." Proc Natl Acad Sci U S A 109(18): 6981-6.

**VITA** (CONTINUED)

PROFESSIONAL PRESENTATIONS

Yeast Conference (GSA), 2009, Toronto, Canada;
Invited Speaker, Travel Award recipient

Biological Sciences Departmental Presentation (4 times)
Oral Research Presentation

ASCB Annual Meeting (ASCB), 2012, San Francisco, CA
Poster Presentation

ASCB Annual Meeting (ASCB), 2007, Washington D.C.
Poster Presentation

ASBMB Graduate Student Symposium, 2010, Chicago, IL
Meeting Organizer and Poster Presentation

BMG Departmental Retreat, 2011, Lake Geneva, WI
Poster Presentation